United States Department of Agriculture

The Geologic, Geomorphic, and Hydrologic Context Underlying Options for Long-Term Management of the Spirit Lake Outlet Near Mount St. Helens, Washington

Gordon E. Grant, Jon J. Major, and Sarah L. Lewis

Forest Service

Pacific Northwest Research Station

General Technical Report PNW-GTR-954

June 2017

Authors

Gordon E. Grant is a research hydrologist, U.S. Department of Agriculture, Forest Service, Pacific Northwest Research Station, 3200 SW Jefferson Way, Corvallis, OR 97331; **Jon J. Major** is a research hydrologist, U.S. Department of the Interior, Geological Survey, Cascades Volcano Observatory, 1300 SE Cardinal Court, Building 10, Suite 100, Vancouver, WA 98683; **Sarah L. Lewis** is a senior faculty research assistant, Oregon State University, College of Earth, Ocean, and Atmospheric Sciences, 104 CEOAS Administration Building, Corvallis, OR 97331.

Cover photo: Hikers above Spirit Lake, Mount St. Helens National Volcanic Monument, Washington. Photo by Keith Routman.

Abstract

Grant, Gordon E.; Major, Jon J.; Lewis, Sarah L. 2017. The geologic, geomorphic, and hydrologic context underlying options for long-term management of the Spirit Lake outlet near Mount St. Helens, Washington. Gen. Tech. Rep. PNW-GTR-954. Portland, OR: U.S. Department of Agriculture, Forest Service, Pacific Northwest Research Station. 151 p.

The 1980 eruption of Mount St. Helens produced a massive landslide and consequent pyroclastic currents, deposits of which blocked the outlet to Spirit Lake. Without an outlet, the lake began to rise, threatening a breaching of the blockage and release of a massive volume of water. To mitigate the hazard posed by the rising lake and provide an outlet, in 1984–1985 the U.S. Army Corps of Engineers bored a 2.6-km (8,500-ft) long tunnel through a bedrock ridge on the western edge of the lake. Locally, the tunnel crosses weak rock along faults, and external pressures in these weak zones have caused rock heave and support failures, which have necessitated periodic major repairs. During its more than 30-year lifetime, the tunnel has maintained the level of Spirit Lake at a safe elevation. The lake approaches its maximum safe operating level only when the tunnel closes for repair. The most recent major repair in early 2016 highlights the need for a reliable outlet that does not require repeated and expensive interventions and extended closures. The U.S. Forest Service, U.S. Army Corps of Engineers, and U.S. Geological Survey developed, reviewed, and analyzed an array of options for a long-term plan to remove the threat of catastrophic failure of the tunnel. In this report, we (1) provide background on natural hazards that can affect existing and alternative infrastructure; (2) evaluate the potential for tunnel failure and consequent breaching of the blockage posed by the current tunnel infrastructure; (3) evaluate potential consequences to downstream communities and infrastructure in the event of a catastrophic breaching of the blockage; (4) evaluate potential risks associated with alternative lake outlets; and (5) identify data and knowledge gaps that need to be addressed to fully evaluate options available to management.

Keywords: Risk assessment, natural dam, potential failure mode analysis, Mount St. Helens, Toutle River, Spirit Lake, flood, lahar, debris flow, volcano, earthquake.

Executive Summary

The landscapes of the U.S. Pacific Northwest are renowned for their magnificent and distinctive volcanoes, cascading rivers, clear mountain lakes, and lush forests. But intrinsic to the scenery and woven into the region's history is a recurring encounter with natural hazards in the form of volcanic eruptions, earthquakes, floods, landslides, and forest fires. In recent times, nowhere have these hazards and their interconnected linkages been more evident than at Mount St. Helens.

The May 18, 1980, eruption of Mount St. Helens was a transformative event in the geological and human history of the Pacific Northwest. Its massive debris avalanche deposited cubic kilometers of material in the upper North Fork Toutle River valley; its energetic blast pyroclastic density current (blast PDC) devastated hundreds of square kilometers of majestic forest; and its lahars (volcanic debris flows) bulldozed hundreds of kilometers of river channels, destroyed many bridges, roads, and other infrastructure, and filled and blocked navigational shipping lanes. At least 57 people lost their lives, and damages exceeded $1 billion.

Along with transforming the landscape, the 1980 eruption left a legacy of heightened hazard in the form of a natural debris dam that blocked the outlet to Spirit Lake, a once picturesque recreational retreat at the foot of the mountain, which bore the full brunt of the eruption. With no outlet, the lake water rose, prompting fears that it would overtop and erode the blockage, and consequently release a cataclysmic flood that would transform into a lahar much larger than had occurred during the eruption, one that could devastate downstream communities.

In recognition of the hazard posed, the U.S. Army Corps of Engineers (USACE) in 1982 established an interim pumping facility to lower and stabilize the surface elevation of the lake while they considered a range of alternatives for providing a stable outlet. In 1984–1985, the Corps constructed a 2.6-km (8,500-ft) long, 3.4-m (11-ft) diameter, gravity-controlled tunnel with a regulating headgate to carry water out of Spirit Lake. The tunnel is bored through bedrock on the western side of Spirit Lake basin and delivers water to South Fork Coldwater Creek, a tributary of the North Fork Toutle River. Subsequent operations and maintenance of the tunnel (and funding thereof) were turned over to the USDA Forest Service (USFS), which manages the tunnel within the broader context of the Mount St. Helens National Volcanic Monument.

The tunnel is bored through both hard and decomposed volcanic bedrock, and it crosses faults, dikes, and shear zones, all of which were recognized at the time of construction. But because the tunnel was constructed rapidly under emergency conditions, it was under-reinforced along some of its length. In the 30+ years

following construction, the tunnel has maintained the level of Spirit Lake at a safe elevation, but several major repairs have been necessary, owing primarily to rock heave and support failure resulting from external pressures in the under-reinforced zones. Major repairs in 1995, 1996, and 2016 entailed extended closures of the tunnel, which allowed the lake to rise to precarious levels.

The most recent episode of tunnel distress, repaired in early 2016, highlights the need for a reliable outlet that does not require repeated and expensive interventions and extended closures. The USFS, working with the (USACE) and U.S. Geological Survey, developed, reviewed, and analyzed an array of options for a long-term plan to remove the threat of catastrophic failure of the tunnel. In this report, we (1) evaluate the potential for tunnel failure and a consequent catastrophic breaching of the blockage posed by the current tunnel infrastructure; (2) evaluate potential consequences to downstream communities and infrastructure in the event of a catastrophic breaching of the blockage; (3) evaluate potential risks associated with alternative lake outlets; and (4) identify data or knowledge gaps that need to be addressed to fully evaluate options available to management.

To do so, we provide context on eruptions and eruption impacts of Mount St. Helens, the character and stability of the debris blockage, and the history of the tunnel. We also identify hydrologic, seismic, and volcanic processes (and their derivative geomorphic hazards) that could potentially affect the tunnel or alternative outlets and consequently induce a breakout flood from Spirit Lake. We combine these analyses to assess the probability of a breakout flood arising from a range of plausible mechanisms by which the tunnel or an alternative lake outlet could fail, and we identify key uncertainties.

Mount St. Helens is by far the most active volcano in the Cascade Range. The 1980s eruptions and subsequent smaller eruptions in 2004–2008 were only the most recent in a long history of eruptive episodes spanning hundreds of thousands of years. Within this rich geological history, the cataclysmic 1980 eruption was average in terms of magmatic output and volcanic ash fall (tephra fall), but it had distinctive elements. The massive debris avalanche that dammed the outlet to Spirit Lake and other tributaries was large (2.5 km^3; 0.6 mi^3) but not unprecedented for this volcano. The blast PDC that flattened 550 km^2 (210 mi^2) of forest was not an event unique to the 1980 eruption, but its scale was unprecedented. Lahars that resulted from rapid melting of snowpack and glaciers swept all major channels draining the volcano. The voluminous (10^8 m^3) North Fork Toutle River lahar traveled at least 100 km (60 mi) and destroyed homes, bridges, roads, rail lines, and

other infrastructure. Though large and destructive, its volume, depth, and discharge pale in comparison to those of ancient lahars in the Toutle River valley caused by breaching(s) of an ancestral Spirit Lake about 2,500 years ago. The 1980 eruption and its aftermath transformed the landscape around Mount St. Helens, resulting in decades of accelerated erosion and problematic downstream sediment delivery. Though there has been much geomorphic and ecologic recovery of the landscape since the 1980 eruption, after three decades local communities and land managers still contend with geologic responses to events that happened within minutes on a single day.

The Spirit Lake blockage is a complex, irregular feature incorporating different stratigraphic units. It ranges in thickness from about 60 m (200 ft) to more than 150 m (500 ft). The bulk of the blockage that impounds Spirit Lake, derived from the debris-avalanche deposit, is composed predominantly of heterogeneous gravelly sand, with some silt and clay as well as rocks up to several meters in diameter. The rock from the mountain is highly shattered and incompetent, and few rocks from the mountain larger than a few meters wide remain. It is mantled by deposits of varying thickness from the blast PDC and subsequent small-to-moderate-sized pyroclastic flows and associated ash clouds. The blast deposit consists of a lower unit of friable, fragmented rock debris larger than coarse sand, overlain by an upper unit of silt- to sand-sized bits of rock. Its thickness within the Spirit Lake blockage ranges from a few centimeters to as much as 12 m (40 ft). The ash cloud deposit is composed mainly of pumiceous sand and silt, and across the blockage this deposit ranges from 1 to 12 m (3 to 40 ft) thick. All of the blockage material is highly erodible. The ash cloud deposit is fragile, subject to internal seepage erosion, and unlikely to hold back rising lake water. Hence the lowest elevation of the contact between the pyroclastic deposits (blast deposit, pyroclastic flow, or ash cloud) and the underlying debris-avalanche deposit (1069 m; 3,506 ft NGVD29) sets the effective elevation of the blockage crest. The blockage itself need not be overtopped to fail.

Both modeling and geologic evidence indicate that breaching of the Spirit Lake blockage would indeed be catastrophic. A 1983 modeling study predicted that flow depths of a lahar resulting from breaching of Spirit Lake could be 18 m (60 ft) at Castle Rock; 9 to 12 m (30 to 40 ft) at Toutle, Silver Lake, Kelso, and Longview; and 4.5 to 6 m (15 to 20 ft) at Toledo; discharges are predicted to be many tens of thousands of cubic meters per second (millions of cubic feet per second). Such a catastrophic event would likely lead to life loss and significant (>$1 billion) economic damages. These unimaginable inundation limits are consistent with mapped

elevations of ancient lahar deposits related to a breaching of an ancestral Spirit Lake about 2,500 years ago. Thus, as unimaginable as the predicted event may be, lahars of that magnitude related to a breaching of Spirit Lake have occurred in the Toutle-Cowlitz river system.

A detailed hydrologic analysis of the Spirit Lake basin and outlet system reveals both the soundness and vulnerabilities of the current infrastructure. Unlike the case of constructed dams, where infrastructure failure can lead to a sudden reservoir release, failure or blockage of the existing tunnel would not result in an immediate release of Spirit Lake. Instead, under most circumstances, many months would be required for the lake to fill to a level that would induce breaching of the blockage. Presumably, this lag time would allow for intervention to prevent a catastrophic lahar.

The currently configured outlet has worked well under most circumstances to pass flow from both normal and historically large storm events. Over its lifetime to date, lake levels have never exceeded the designated maximum safe operating elevation of 1055 m (3,460 ft). This elevation is conservative; based on current knowledge a potential failure of the debris blockage is remote unless the lake level approaches or exceeds 1069 m (3,506 ft), which is the lowest elevation of the pyroclastic-deposit (mostly ash cloud) contact along the blockage crest. Even a succession of very large storms would be unlikely to raise the lake from its normal operating level (1049 m; 3,440 ft) to this critical elevation, but they can significantly reduce its capacity to safely accommodate input from additional storms.

Despite the overall success of the existing tunnel, hydrological analysis has revealed the potential for a breakout flood to be significantly heightened after extended closure for repair. The highest lake levels over the past 32 years have been associated with three periods of closure for tunnel repair. During these periods, lake levels approached the designated maximum safe operating level. Inflows from storms associated with historically large floods can promote precariously high lake stands if they occur during times of closure, but they are not required to raise the lake level to the maximum safe operational threshold. Average inflows during closure can also raise the lake level. In contrast, when the tunnel is operable, inflows from storms associated with large floods have not resulted in high lake stands.

Routing of the probable maximum flood (PMF), the largest conceivable extreme hydrologic event, through the lake basin revealed that dangerously high lake levels could occur if a PMF-type event occurred while the lake was artificially elevated above its normal operating level by even a few meters. Although a PMF event has a very low annual exceedance probability (annual chance of occurring

≤0.001), the combination of a PMF and high antecedent lake level could be catastrophic. Of the alternative outlet options considered, only an open channel across the blockage would consistently maintain the lake level below its maximum safe operational threshold, because outflow through a channel scales directly with basin inflow and lake level. An open channel option also would limit the duration of lake high stands and would drain the lake more rapidly following large storms. There is a moderate to high degree of uncertainty about the absolute magnitude of the PMF, which could be resolved with additional analysis.

The Mount St. Helens region is subject to three principal types of regional earthquakes: great megathrust earthquakes along the Cascadia subduction zone, deep earthquakes formed within the subducting oceanic plate, and crustal earthquakes resulting from stresses induced by tectonic block rotation and plate interactions. The region also experiences earthquakes that have been triggered by volcanic eruptions. Historical earthquakes in the Pacific Northwest have been of the latter three varieties; there have been no great megathrust earthquakes since 1700, before Euro-American settlement. Neither a probabilistic seismic hazard analysis nor a site-specific seismic response analysis has been conducted for the Spirit Lake outlet project, but regional seismic hazards have been evaluated. The tunnel intake structure was designed with deep intraslab and volcano seismicity considered, seismicity reasonably well understood at the time of design. An initial assessment of the seismic stability of the debris blockage in 1981 concluded that it is stable under forces from the types of probable earthquakes known about at the time. However, neither Cascadia megathrust earthquakes (M8–9) nor smaller, but more local, earthquakes along the crustal St. Helens seismic zone were considered as potential contributors to seismic hazard.

Over its 300,000-year history, Mount St. Helens has erupted many volcanic products. It has erupted ash falls, pyroclastic density currents (flows and surges), lava domes, and lava flows, and has spawned lahars and debris avalanches. In the past 2,500 years, the volcano has variously erupted dacite, andesite, and basalt, sometimes all within the same eruptive period. Thus we cannot assume that eruptions of more effusive products (andesite, basalt) portend less explosive activity, or that more explosive dacite eruptions cannot eventually lead to effusive activity that can produce long-traveled lava flows. Unless a new vent opens on the flanks of the volcano, the present geometry indicates that future eruptive activity will be focused in the north-facing crater, and that areas north of the volcano will be at highest risk of impact from eruptions and associated eruptive products. The frequency of eruptions over the past 4,000 years, and distribution of eruptive products, indicate a high probability that the area immediately north of the volcano will be affected by

these processes. Lahars and ash falls are the most likely, with approximate annual exceedance probabilities of ≤ 0.01.

There are limited practical approaches to providing a safe lake outlet. The most promising approaches were evaluated using a USACE standardized dam-safety risk-assessment procedure. These alternatives are the existing tunnel, a fully rehabilitated tunnel, a conduit buried across the blockage, and an open channel across the blockage. Potential modes of failure of these drainage options were identified, and probabilities that those failure modes will lead to a catastrophic breaching of the blockage were broadly quantified. Lack of specific designs for several approaches limited risk quantification.

There is no risk-free way to remove water from the lake. A key finding is that all failure modes for all possible lake outlets involve cascading and coupled sequences of processes, each of which has a finite but difficult-to-quantify probability of occurrence. Therefore, the risk assessment of any mode involves a joint probability with a large degree of uncertainty. The alternative outlets considered required some external driver (i.e., landslide, volcanic flow, seismic event, extremely large inflow of water, or a volcanically induced wave on the lake) to render an outlet inoperable and allow for consequent lake rise and a breakout flood. But an additional potential failure mechanism for an open channel, which does not require a blocked outlet or a rising lake level, involves a volcanic or hydrologic event triggering development of upstream-migrating erosion. This erosion, which moves upstream as a steep step in the channel profile (known as a knickpoint), could undermine the channel bed and capture the lake.

Overall, the probability that failure of any alternative outlet will lead to catastrophic breaching of the blockage is generally remote to low (10^{-5} to $<10^{-6}$ annual probability). The probability that a potential blockage of an open channel would lead to a release of some lake water is greater (10^{-4} to 10^{-5} annual probability). In the latter case, the amount of water released would be determined by the volume impounded by an in-channel blockage, which would likely be far less than that associated with a full breaching of the Spirit Lake blockage. As noted above, however, the potential for conditions leading to catastrophic breaching is substantially heightened when the lake is at a precariously high stand induced by extended closure for tunnel repair. Thus there is an inevitable tradeoff between the risk associated with a conduit subject to the vagaries of infrastructure failure and an open channel subject to the vagaries of exposure to an active volcano and associated volcanic and geomorphic processes.

Beyond being susceptible to in-channel blockages, additional uncertainties and potential risks are associated with an open channel. The gradient between the

present normal operating level of Spirit Lake and the channels downstream of the blockage, into which an open channel would have to connect, is steep (roughly 2 to 3 percent). Along such a gradient, a simple Shields stress analysis shows that a flow depth as low as 1 m (3 ft) can transport particles as large as 50 cm (1.6 ft) diameter. Under much deeper flows (such as would be associated with a PMF-type event), particles a few meters (>10 ft) in diameter could be mobilized. Thus, an open channel would have to be designed as a heavily reinforced, engineered spillway to prevent failure, and possible lake capture, by incision or channel destabilization. Furthermore, a channel across the blockage would require excavation of a trench possibly tens of meters deep. As such, it would be subject to more potential failure modes than any of the other outlets considered. In addition to the erosive force of runoff from Spirit Lake, it would be subject to volcanic flows (lahars, pyroclastic flows, lava flows), to headward erosion of other channels across the debris avalanche, to extrafluvial landslides, or to fluvial geomorphic processes triggered by the dynamism of existing channels in this evolving landscape.

The semiquantitative risk assessment presented here is burdened by significant uncertainties. Events from three principal regional hazards (floods, earthquakes, eruptions) and their derivative geomorphic hazards are fundamentally stochastic. Physical properties of the blockage are known only moderately well, and its performance under some events (e.g., a Cascadia megathrust earthquake) is unknown. The dynamic landscape of the blockage has a propensity for rapid, substantial, and efficient geomorphic change. And the speed with which the lake can rise to compromising elevations, especially if it is already in an elevated state, may in some circumstances hinder intervention to prevent an ultimately catastrophic failure. These uncertainties must be borne in mind when contemplating the utility of any potential drainage outlet.

Contents

Chapter 1: Introduction and Context

The landscapes of the U.S. Pacific Northwest are known worldwide for their magnificent and distinctive volcanoes, cascading rivers, clear mountain lakes, and lush forests. Yet this landscape comes with a price. Intrinsic to the scenery and woven into the history of the region are a cornucopia of natural hazards: volcanic eruptions, earthquakes, landslides, forest fires, and floods. Living in this corner of the globe inevitably means living with the risks posed by such hazards and coming to terms with the uncertainties of their episodicity.

Nowhere were the interconnected linkages between hazards and risks more evident than on May 18, 1980, when Mount St. Helens erupted. The eruption began with a colossal failure of the volcano's north flank. The resulting rockslide-debris avalanche occurred as a series of slide blocks that gutted the volcano. As the slide blocks moved off the volcano, volatiles released from the suddenly unroofed magmatic and hydrothermal systems unleashed a massive horizontal explosion that initiated a hot, sweeping, topographically unconstrained pyroclastic density current (hereafter called the blast PDC). Snow and ice melted by the blast PDC, and dewatering of the debris-avalanche deposit, generated large lahars (volcanic debris flows) that raced down all major channels draining the volcano. These flows washed away houses, bridges, and roads along the affected river channels, and the largest flow traveled all the way to the Columbia River, where it blocked the navigational channel. Later that day, partial collapses of the billowing eruption column that developed shortly after the onset of eruption produced small to moderate pumiceous pyroclastic flows—dense, hot flows of coarse pumice, ash, and gas—that spewed from the newly created crater and mantled the freshly deposited avalanche and blast PDC sediment at the northern foot of the volcano.

In all, the eruption caused 57 fatalities and more than $1 billion in damages. Subsequent eruptions in summer 1980 added additional ashy sediment to the mantle of pyroclastic debris atop the avalanche deposit. Subsequent eruptions in the 1980s generated lahars that both eroded and deposited sediment across the proximal reaches of the avalanche deposit.

Spirit Lake, formerly a picturesque lake nestled at the northern foot of Mount St. Helens, bore the full brunt of the eruption. Part of the debris avalanche swept through Spirit Lake basin, raising the lake's surface elevation by 60 m (200 ft), nearly doubling its footprint. The avalanche also reduced the maximum depth of the lake by 30 m (100 ft) and blocked its outlet to the North Fork Toutle River. Thus, the Spirit Lake watershed became a closed basin. Water and snowmelt from the hillslopes surrounding the lake could no longer drain into the North Fork Toutle River but instead could only raise the lake level.

Following the eruption, interconnections among regional hazards and risks in the landscape became more focused. A legacy of the eruption that swiftly became apparent was a new and potentially catastrophic hazard: a sudden release of Spirit Lake caused by rising water possibly leading to breaching and erosion of the blockage. The resulting breakout flood would be disastrous for the downstream communities of Castle Rock, Kelso, and Longview. An emergency presidential order signed August 19, 1982, directed the Federal Emergency Management Agency (FEMA) to develop a mitigation strategy to prevent breaching of the blockage. FEMA, in turn, directed the U.S. Army Corps of Engineers (USACE) to design and construct a permanent outlet for the lake. In 1982, the USACE established an interim pumping facility to reduce and stabilize the lake level while considering a range of alternatives for providing an outlet. In 1984–1985, the Corps constructed a 2.6-km (8,500-ft) long, 3.4-m (11-ft) diameter, gravity-controlled tunnel with a regulating headgate to carry water out of Spirit Lake. The tunnel is bored through bedrock on the western side of the Spirit Lake basin and delivers water to South Fork Coldwater Creek, a tributary to the North Fork Toutle River. Subsequent operations and maintenance (and funding thereof) of the tunnel was turned over to the USDA Forest Service (USFS), which manages the tunnel within the broader context of the Mount St. Helens National Volcanic Monument.

The tunnel is bored through Tertiary tuffaceous and mafic bedrock. It crosses faults, dikes, and shear zones, all of which were recognized at the time of construction. But because the tunnel was constructed under emergency conditions, and owing to limitations of the tunnel boring machine that was used, the tunnel was under-reinforced along some of its length. In the 30+ years following construction, several major repairs have been necessary, owing primarily to rock heave and support failure as a result of external pressures. Major repairs in 1995, 1996, and 2016 entailed extended closures of the tunnel, which allowed the lake to rise to precarious levels. Had the lake risen a few meters higher during or after these closures, the consequences could have been severe.

The most recent episode of tunnel distress, repaired in early 2016, highlights the need for a reliable outlet that does not require repeated and expensive interventions. In September 2015, members of Congress in Washington state (Senators Maria Cantwell and Patty Murray, and Representative Jaime Herrera Beutler) wrote to the Chief of the Forest Service, the Assistant Secretary of the Army (Civil Works), and the director of the U.S. Department of the Interior Geological Survey (USGS), requesting that the USFS "…fund and develop a report in cooperation with the USACE and USGS that will review and analyze an array of options for a long-term plan that removes the threat of catastrophic failure of the tunnel and takes the unstable nature of the surface geology into account."

Purpose and Scope

This report is a direct response to the congressional request. It is also part of a broader review of hazard mitigation in the Toutle River watershed, a review that also includes an analysis by the National Academies of Sciences, Engineering, and Medicine (see http://www8.nationalacademies.org/cp/projectview.aspx?key=49785). The specific objectives of our analysis are:

- Evaluate the potential for tunnel failure and consequent catastrophic dam breach posed by current conditions and the configuration of both the tunnel and the debris blockage.
- Evaluate potential consequences to downstream communities and infrastructure in the event of a catastrophic breaching of the blockage.
- Evaluate potential risks associated with alternative lake outlets.
- Identify any data or knowledge gaps that would need to be addressed to fully evaluate the options available to management.

To provide context for understanding the blockage and remediation efforts, we begin with a summary of the effects and consequences of the 1980 eruption, a description of the Spirit Lake blockage, and a review of the history and operation of the drainage tunnel. We then provide a summary of regional hydrology, seismicity, and volcanic processes that could affect the Spirit Lake basin. We use this context to examine a range of mechanisms by which the tunnel, potential alternative outlets, or the blockage could fail, and consider the consequences of failures. Specifically, we explore how key hydrologic, volcanic, and seismic processes are likely to interact with built infrastructure. We highlight key lessons that have emerged which provide context and guidance for any decisions regarding a permanent lake outlet, but we do not make specific recommendations as to which alternative outlet is the best solution. We conclude by identifying critical knowledge gaps and uncertainties that may need to be resolved to move forward with decisions on the long-term management of the lake.

Sources of Information

In this report, we rely primarily on existing public information relevant to the management issues at Spirit Lake. To provide a foundation for a risk assessment of the existing infrastructure and potential alternative outlets, we arranged for the USACE Portland District Office to conduct a potential failure mode analysis (PFMA), including a semiquantitative risk assessment (SQRA). Both the PFMA and SQRA are formal, facilitated processes that USACE and the U.S. Bureau of Reclamation (BOR) use to assess the potential for and probability of dam failures. The debris

blockage at Spirit Lake is not a constructed dam, nor is it operated like one. Unlike a constructed dam, the failure of which could lead to an immediate downstream catastrophe, the Spirit Lake outlet infrastructure and the lake blockage are a multicomponent system; failure of the lake outlet does not result in an immediate or necessarily imminent failure of the blockage. The ultimate failure of the debris blockage is a two-step process: first, the outlet for Spirit Lake must fail so that water cannot exit the lake, then the lake must rise over a span of months to a level that induces breaching of the blockage. Nevertheless, the PFMA process provides a means of assessing potential risk. Time and data constraints did not allow for a fully probabilistic PFMA to be conducted; instead, the SQRA is a more generalized but still quantitative analysis of potential failure mechanisms and their risks. The PFMA was conducted from February 29 to March 7, 2016, at the USACE Portland District office. Both senior authors of this report participated in this process. Other agencies participating in the PFMA included representatives from USACE, BOR, and USFS. The panel conducting the analysis included geotechnical, structural, hydrologic, and hydraulic engineers; geologists; geomorphologists familiar with fluvial and volcanic processes; and an economist. For this report, we draw on the outcome of the PFMA/SQRA analysis along with other published sources.

Chapter 2: Geological History and Background of Mount St. Helens

Mount St. Helens is by far the most active of the major volcanoes in the Cascade Range of the Pacific Northwest (fig. 2-1). The volcano as we see it is a youthful feature on the landscape. The bulk of the modern edifice above 1800 m (5,900 ft) altitude prior to the major 1980 eruption was constructed mostly over the past 4,000 years, but a volcanic center has existed there for at least 300,000 years (Clynne et al. 2005, 2008). During the long period of intermittent volcanism that extended from about 300,000 to 2,800 years ago (fig. 2-2), Mount St. Helens erupted mostly dacitic products (containing 63 to 68 percent silicon dioxide [SiO_2]) and consisted of clusters of dacite domes with summit altitudes ranging from about 1800 to 2100 m (5,900 to 6,900 ft) (Clynne et al. 2005, Crandell 1987, Mullineaux and Crandell 1981) (fig. 2-2). By about 2,500 years BP, the volcano began erupting andesite (53 to 63 percent SiO_2) and basalt (<53 percent SiO_2) as well as dacite (Clynne et al. 2008, Crandell 1987, Mullineaux and Crandell 1981). By about 1750 CE the volcano had attained its pre-1980 form with a summit altitude of 2950 m (9,675 ft) (Clynne et al. 2005) (fig. 2-2). In the mid-1800s, travelers witnessed dome-building eruptions on the volcano's flank (Yamaguchi et al. 1995) (fig. 2-3) (see chapter 7 for further

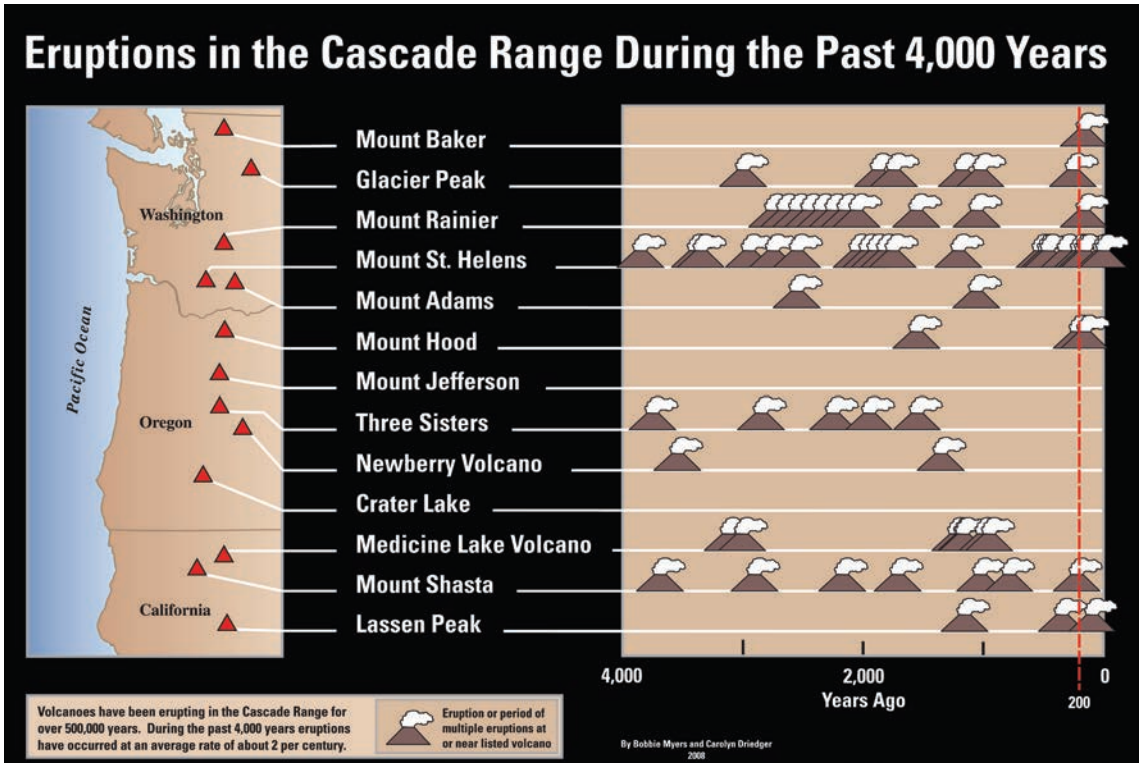

Figure 2-1—Schematic representation of eruption frequency of volcanoes in the Cascade Range (Myers and Driedger 2008).

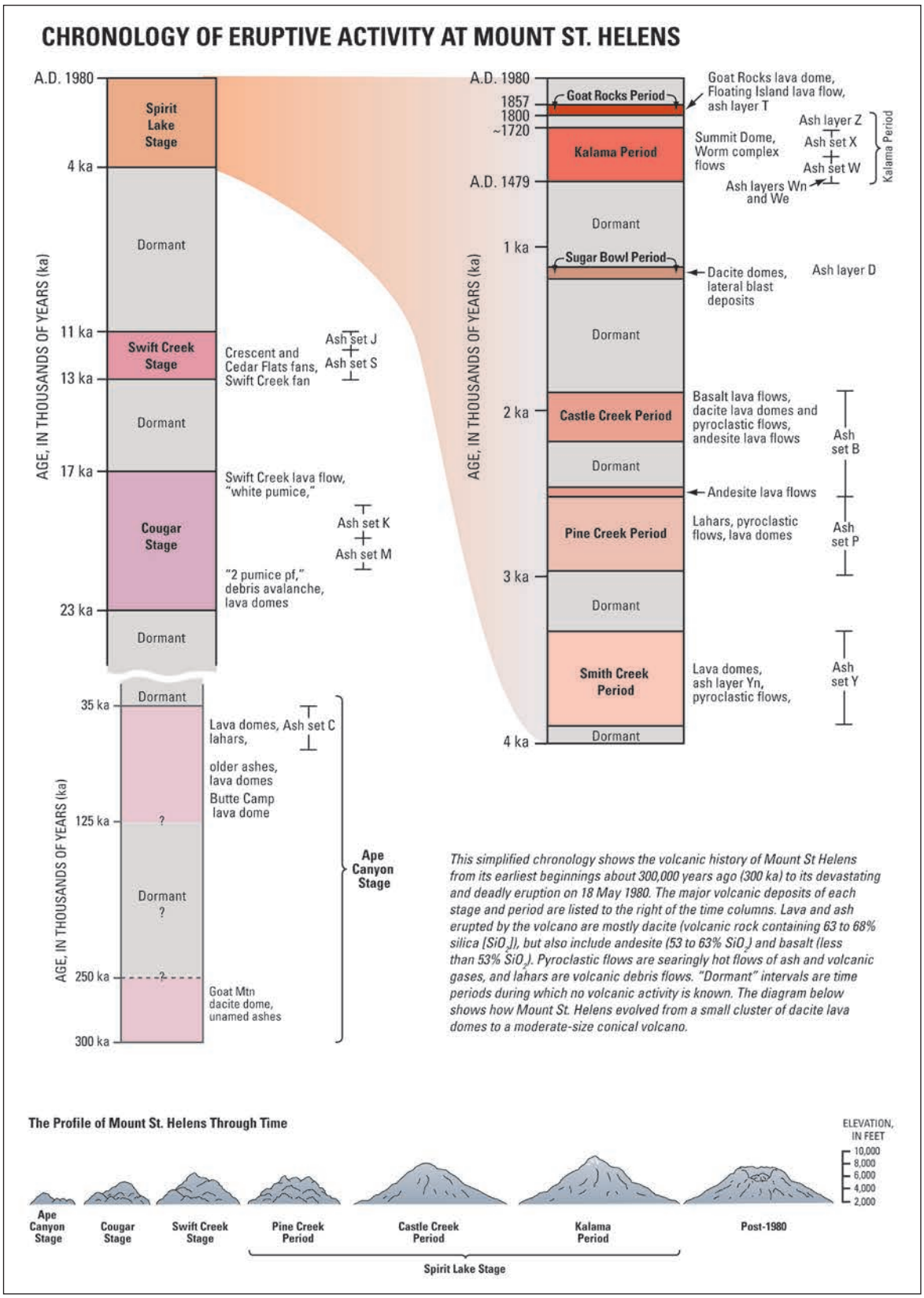

Figure 2-2—Chronology of eruptive activity at Mount St. Helens, and profiles of the volcano through time (from Clynne et al. 2005).

Figure 2-3—North-flank eruption of Mount St. Helens painted by Canadian artist Paul Kane. Although Kane used much artistic license to create this studio painting, he did witness an eruption of the volcano on March 26, 1847 (see Yamaguchi et al. 1995). Published with permission of the Royal Ontario Museum© ROM.

details). The volcano is underlain by both shallow (2 to 3.5 km [~1 to 2 mi] below sea level) and deep (>7 km; >4 mi) zones of magma storage that vent intermittently to the surface (Kiser et al. 2016, Pallister et al. 1992, Waite and Moran 2009).

The volcano sits upon a deeply eroded terrain of gently folded and altered volcanic and plutonic rocks that represent the Tertiary Cascade magmatic arc (Evarts and Swanson 1994, Evarts et al. 1987). The arc is associated with subduction of the oceanic Juan de Fuca plate beneath the continental North American plate. But much of that older terrain is deeply buried beneath a thick fill of shed volcanic detritus (fig. 2-4). The volcano lies along the strike of the 90-km (55-mi) long St. Helens seismic zone, a crustal earthquake zone defined by small- to moderate-magnitude (M2.5 to 5.5) earthquakes (Parsons et al. 1998, Stanley et al. 1996, Weaver and Smith 1983) (see chapter 6 for further details). Pringle (2002) provided a synopsis of the roughly 40 million years of volcanic activity in the region prior to the 1980 eruption.

The 1980s Eruptions

The cataclysmic eruption that caused the dramatic landscape change at Mount St. Helens—and which led to the hazard mitigation issues surrounding Spirit Lake and the Toutle River valley—occurred on May 18, 1980. Between March and May

Figure 2-4—Mount St. Helens area before the 1980 eruption. Dashed lines denote the approximate limit of the volcaniclastic debris apron. Fragmental deposits derived from Mount St. Helens extend down all drainages (adapted from Clynne et al. 2008).

1980, dacite magma intruded the cone and caused severe deformation of the volcano's north flank (fig. 2-5). During April and May 1980, the flank of the volcano deformed horizontally at rates to 1.5 to 2.5 m (5 to 8 ft) per day (Lipman et al. 1981) and formed the so-called "north flank bulge." The eruption consisted of an ensemble of volcanic processes that reconfigured the landscapes of several watersheds (Lipman and Mullineaux 1981) (table 2-1). Within minutes to hours of the eruption's onset, hundreds of square kilometers of landscape were variously transformed by a voluminous debris avalanche, a directed pyroclastic density current (hereafter called the blast PDC), lahars (volcanic debris flows), pumiceous pyroclastic flows related to fountaining and collapse of the vertical eruption plume, and extensive tephra fall (figs. 2-6 through 2-9) (see box 1). The nature and severity of impacts in a particular watershed depended on the disturbance process(es) and proximity to the volcano. Multiple processes affected both hillslopes and channels in basins broadly north, east, and within 10 km (6 mi) of the volcano, whereas single processes chiefly affected either hillslopes or channels in basins to the west, south, and those beyond 10 km (6 mi) from the volcano.

The eruption began at 8:32 a.m. with a colossal failure of the volcano's north flank (Voight 1981). The resulting debris avalanche released as a series of slide blocks (Glicken 1996) (fig. 2-5) that was famously captured in a sequence of iconic photographs (see Voight 1981). Slide block I consisted chiefly of the upper outer skin of the edifice and was composed mainly of mafic rocks (andesite, basaltic andesite, and basalt) that formed much of the upper third of the volcano, modern dacite of the summit dome, and some of the older dacite that composed the interior of the volcano. Slide block II began moving before the first block had completely left the volcano. It gutted more of the interior of the volcano. It was in motion when volatiles released from the suddenly unroofed magmatic and hydrothermal systems ripped through the moving slide blocks, triggering the devastating blast PDC. A further large block or series of retrogressive slides, known as slide block III, followed slide block II and occurred coincident with the blast PDC. This block completed the gutting of the volcano and produced the gross edifice morphology that we see today, including a steep-walled, U-shaped (in plan view) crater.

The debris avalanche deposited 2.5 km^3 (0.6 mi^3) of poorly sorted rock, soil, ice, and organic debris in the upper North Fork Toutle River valley (figs. 2-6, 2-7, 2-8A, and 2-10) (Glicken 1996); buried 60 km^2 (23 mi^2) of the valley to a mean depth of 45 m (150 ft); truncated tributary channels; created new or enlarged existing lakes behind tributary blockages; and disrupted the watershed's drainage pattern (Janda et al. 1984, Lehre et al. 1983). Part of the debris avalanche swept through the Spirit Lake basin, and part rode up and over Johnston Ridge and

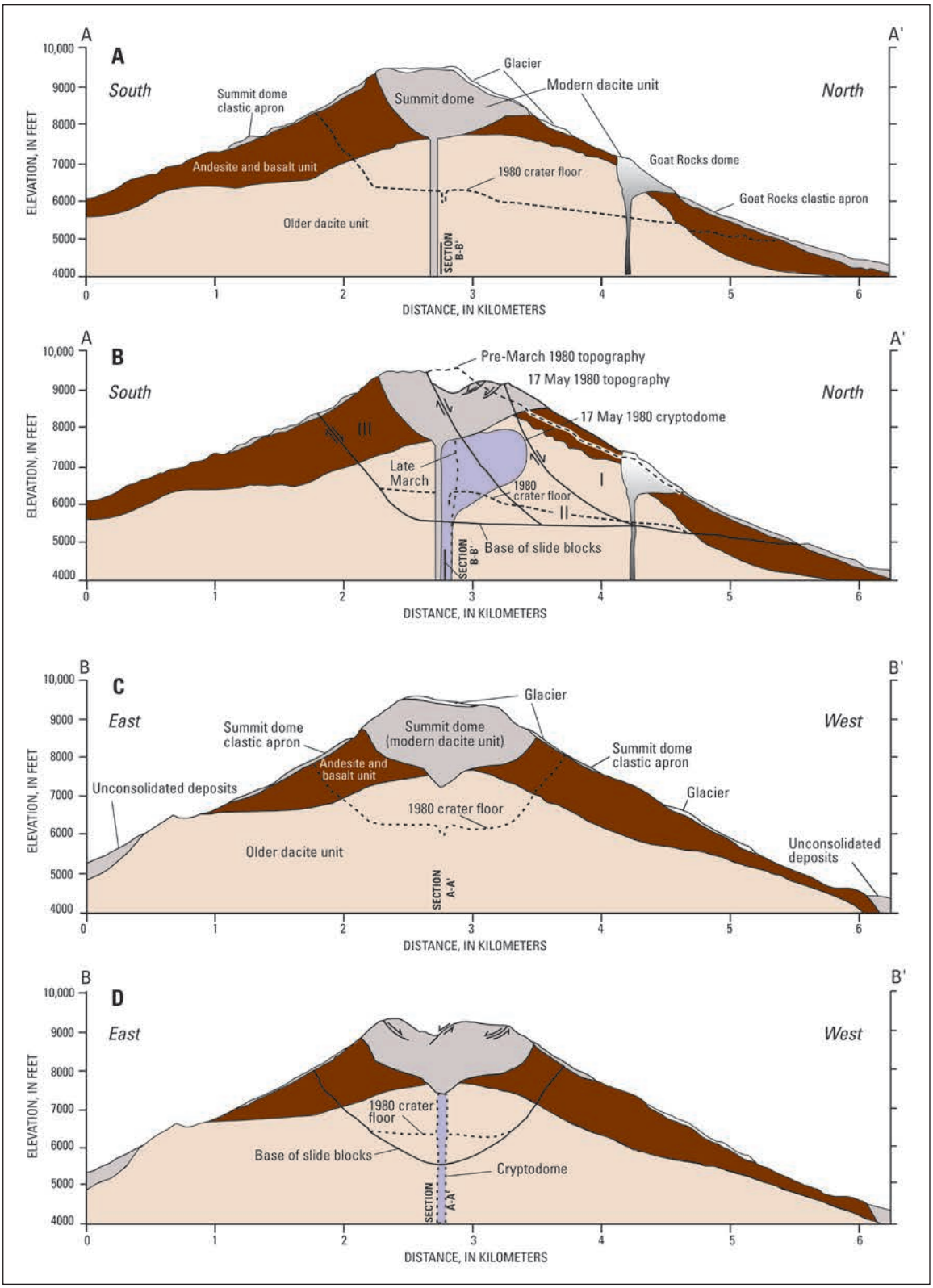

Figure 2-5—Schematic cross sections through Mount St. Helens (from Glicken 1996): (A) south-north before 1980; (B) south-north on May 17, 1980, the day before its cataclysmic eruption; (C) east-west before 1980; (D) east-west on May 17, 1980. Note the generalized distribution of rock types and the approximate geometry of the 1980 slide blocks.

Table 2-1—Characteristics of deposits from the May 18, 1980, Mount St. Helens eruption[a]

Event	Volume of uncompacted deposit	Area affected	Deposit thickness
	Cubic kilometers	*Square kilometers*	*Meters*
Debris avalanche	2.5	60	10–195
Blast PDC	0.20	550	0.01–1
Lahars	0.05	50	0.1–3
Pyroclastic flows	0.12	15	0.25–40
Proximal tephra fall	0.1	1100	>0.01

PDC = pyroclastic density current.

[a] Data are from Lipman and Mullineaux (1981).

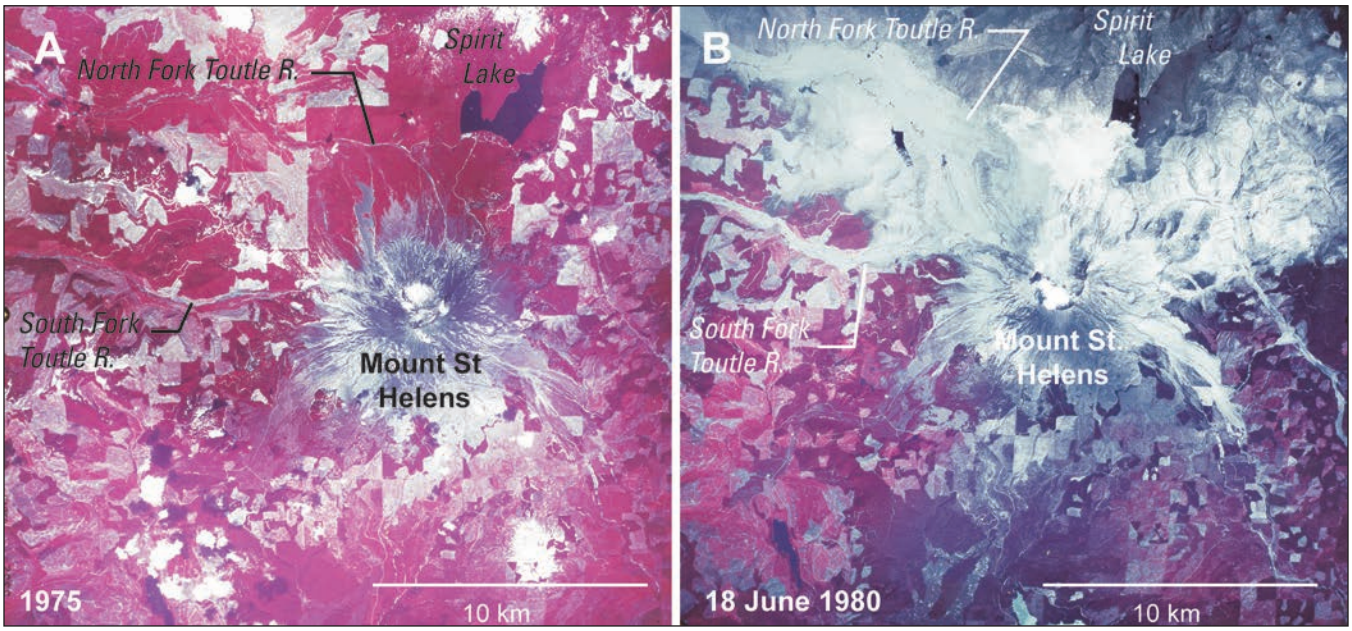

Figure 2-6—High-altitude infrared images of Mount St. Helens from (A) 1975, and (B) June 18, 1980. Source: U.S. Geological Survey National High Altitude Photographs.

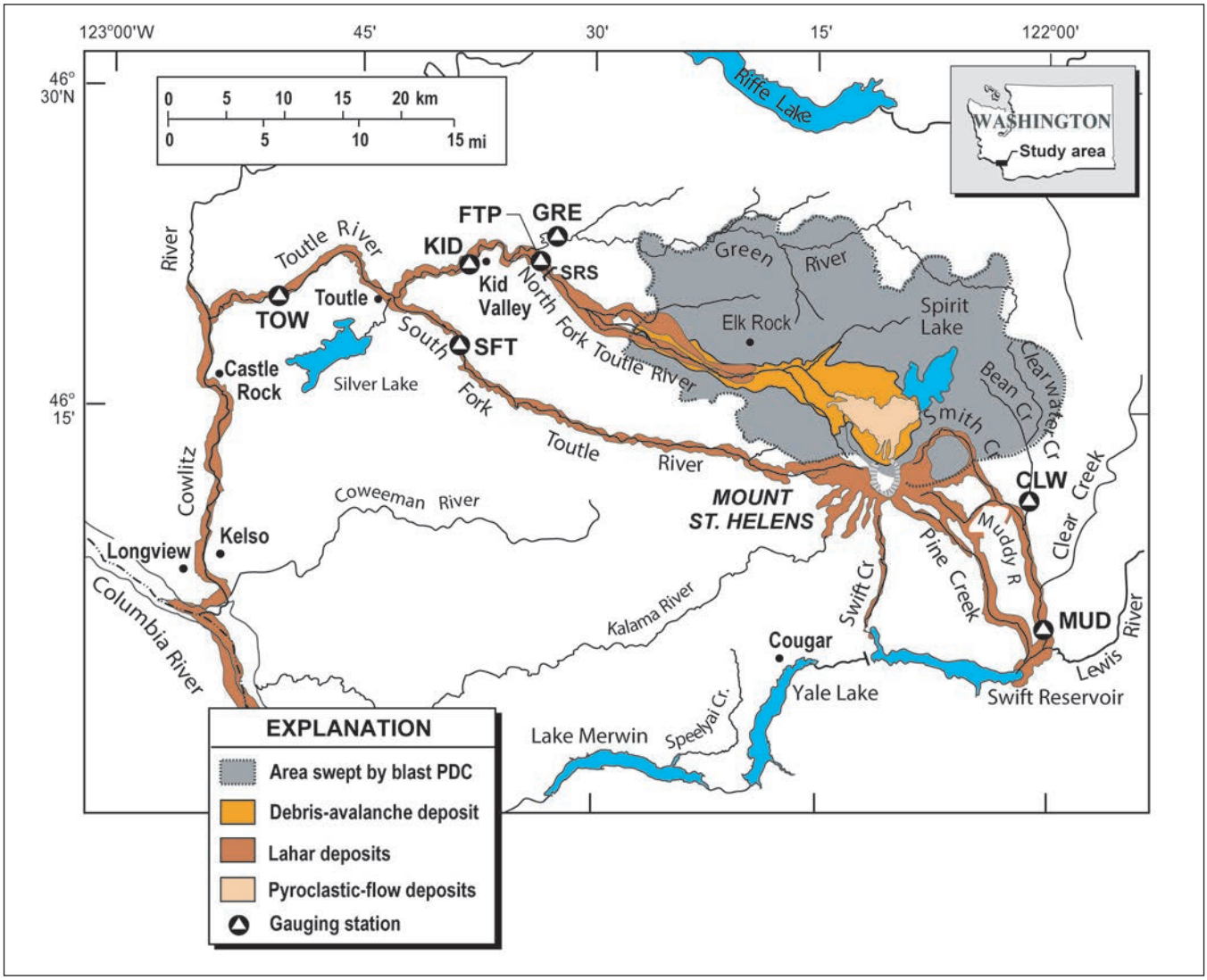

Figure 2-7—Distribution of major volcaniclastic deposits of the 1980 eruption and locations of gauging stations (e.g., Toutle River, TOW); SRS identifies the U.S. Army Corps of Engineers sediment retention structure. PDC = Pyroclastic density current; CLW = Clearwater creek; FTP = North Fork Toutle River; GRE = Green River; KID = North Fork Toutle River; MUD = Muddy River; SFT = South Fork Toutle River.

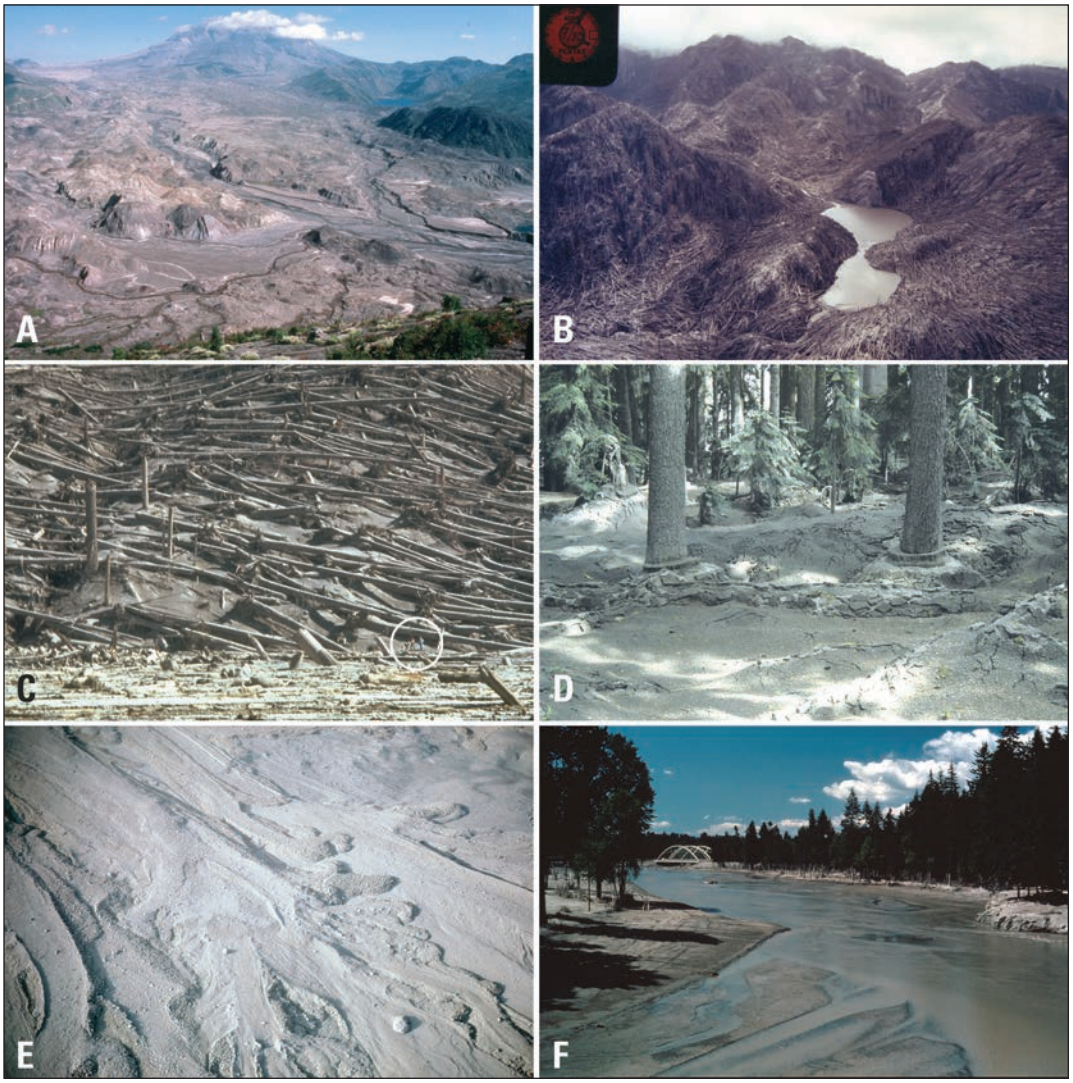

Figure 2-8—Images of landscape disturbances caused by the May 18, 1980, eruption: (A) hummocky debris avalanche in upper North Fork Toutle valley; field of view is about 4 km (2.5 mi) across; U.S. Geological Survey (USGS) photograph. (B, C) tephra-mantled hillslopes with trees blown down by blast pyroclastic density current (PDC). Note people in circle for scale. USGS, July 6, 1980, and September 24, 1980. (D) Tephra-mantled landscape east of volcano beyond zone of blast PDC, summer 1980. Tree trunks about 0.5 m (1.5 ft) across. Photograph courtesy of Joe Antos, University of Victoria. (E) Pyroclastic flow deposits mantling debris avalanche in upper North Fork Toutle valley. Individual flow lobes about 30 to 50 m (100 to 150 ft) across. USGS, October 4, 1980. (F) Lower Toutle River valley transformed from cobble-bedded channel to sand-bedded channel by large lahars. Field of view about 80 m (260 ft) across. USGS, July 6, 1980.

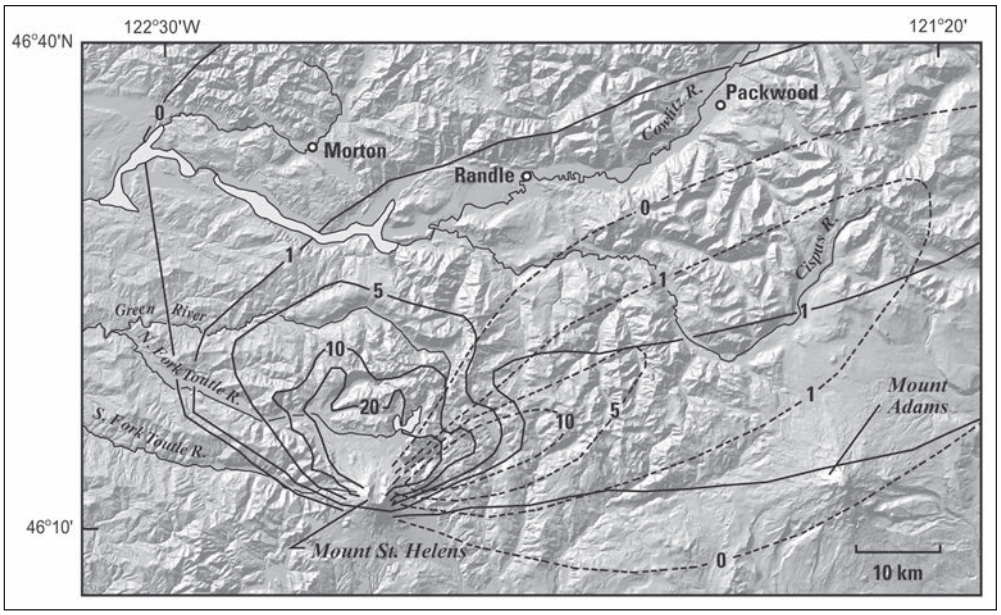

Figure 2-9—Isopach map of May 18, 1980, blast PDC, including fall facies (solid lines), and proximal Plinian tephra fall (dashed lines); values in centimeters. Map adapted from Waitt and Dzurisin (1981).

Box 1

Volcanic Process Terminology

Tephra—A general term for volcanic particles of any size, shape, or composition ejected from volcanoes.

Tephra fall—Rain of volcanic particles falling to the ground after eruption, also known as ash fall or airfall tephra.

Pyroclastic density current—Hot, ground-hugging mixture of particles and gas remaining denser than the surrounding atmosphere and moving under the influence of gravity. Individual currents typically exhibit a diversity of flow regimes from dense, granular flows (pyroclastic flow) to dilute, turbulent suspensions (pyroclastic surge).

Debris avalanche—Flowing mixture of unsaturated or partially saturated volcanic particles and water (± ice) initiated by the gravitational collapse of part of a volcanic edifice.

Lahar—Water-saturated flow of volcanic rock particles and water (± ice). A lahar having >50 percent solids by volume is termed a debris flow; one having roughly 10 to 50 percent solids by volume is termed a hyperconcentrated flow. Flow type can evolve with time and distance along a flow path. Muddy water floods typically are <10 percent solids by volume.

Grain size terminology can vary depending on one's scientific background. Some researchers use sedimentological terms based on the Wentworth grain-size classification (Folk 1980), and others use volcanological terms (White and Houghton 2006).

Box 1 (continued)

Grain size terms used in volcanology and sedimentology:

Diameter	Volcanology	Sedimentology
>64 mm	Blocks, bombs[a]	Cobbles, boulders
2–64 mm	Lapilli	Granules, pebbles
<2 mm	Ash	Sand
<250 μm	Fine ash	Fine sand to silt

[a] Bombs have fluidal morphology.

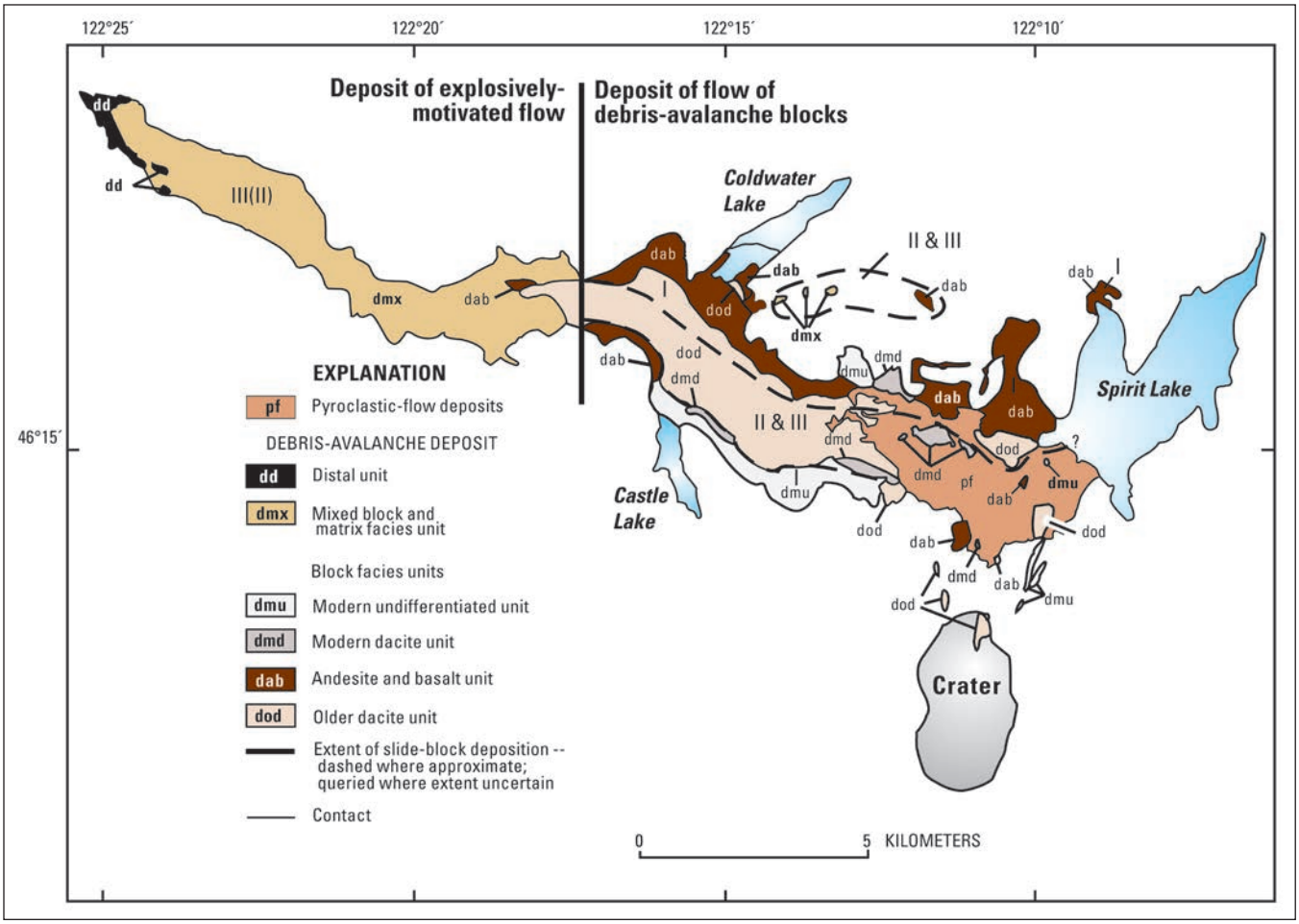

Figure 2-10—Generalized lithologic map of debris-avalanche deposit, showing interpretations of areas of deposition of slide blocks (see fig. 2-5). (II) indicates primarily slide block III but includes subordinate volume of slide block II (Source: Glicken 1996).

through South Coldwater Creek valley, but the bulk buried the upper North Fork Toutle valley (fig. 2-11). The part that swept through Spirit Lake basin raised the lake level by 60 m (~200 ft), nearly doubled the lake's footprint (from ~5 km^2 to 9 km^2; 1.9 to 3.5 mi^2), reduced maximum lake depth from 60 m (~200 ft) to 30 m (~100 ft) (fig. 2-12), and completely blocked its outlet.

The blast PDC is the event that devastated ~550 km^2 (~210 mi^2) of rugged, forested landscape in a roughly 180-degree arc north of the volcano, and blanketed the terrain with up to 1 m (3 ft) of gravel- to silt-sized tephra (figs. 2-7, 2-8B, and 2-8C) (Hoblitt et al. 1981, Waitt 1981). Close to the volcano, the blast PDC (and the debris avalanche) stripped vegetation and soil from the landscape. With increasing distance from the volcano, it toppled but did not remove trees. In the basins of Green River, Smith Creek, Bean Creek, and upper Clearwater Creek (fig. 2-7), the blast PDC ravaged hillslopes but had relatively little impact on stream channels aside from locally toppling mature trees into them.

Extensive lahars (imagine rivers of slurry or wet concrete) swept all major channels draining the volcano and deposited tens to hundreds of centimeters of gravelly sand on valley floors and flood plains. The voluminous (10^8 m^3) and

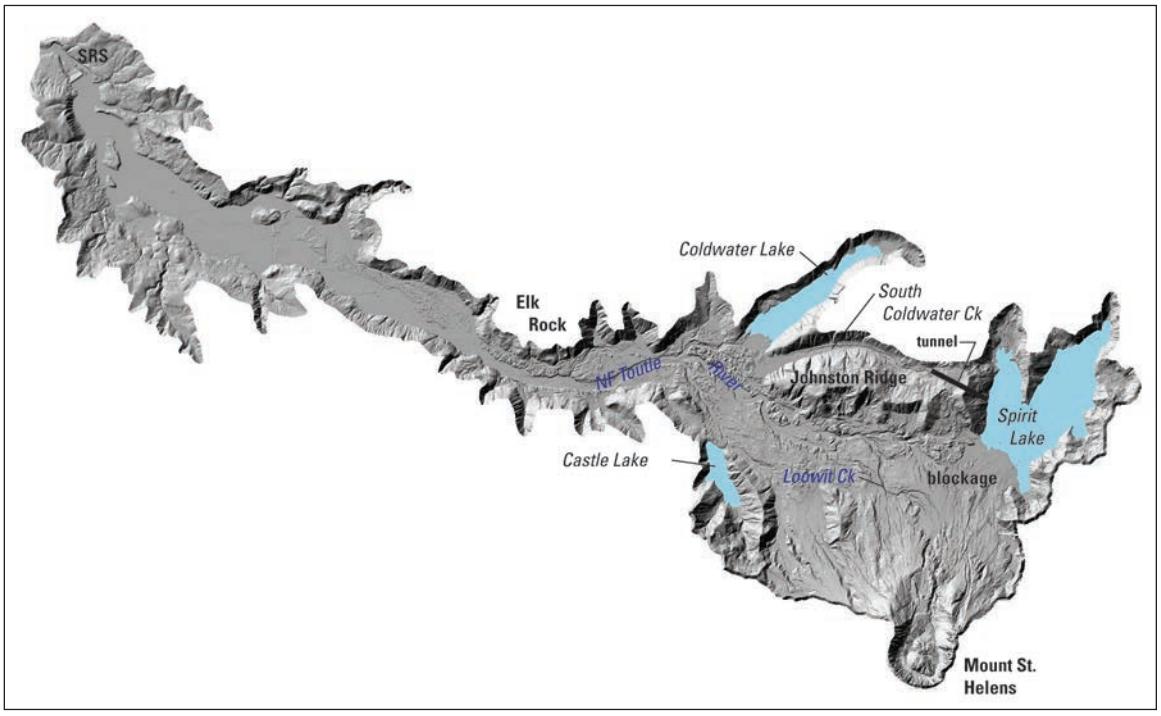

Figure 2-11—Digital elevation model of upper North Fork Toutle River valley derived from an airborne LiDAR survey in 2009. Note locations of Spirit Lake, blockage, tunnel, and sediment retention structure (SRS). The tunnel extends from the west side of Spirit Lake through Harry's Ridge and exits into South Coldwater Creek.

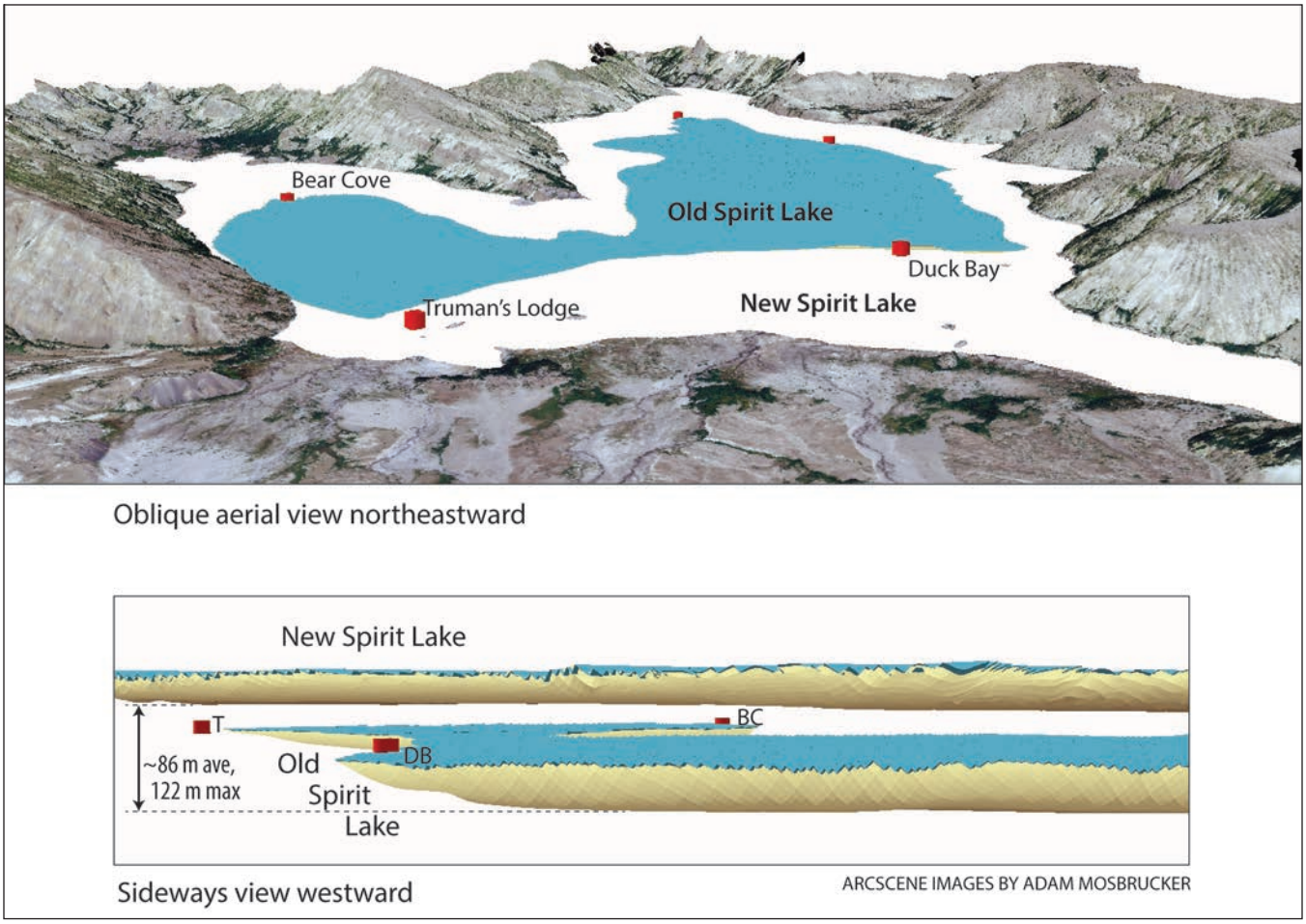

Figure 2-12—Oblique view of Spirit Lake derived from 2009 LiDAR DEM comparing footprint of post-1980 lake to that of pre-1980 lake. Lower image shows south-north section through the lake showing change in elevation of lake bed and surface. T = Truman's lodge; DB = Duck Bay; BC = Bear Cove.

highly destructive North Fork Toutle lahar traveled at least 100 km (60 mi) along the North Fork Toutle, Toutle, and Cowlitz Rivers (fig. 2-7) (Fairchild 1987, Janda et al. 1981, Major et al. 2005). On the volcano's western, southern, and eastern flanks, large but less voluminous (to 10^7 m^3) lahars traveled up to tens of kilometers (Fairchild 1987, Janda et al. 1981, Major and Voight 1986, Pierson 1985, Scott 1988a, Waitt 1989). Notably large flows swept the channels of the South Fork Toutle and Muddy Rivers (fig. 2-7). Overall, the lahars bulldozed riparian corridors, straightened and smoothed river channels (fig. 2-8F), and transformed them from sinuous, gravel-bedded, pool-riffle to streamlined, sand-bedded systems.

The fallout from a billowing eruption column, which developed shortly after the onset of the eruption, blanketed proximal areas east-northeast of the volcano with gravelly to silty pumice fallout as thick as tens of centimeters (Waitt and Dzurisin 1981) (fig. 2-9). Partial collapses of the eruption column also generated pumiceous

pyroclastic flows that accumulated atop the debris-avalanche deposit (figs. 2-7 and 2-8E). Close to the volcano, tephra fall and pyroclastic flows augmented deposition on an already devastated landscape, but beyond 15 km (10 mi) east of the volcano, accumulations of fallout tephra caused the primary disturbance in many watersheds (figs. 2-8D and 2-9) (Sarna-Wojcicki et al. 1981, Waitt and Dzurisin 1981). Fallout greater than ~5 cm (2 in) thick significantly damaged the forest understory (Antos and Zobel 2005).

Deposits from several smaller eruptions in 1980 augmented the landscape disturbances caused by the May 18 eruption. Eruptions from late May to October 1980 deposited additional pyroclastic fill atop the debris-avalanche deposit and veneers of fallout tephra in neighboring watersheds. Minor eruptions from 1980 through 1986 built a 90-million-m^3 (120-million-yd^3) lava dome in the volcano's crater and triggered a few snowmelt-induced lahars (the largest ~10^7 m^3) (fig. 2-13) and sediment-laden water floods (Major et al. 2005, Pierson 1999, Waitt et al. 1983). As volcanic activity waned, snow and rock accumulated in the shaded rear of the volcano's crater and by the late 1990s had formed a 120-million-m^3 (~160-million-yd^3) debris-laden glacier that wrapped around the lava dome (fig. 2-14) (Schilling et al. 2004).

2004–2008: A Volcano Rekindled

In 2004, the volcano erupted again. Seismic unrest that began on September 23, 2004, rapidly culminated in localized deformation within the volcano's crater, phreatic (water-dominated) explosions, and ultimately extrusion of solidified lava that formed another lava dome (Scott et al. 2008). Solidified lava spines first breached the surface on October 11, 2004. For the 39 months that followed, the dome grew continuously through a combination of solidified lava extrusion and endogenous intrusion. The 2004–2008 eruption produced a series of solidified lava spines that grew, crumbled, and migrated about an ice-filled moat between the 1980s lava dome and the south crater wall (fig. 2-15) (Major et al. 2008, Schilling et al. 2008, Scott et al. 2008, Vallance et al. 2008). In January 2008, the dome stopped growing, and associated seismicity, local deformation, and gas efflux diminished to very low levels (Dzurisin et al. 2015).

Emplacement of the 2004–2008 lava dome complex deformed Crater Glacier and caused its arms to advance northward toward the crater mouth. As of 2016, the glacier surrounds both the 1980s and 2000s dome complexes, and its snout has advanced to the headwaters of the channel system draining the crater.

Figure 2-13—Oblique aerial photograph of March 1982 snowmelt-triggered lahar. View to south. The flow originated after a water flood from the crater entrained sediment along the steep north flank and increased its ratio of solids to fluid. Most of the flow traveled west (right) down the North Fork Toutle valley, but a substantial fraction flowed into Spirit Lake (on left). U.S. Geological Survey, March 21, 1982.

Figure 2-14—Oblique aerial view toward the southwest of Mount St. Helens crater showing 1980s lava dome and glacier that developed in rear of crater. U.S. Geological Survey, approximately October 2000.

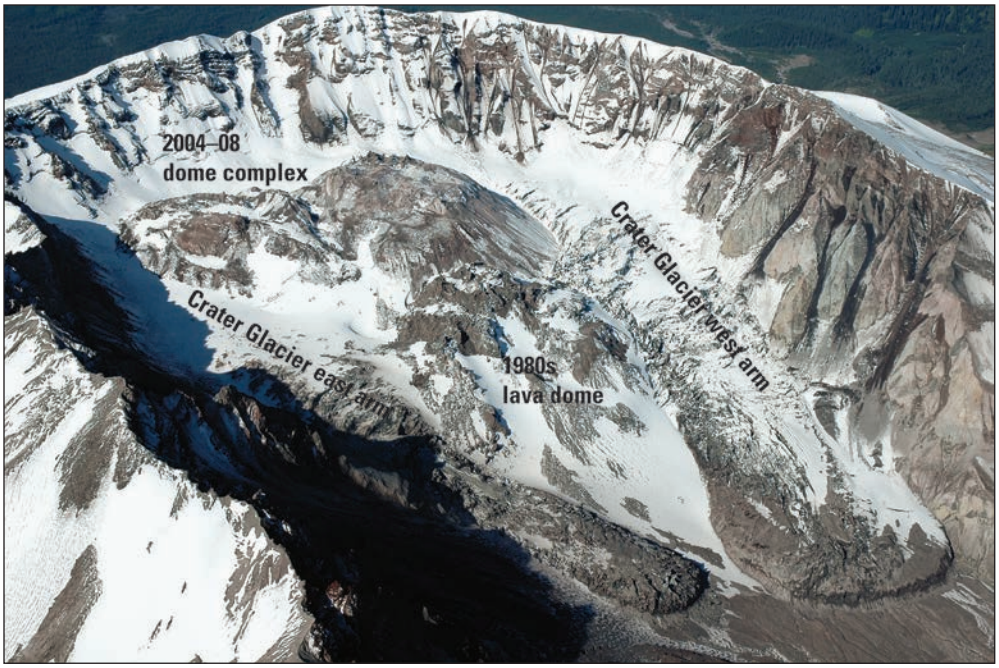

Figure 2-15—Oblique aerial view toward the southwest of Mount St. Helens crater showing 1980s lava dome, the younger 2004–2008 lava dome complex, and the advanced arms of Crater Glacier. U.S. Geological Survey, June 26, 2007.

Hydrologic and Geomorphic Impacts of the 1980 Eruption in the Toutle River Valley

Hydrologic Impacts

In the Toutle River watershed, the 1980 eruption draped hillslopes with flow and fall deposits, filled channels, and caused significant channel modification and instability. With the exception of the upper North Fork Toutle valley, gross pre-eruption landforms remained mostly intact. Large lahars that swept the Toutle watershed generally paved channels with up to a few meters of gravelly sand, lowered flow capacity, simplified structure and complexity, and reduced roughness. Along the lower Cowlitz River, the North Fork Toutle lahar was mostly confined by levees that lined the channel. There, the lahar deposited more than 38 million m^3 (50 million yd^3) of sediment and raised the channel thalweg by ~5 m (16 ft). This change in bed elevation dramatically reduced channel conveyance capacity. The pre-eruption discharge at flood stage on the Cowlitz River at Castle Rock (fig. 2-7) was ~2150 m^3/s (~75,900 cfs). After the lahar, the discharge at flood stage was reduced to ~10 percent of its pre-eruption magnitude (Lombard et al. 1981). The North Fork Toutle lahar also deposited ~34 million m^3 (45 million yd^3) of sediment in the Columbia River, and locally raised the channel bed by ~8 m (25 ft) near its confluence with the Cowlitz River.

The 1980 eruption caused geophysical and ecological perturbations that radically altered landscape hydrology. The eruption destroyed mature forest over hundreds of square kilometers, broadly deposited tephra having a nearly impervious surface over more than 1000 km^2 (>400 mi^2), and greatly altered the character of major channels that drained the volcano. Infiltration capacities of slopes ravaged by the blast PDC were reduced from ~75 to 100 mm h^{-1}, typical of forested soils in the Cascade Range (Johnson and Beschta 1980, Leavesley et al. 1989), to as little as 2 mm h^{-1} (Leavesley et al. 1989). One year after the eruption, spatially averaged infiltration capacities within this disturbance zone remained at <10 mm h^{-1} (Leavesley et al. 1989, Swanson et al. 1983), and after nearly 20 years, plot-specific infiltration capacities remained only 20 to 30 percent that of predisturbance capacities (Major and Yamakoshi 2005).

The volcanic impacts modified the typical modes of landscape water transfer and altered hillslope hydrology in the most heavily affected basins (Dunne and Fairchild 1984, Major and Mark 2006, Pierson and Major 2014). Normally, hillslope-storage and subsurface flow are the dominant components of forest hydrology in the Cascade Range (e.g., Jones 2000, Wigmosta and Burges 1997). Vegetation loss and greatly reduced infiltration radically modified the amount of precipitation reaching the surface, the evaporative and infiltration losses, hillslope-storage, subsurface flow, and the dynamics of snow accumulation and melt. Consequently, substantially more rainfall and snowmelt ran off hillslopes rapidly as overland flow (e.g., Pierson and Major 2014).

Channel changes had variable hydrological impacts. Straightening and smoothing of channels by lahars enhanced flow efficiency by reducing hydraulic roughness. In contrast, disruption of the upper North Fork Toutle valley by the debris-avalanche deposit temporarily diminished channel flow. The debris-avalanche deposit blocked several channels tributary to the North Fork Toutle River and, because of its irregular surface of hummocks and closed depressions, disrupted through-going flow. Drainage development on the debris-avalanche deposit began shortly after emplacement when ponds that formed in depressions on the deposit breached (Janda et al. 1984). Channel development was augmented in several ways: breakouts of lakes impounded adjacent to the avalanche deposit; controlled releases from the largest lakes impounded along the deposit margin; pumping water from Spirit Lake across the deposit surface; meltwater floods and lahars issuing from the crater; and runoff erosion. Many lakes and ponds that formed adjacent to and on the surface of the avalanche deposit trapped and released local runoff slowly, though some breached uncontrollably and released water rapidly. It took nearly 3 years for a fully integrated new drainage network to form across the deposit (Meyer 1995,

Simon 1999), and much of that integration was accomplished by artificial means (i.e., pumping water from Spirit Lake; controlled releases from other lakes) (Janda et al. 1984).

Eruption-induced landscape changes generally amplified peak flows from severely disturbed basins (Dunne and Fairchild 1984, Major and Mark 2006). But peak flow responses to the eruption were complex, relatively short lived, and varied with respect to the nature of volcanic disturbance, season, discharge magnitude, and time since the eruption. Hydrological responses to the volcanically induced landscape disturbances were strongest from basins in which both hillslope hydrology and channel hydraulics were altered, but weakest from basins affected only by moderate to minor tephra fallout, and flow amplification occurred predominantly in autumn (Major and Mark 2006). Small and large autumn peak flows from all heavily disturbed basins were amplified by several percent to many tens percent through 1984, and amplified to a lesser extent from 1985 through 1989 on the Toutle River (Major and Mark 2006). After 1990, differences between pre- and post-eruption peak flows are indistinguishable. Although peak flow responses to the eruption were distinctly seasonal, the nature of the responses varied with flow magnitude. In some basins (Toutle River, South Fork Toutle River, Muddy River), both small and large autumn peaks were amplified nearly proportionately, whereas in others (North Fork Toutle River, Green River), small to moderate peaks were amplified disproportionately relative to the larger peaks. The variations in discharge among different basins, seasons, and flow magnitudes show that the hydrological response to the 1980 eruption was complex and inconsistent, and also indicate changes to channel hydraulics, and not just to hillslope hydrology, played a prominent role in the hydrological response (Major and Mark 2006).

Geomorphic Impacts

The style of post-eruption channel adjustments varied with the type of disturbance, but generally followed complex cycles of incision, aggradation, and widening. Channel development on the debris-avalanche deposit began during an initial phase of localized liquefaction and dewatering, which triggered fill and spill of small ponds and erosion by the North Fork Toutle lahar. Channel adjustments subsequently followed a sequence of incision, aggradation, and widening (Meyer and Martinson 1989, Mosbrucker et al. 2015, Zheng et al. 2014). In general, channels on the debris-avalanche deposit incised tens of meters and widened hundreds of meters, revealing the debris-avalanche sediment as very erodible. Similar, but less dramatic, adjustments occurred along other channels affected by lahars. Lahar-affected channels generally incised up to several meters, widened by tens of meters,

and locally aggraded by as much as a couple of meters (Meyer and Janda 1986, Meyer and Martinson 1989, Mosbrucker et al. 2015, Simon 1999).

Rates of channel stabilization varied greatly among channels affected by the debris avalanche and lahars, but dramatic adjustments and consequent extraordinary sediment transport declined sharply within a few years of the eruption. Channel adjustments occurred most rapidly through 1981 as channels incised and widened (Meyer and Martinson 1989, Mosbrucker et al. 2015, Zheng et al. 2014). Within 5 years, dramatic channel changes were largely complete, but some reaches, especially along the upper North Fork Toutle River across the debris-avalanche deposit, still exhibit progressive change even more than three decades after the eruption (Major et al., in press; Mosbrucker et al. 2015) (fig. 2-16). Hence, massively high sediment loads swiftly declined, but loads remain elevated above pre-1980 levels (Major et al. 2000, in press) (fig. 2-17).

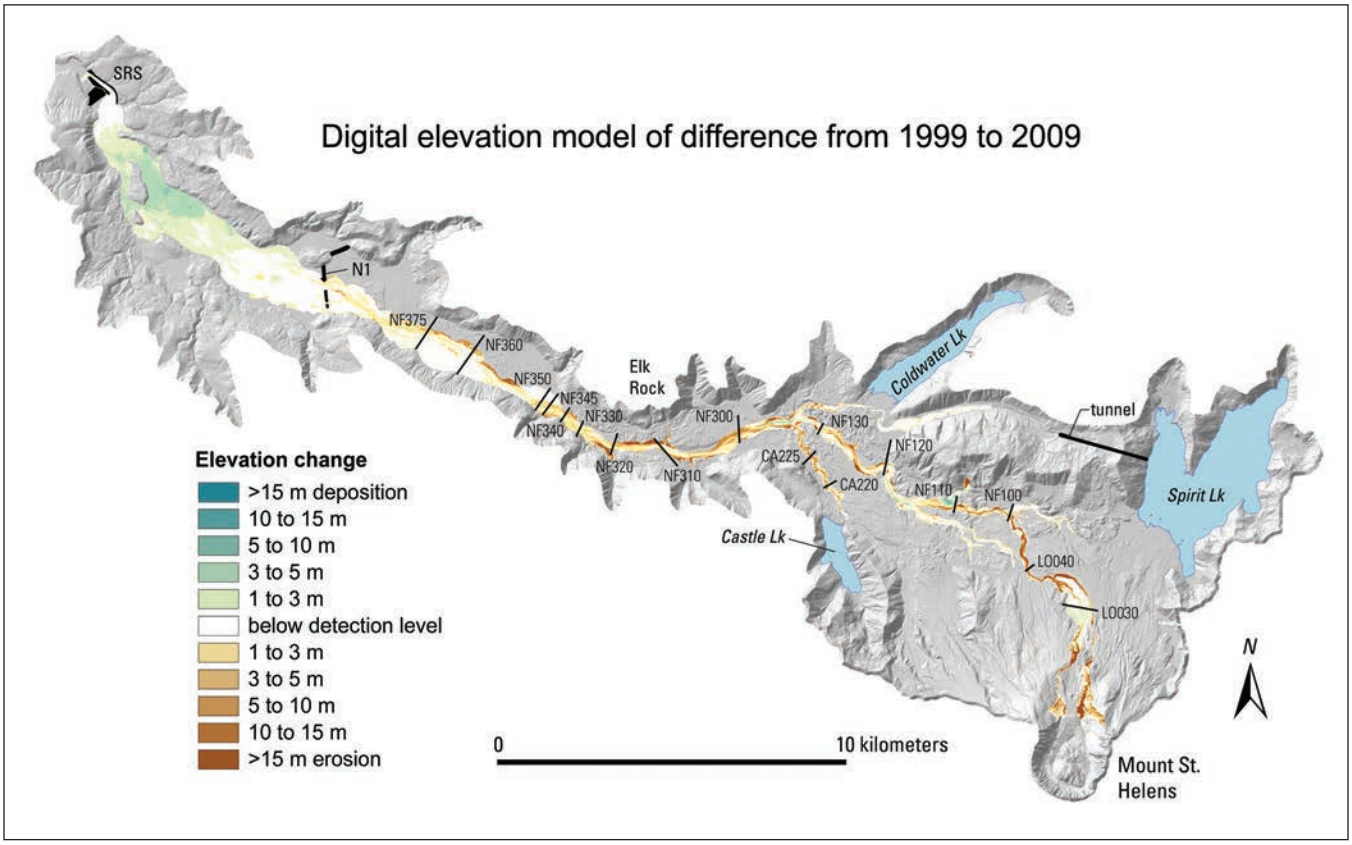

Figure 2-16—Digital elevation model of topographic difference (DoD) created by differencing digital elevation models derived from aerial photography in 1999 and an airborne LiDAR survey in 2009. The DoD has been draped over a hill-shaded topographic model derived from the 2009 LiDAR survey. Locations of various cross sections that track changes in channel geometry are shown. SRS is the sediment retention structure; N1 is the remnant of an initial retention structure built in the early 1980s but which was quickly overwhelmed. Source: Major et al. (in press).

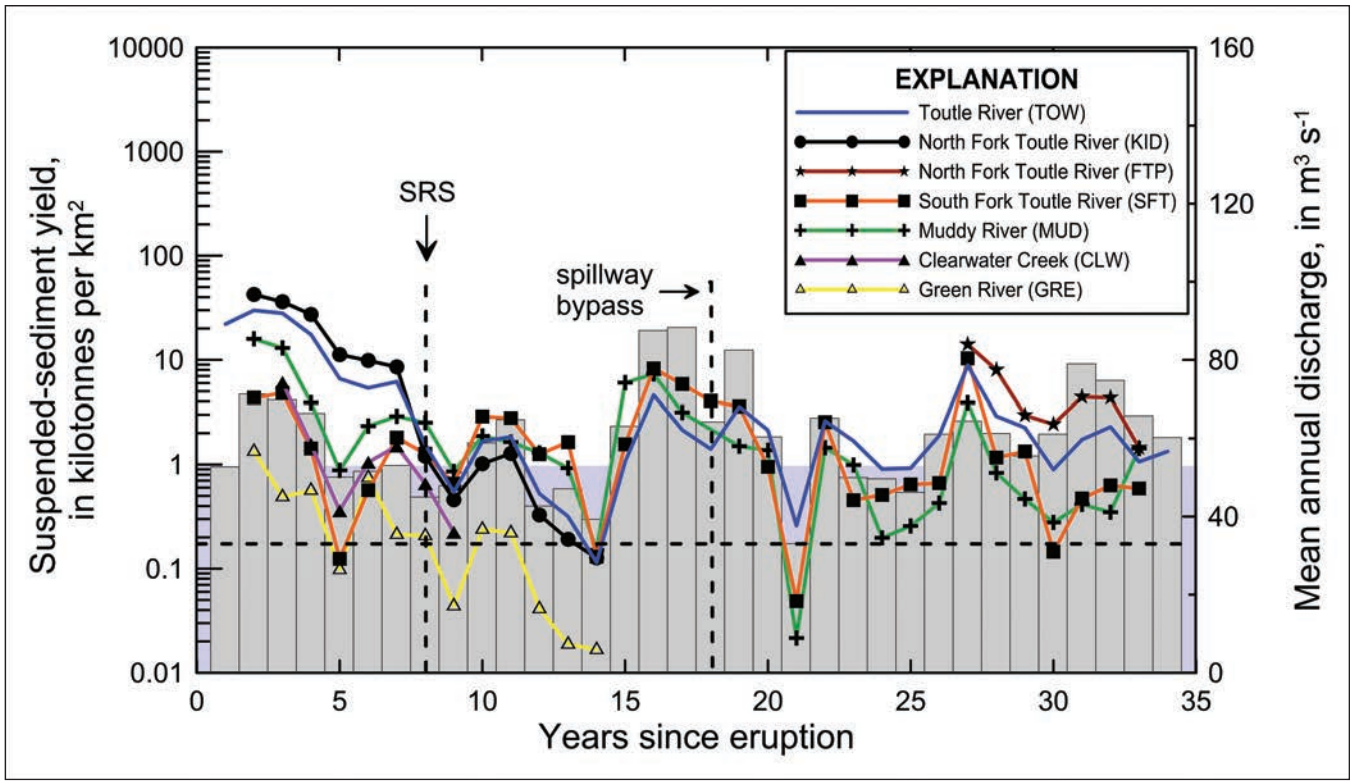

Figure 2-17—Time series of suspended-sediment yield (load per unit basin area) at Mount St. Helens. See figure 2-7 for basin disturbances and gauge locations. Bluish background shading highlights range of average annual yields from several western Cascade Range rivers. Dashed horizontal line is the approximate mean value of that range of average annual yields. The gray histogram shows mean annual discharge measured at TOW gauging station on Toutle River. SRS line marks completion date of sediment retention structure on North Fork Toutle River in 1988. Spillway bypass line indicates when water and sediment began passing over the SRS spillway in 1998. Source: Major et al. (in press).

Substantial post-eruption channel aggradation is endemic to volcanoes in the Cascade Range. Thick post-eruptive alluvial fills have been described along channels draining Mount St. Helens, Mount Hood, and Mount Rainier (Crandell 1987, Pierson et al. 2011, Zehfuss et al. 2003). Persistent erosion and sedimentation problems should be anticipated following emplacement of large volcanic debris avalanches and lahars, and measures designed to mitigate problems related to sediment redistribution need to remain functional for several decades or longer.

Social and Economic Impacts of the 1980 Lahars and Post-Eruption Sediment Transport

The 1980 lahars destroyed or severely damaged civil works along all of the major river systems that drain the volcano, caused lesser damage along the Cowlitz River, and caused no damage but affected commercial transport along the Columbia River

(Schuster 1983). The 1980 eruption, including lahars, caused more than $1 billion in losses (Foxworthy and Hill 1982, Willingham 2005). Along the Toutle River valley, the North Fork Toutle and South Fork Toutle lahars together destroyed or heavily damaged numerous homes, bridges, roadways, logging camps, and privately and publicly owned water supply and sewage disposal systems. The Interstate 5 highway and Burlington Northern railway bridges that cross the Toutle River near its confluence with the Cowlitz River, and link Portland and Seattle, sustained only minor damage. To lessen the possibility of subsequent flood damage to these structures, the U.S. Army Corps of Engineers (USACE) dredged sediment from the lower 20 km (12 mi) of the Toutle channel through May 1981 (Schuster 1983, Willingham 2005).

Along the Cowlitz River, the North Fork Toutle lahar drastically affected operations of municipal water supply and sewage disposal systems of cities and towns located along the flood plain. The flow caused no permanent damage, but it took weeks before systems and services were fully restored. To restore the original channel and manage future flooding, the USACE dredged ~43 million m^3 (55 million yd^3) of sediment from the channel by October 1981 (Schuster 1983, Willingham 2005).

Sediment deposited by the North Fork Toutle lahar blocked the navigation channel of the Columbia River and affected regional commerce. Ocean-going traffic to and from Portland, Oregon, and Vancouver, Washington, was halted for about a week until a partial deep-draft channel could be dredged. The full channel took months to restore. Closure of the shipping channel resulted in combined daily revenue losses of $5 million (1980 dollars) for the ports of Portland and Vancouver. From May 1980 to October 1981, the USACE dredged nearly 77 million m^3 (100 million yd^3) of eruption-related sediment from the Toutle, Cowlitz, and Columbia Rivers (Schuster 1983, Willingham 2005), a volume equivalent to a mere 3 percent of the total volume of debris-avalanche sediment deposited in the upper North Fork Toutle River valley.

Between 1980 and 1990, the federal government spent more than $1 billion mitigating problems caused by the 1980 lahars, the colossal debris avalanche, and post-eruption sediment redistribution (Willingham 2005). The bulk of the costs entailed channel dredging, design and construction of a large sediment retention structure (SRS) to trap sediment in the North Fork Toutle River valley (figs. 2-7 and 2-18), design and construction of a bedrock tunnel to provide an outlet for Spirit Lake, and temporary pumping of the lake until the outlet tunnel could be completed. By 1998, sediment behind the SRS had filled to the level of the spillway. At that time, substantial amounts of sandy sediment bypassed the SRS, and within a decade, the USACE had to resume dredging of the lower Cowlitz River. They are

Figure 2-18—Mitigation of post-1980 sediment transport along the Toutle-Cowlitz River system. (A) Sediment dredging along Cowlitz River. U.S. Geological Survey, February 2, 1981. (B) Oblique aerial view to east of sediment retention structure constructed on North Fork Toutle River valley. Photo by Bill Johnson, U.S. Army Corps of Engineers. Source: Major et al. (2005).

currently conducting a comprehensive assessment of sediment erosion, transport, and deposition in the Toutle watershed and have adopted an adaptive and phased sediment-management plan that incorporates minor raises of the SRS spillway, construction of grade-building structures on the sediment plain behind the SRS, and limited dredging of the lower Cowlitz River as needed (USACE 2014a).

Prehistoric Eruptive Impacts in the Toutle River Watershed

The 1980 eruption of Mount St. Helens is not the only eruption to severely affect the Toutle River valley. Outcrops show that at least 35 lahars have inundated the Toutle River valley >50 km (30 mi) from the volcano near the confluence of the

North Fork Toutle and South Fork Toutle Rivers over the past 50,000 years (Crandell 1987, Scott 1989). Several lahars inundated valley flood plains during the Swift Creek eruptive stage (16,000 to 12,800 years BP), and the Smith Creek (3,900 to 3,300 years BP) and Pine Creek (3,000 to 2,500 years BP) periods of the Spirit Lake eruptive stage (fig. 2-2) (Scott 1988a).

The largest lahars that have been identified at Mount St. Helens occurred in rapid succession in the Toutle River valley about 2,500 to 3,000 years BP (during the Pine Creek eruptive period). A series of four lahars occurred, the largest of which exceeded 10^9 m^3 (Scott 1988b) (fig. 2-19). The largest of these flows vastly exceeded the depth, discharge, and volume of the destructive 1980 North Fork Toutle lahar (figs. 2-20 and 2-21). Near Kid Valley, 50 km (30 mi) downstream from the volcano (see fig. 2-7), peak flow depth of the largest ancestral lahar was about 35 m (115 ft) compared to about 8 m (26 ft) for the 1980 lahar (fig. 2-20). Likewise, peak discharge of the ancestral lahar was about 200 000 m^3 s^{-1} (7 million cfs) compared to about 10 000 m^3 s^{-1} (350,000 cfs) for the 1980 lahar (fig. 2-21). These ancestral flows were associated with successive breaching of one or more landslide dams, which presumably dammed an ancestral Spirit Lake given the required volumes of water to generate such huge lahars. These lahars formed through erosion and entrainment of sediment by flows that began as breakout flood surges (Scott 1988b). The largest flood surge entrained sediment for more than 20 km (12 mi) before it transformed into a lahar. A sudden release of an ancestral Spirit Lake is the only possible source of the flood surge that produced the huge lahar in this series. Deposits of two prehistoric debris avalanches from the north flank of Mount St. Helens have been identified and are dated between 2,500 and 3,000 years BP (Hausback and Swanson 1990). These debris avalanches probably blocked the outlet from, and caused enlargement of, Spirit Lake, as did the 1980 debris avalanche. The sequence of lahars that began as large flood waves, therefore, provides an analog for what could have happened from breakouts of major lakes formed or enlarged by the 1980 eruption had lake levels not been stabilized by engineering intervention.

Frequency of Large Lahars in the Toutle River Valley

Large lahars at Mount St. Helens occur frequently. Lahars large enough to inundate flood plains in the Toutle River valley >50 km (30 mi) from the volcano have occurred at least 35 times in roughly 50,000 years, at least 26 times in the past 14,000 years, and at least 15 times in the past 4,500 years (Scott 1989). Unlike meteorologic floods that generally are considered independent events distributed randomly in time, large lahars at Mount St. Helens are interdependent, nonrandom events

Figure 2-19—Pine-Creek age lahar deposits along Toutle River valley near North Fork Toutle River–South Fork Toutle River confluence. These deposits resulted from lahars formed during breakouts from an ancestral Spirit Lake dammed by debris avalanche(s) from an eruption of Mount St. Helens approximately 2,500 to 2,900 years ago. Lahar PC1 was the largest of a sequence of four lahars, and had a volume of order 10^9 m^3 (Scott 1988b). The dashed line highlights a clast of debris avalanche deposit entrained by the lahar. Geologists are standing about 5 to 10 m (15 to 30 ft) above the present river level, which is similar to the river level at the time these lahars passed through. U.S.Geological Survey, June 15, 2016.

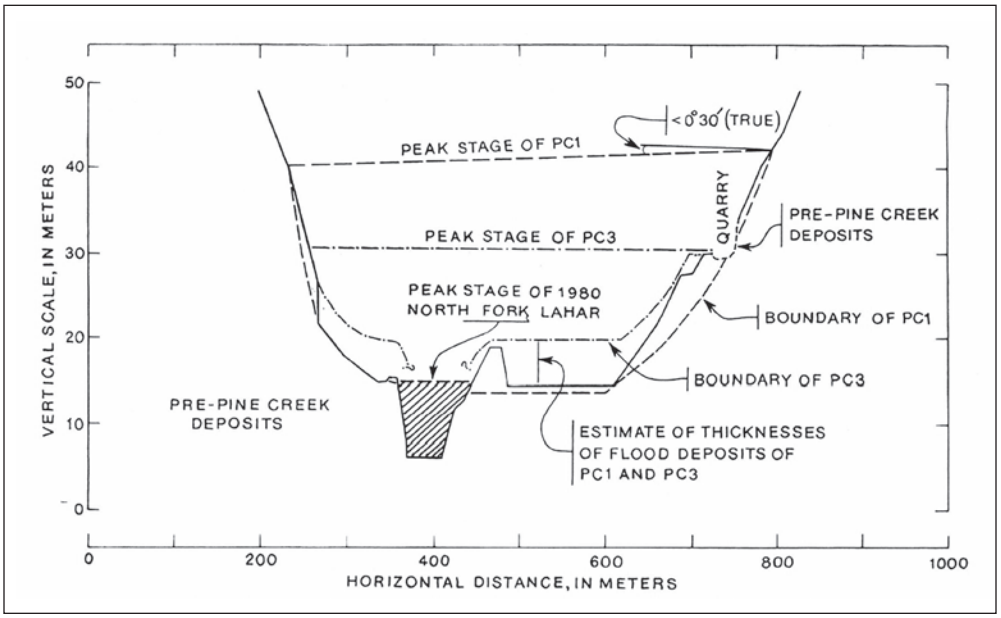

Figure 2-20—Reconstructed cross sections of the peak stage of lahars PC1 and PC3 at Kid Valley. The flow cross section of the 1980 North Fork Toutle lahar is shown for comparison (Source: Scott 1988b).

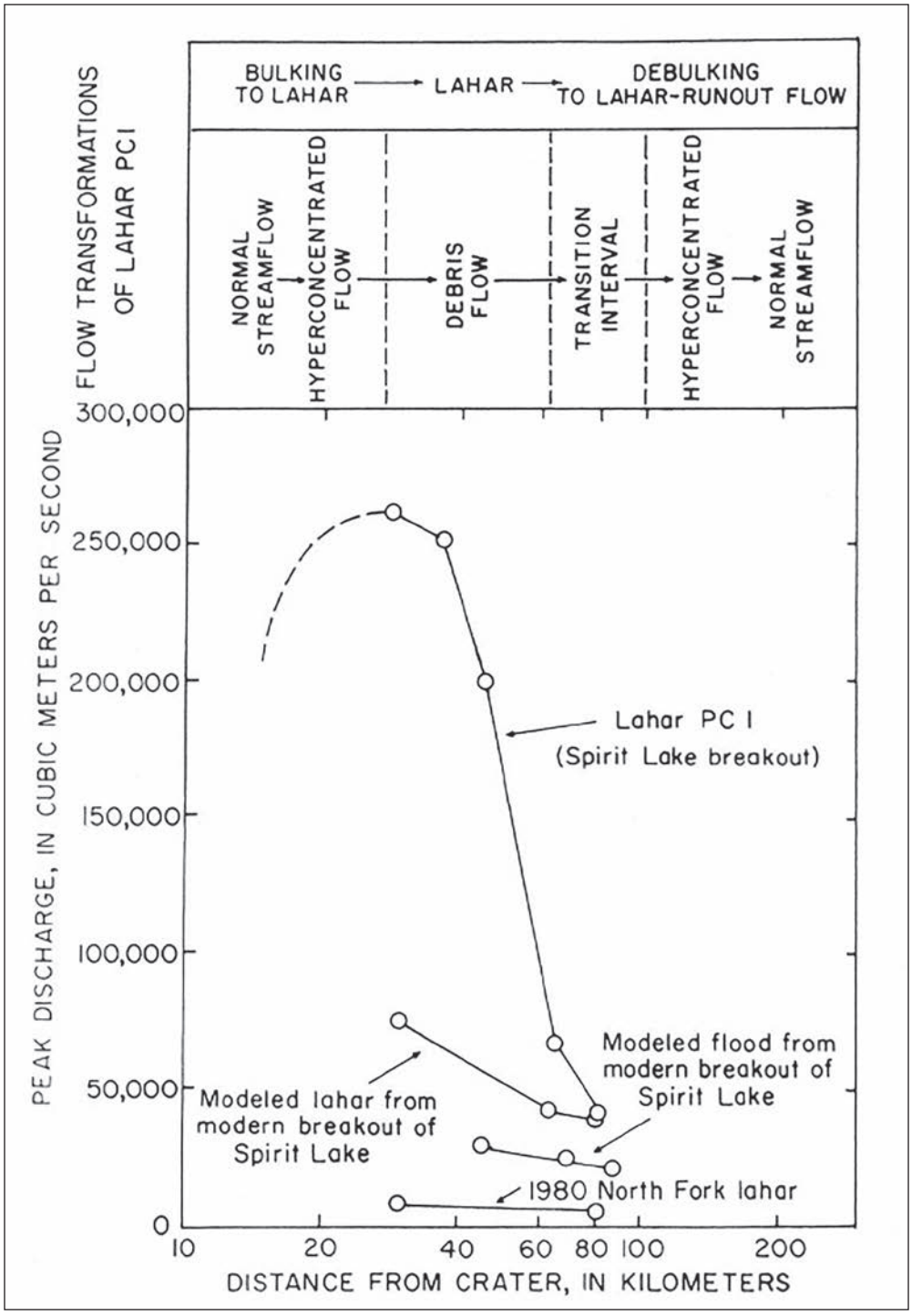

Figure 2-21—Peak discharges of lahar PC1, a modeled lahar from a modern breakout of Spirit Lake (Swift and Kresch 1983), and a modeled flood from a modern breakout of Spirit Lake (Bissell and Hutcheon 1983). Peak discharge of the 1980 North Fork Toutle lahar (Fairchild and Wigmosta 1983) is shown for comparison (Source: Scott 1988b).

drawn from highly skewed populations. They occur during distinct eruptive periods that are separated by dormant intervals lasting a few to many tens of centuries (fig. 2-2). Furthermore, within each eruptive period, lahars commonly are clustered in time within a few to several tens of years, and variations in triggering mechanisms strongly affect their occurrence.

Estimating recurrence intervals for large lahars is conditional upon the state of the volcano. A simplistic frequency analysis based on a sum of flows over a specified time interval provides only a minimum estimate of recurrence. For example, the average recurrence interval of lahars in the Toutle River valley over the past 4,500 years is about 300 years (15 events). But many of these events were clustered, and when the volcano is in a period of eruption, lahars are more likely to occur. Owing to nonrandom occurrence, perhaps a more useful estimate of average recurrence interval of large lahars in the Toutle River valley can be gleaned by considering only those periods when the volcano was active. Thus, the average recurrence interval of large lahars during periods of eruption over the past 4,500 years is 130 years (based on at least 15 overbank flows during the 1,930 years considered to be within eruptive periods) (Scott 1989). The volcano today is considered to be in an active eruptive period.

Chapter 3: Characteristics and Hazards of the Spirit Lake Blockage

The Spirit Lake blockage lies in the upper North Fork Toutle River valley at the foot of Mount St. Helens. It is composed largely of the deposit of the massive debris avalanche that swept off the volcano during the May 18, 1980, eruption. The dimensions of the actual blockage itself are hard to define because it does not have a simple shape or resemble the typical shape of an earthen dam, nor is there a sharp break in slope to define its toe. Glicken et al. (1989) selected the western boundary of the blockage based on an abrupt change from hummocky to smooth topography near the western end of the embayment up which the debris avalanche overrode Johnston Ridge (fig. 3-1). That boundary is about 1950 m (6,400 ft) from the toe of Harry's Ridge at the southwest shore of Spirit Lake and about 1100 m (3,600 ft) from the crest of the blockage. As defined, the toe of the blockage is at 1027 m (3,370 ft) elevation NGVD29, about 23 m (75 ft) below the current average lake level. The northern boundary of the blockage abuts Johnston Ridge; the southern boundary of the blockage is even more subjectively defined. Overall, Glicken et al. (1989) estimated the blockage to be about 1465 m (4,800 ft) in width from north to south and about 1950 m (6,400 ft) in length from east to west.

The debris-avalanche deposit consists entirely of rocks from the Mount St. Helens edifice. It is composed dominantly of heterogeneous gravelly sand but contains silts and clays as well as rocks that are meters in diameter (Glicken et al. 1989). The texture of the deposit is extremely variable. Close to the volcano, shattered but intact remains of original edifice stratigraphy are preserved; farther downstream the deposit has a more blended appearance with little original stratigraphy evident. But there is little widespread competent rock preserved. Instead, much of the rock from the mountain is highly shattered; few rocks meters wide from the mountain remain (Glicken 1996). Along the crest of the blockage the debris-avalanche deposit ranges from about 60 m (200 ft) to more than 150 m (500 ft) thick (Glicken 1996) (fig. 3-2). It is mantled by deposits from the blast PDC (the "blast deposit") and pyroclastic-flow and ash cloud deposits from several later flows. Thicknesses of these mantling deposits are highly variable.

The blast deposit consists of a lower unit of angular, unstratified, clast-supported rock debris larger than coarse sand, overlain by an upper unit of silt to sand-sized sediment composed of ground-up bits of rock. Its thickness within the Spirit Lake blockage ranges from a few centimeters to as much as 13 m (43 ft) (Glicken et al. 1989). The ash cloud deposit is composed mainly of sand (40 to 60 percent) and silt (40 to 60 percent). Across the blockage, it ranges from <1 to 12 m (<3 to 40 ft) thick (Glicken et al. 1989).

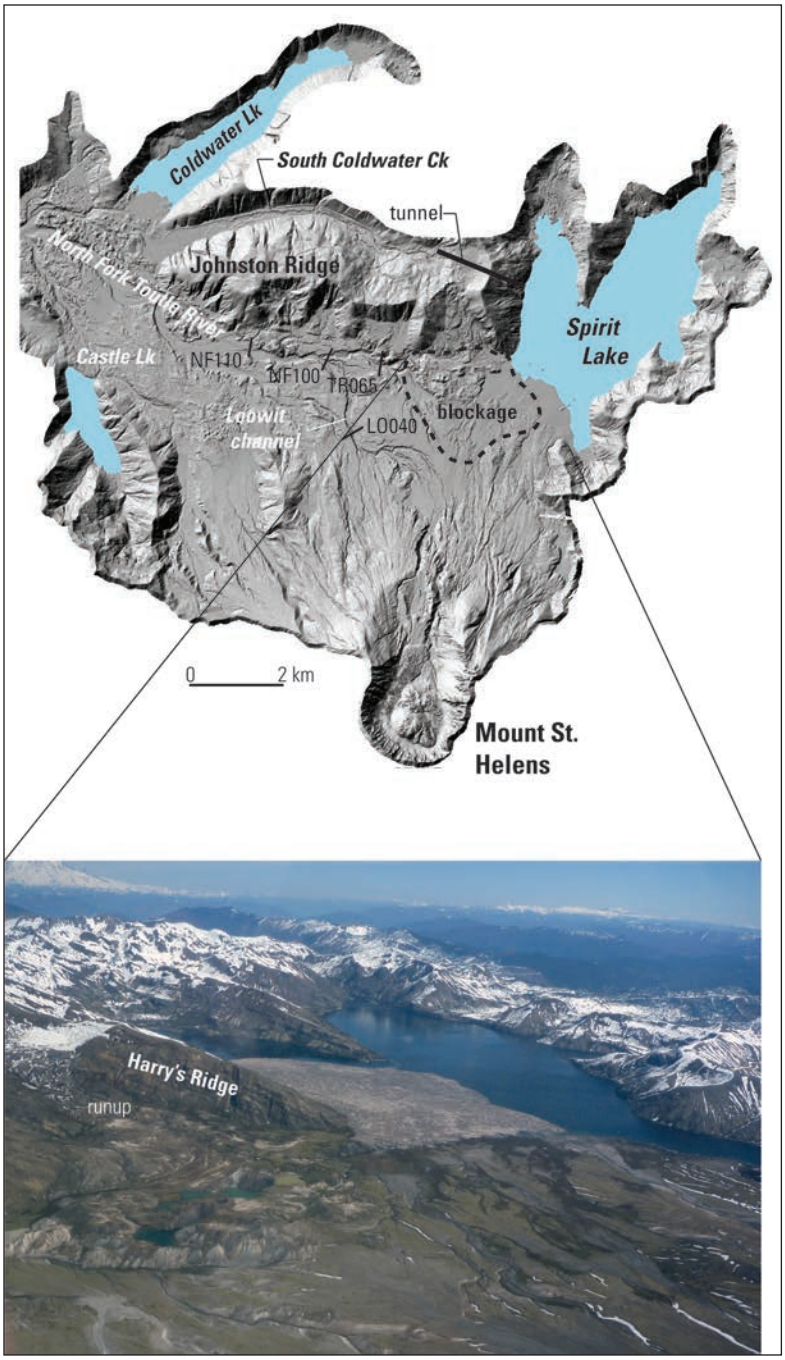

Figure 3-1—Portion of digital elevation model of upper North Fork Toutle River valley derived from an airborne LiDAR survey in 2009. Dashed line shows approximate dimensions of the part of debris avalanche and overlying pyroclastic deposits known as the Spirit Lake debris blockage. U.S. Geological Survey photograph, April 18, 2016, shows oblique aerial view to northeast of blockage and Spirit Lake. Note log mat in western arm of the lake.

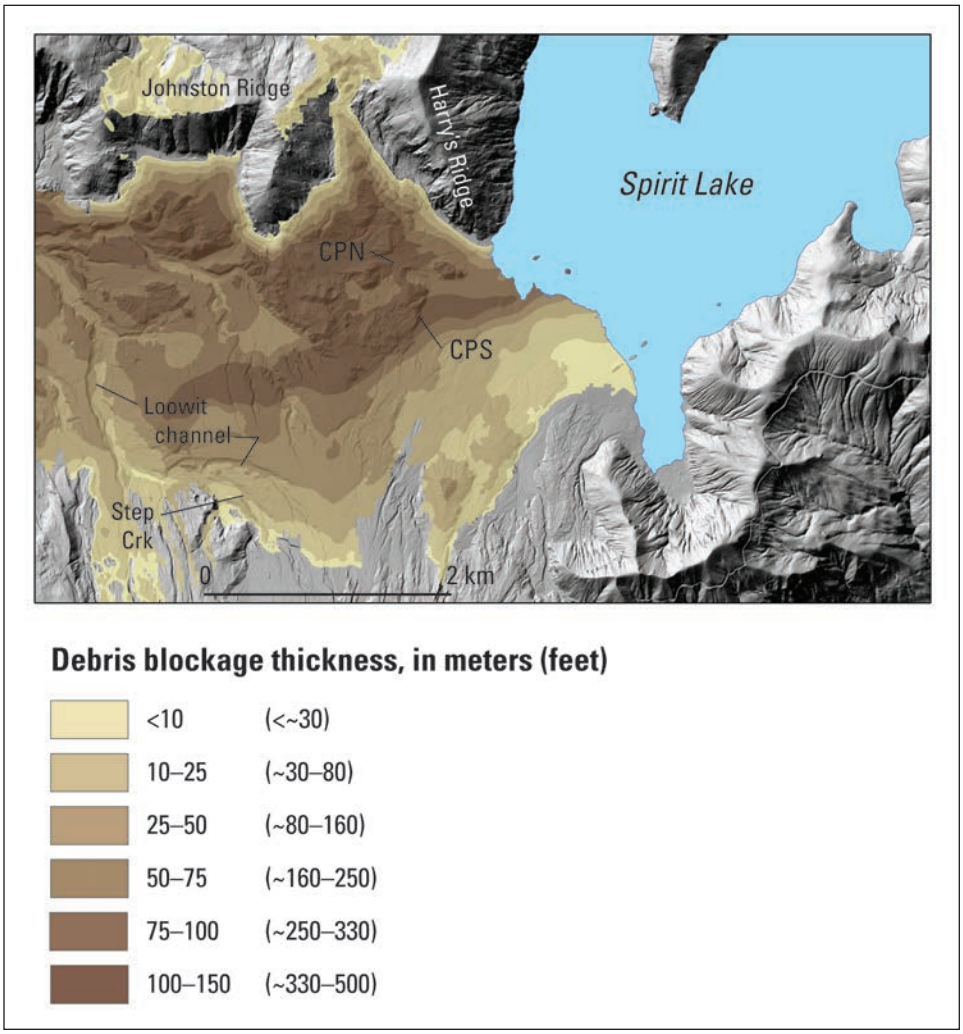

Figure 3-2—Isopach map of debris-blockage thickness draped over hill-shaded topographic model derived from the 2009 LiDAR survey. The lowest elevations of the contact between the debris-avalanche and overlying pyroclastic deposits along the crest of the blockage are at critical point north (CPN, 1071 m; 3,513 ft) and critical point south (CPS, 1069 m; 3,506 ft) (Glicken et al. 1989). Map derived by Adam Mosbrucker, U.S. Geological Survey. Original isopach data are summarized in Glicken (1996).

Both the debris-avalanche sediment and overlying pyroclastic sediment are highly erodible, though the pyroclastic sediment erodes more swiftly. Channels near the northern and western edges of the blockage incised tens of meters and widened by at least a hundred meters within months to a couple of years (fig. 3-3). Examples of deep gullies across the blockage and seepage erosion pipes within the ash cloud deposit are shown in figure 3-4.

An initial blockage stability analysis performed by Youd et al. (1981) assumed that the pyroclastic deposits overlying the blockage crest comprised a thin mantle atop the debris-avalanche deposit, and that physical overtopping by a rising lake

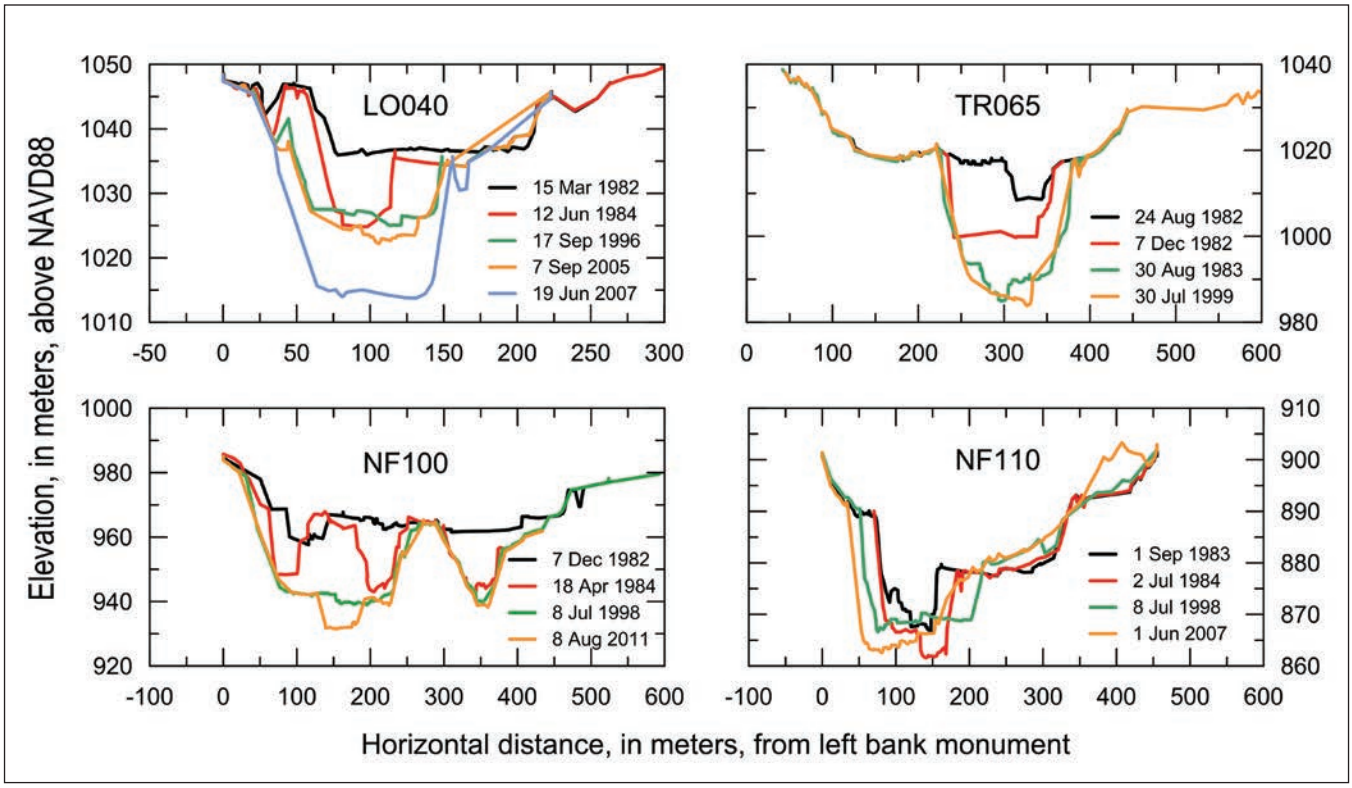

Figure 3-3—Time series of cross-section profiles of channels developed on debris-avalanche deposit near Spirit Lake blockage. See figure 3-1 for section locations. Data from Mosbrucker et al. (2015).

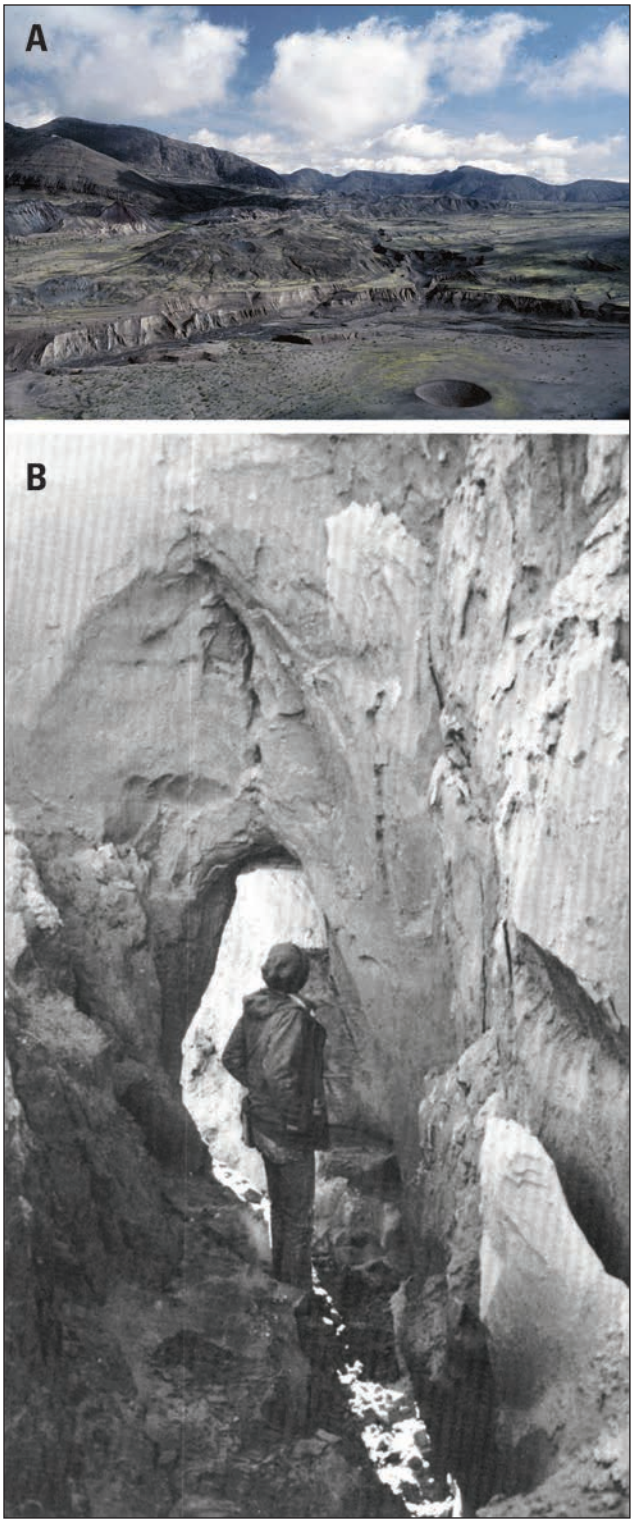

Figure 3-4—Photographs of erosion of Spirit Lake debris blockage. (A) U.S. Geological Survey photograph of surface erosion channels. (B) Photograph of seepage erosion pipe within ash cloud deposit. Image from Glicken et al. (1989).

level was the principal potential failure mode of the blockage. Subsequent field analysis revealed the pyroclastic deposits to be much thicker, highly erodible, and unlikely to hold back the impounded lake. The U.S. Geological Survey (USGS) and U.S. Army Corps Engineers (USACE) thus implemented a drilling program to identify the lowest elevation of the contact between the debris-avalanche deposit and overlying pyroclastic deposits along the blockage crest, better define thicknesses of the pyroclastic deposits, and obtain samples for analyses of material properties (Glicken et al. 1989, USACE 1983).

The USGS conducted consequent stability analyses on the Castle Lake blockage farther downstream (Meyer et al. 1994). The Castle Lake blockage, formed of debris-avalanche sediment virtually identical to that in the Spirit Lake blockage, is much smaller than the Spirit Lake blockage. It is about 600 m (2,000 ft) long and about 425 m (1,400 ft) in width from the lake to the downstream toe. The stability analyses showed this blockage to be stable against failure by piping, but potentially locally unstable against heave and internal erosion.

Estimates of Critical Lake Elevations

An initial USACE estimate of the elevation of the contact between the debris-avalanche deposit and the overlying pyroclastic deposits—called the effective dam crest elevation—is 1064 m (3,490 ft) (USACE 1983). Subsequent interpretation of drilling and field mapping data by Glicken et al. (1989) identified two critical low points of the crucial geological contact along the crest of the blockage: critical point north (CPN) at elevation ~1071 m (~3,513 ft) and critical point south (CPS) at elevation 1069 m (3,506 ft) (see fig. 3-2).

Recognition that the pyroclastic deposits would likely be unable to hold back water, in conjunction with a rising lake level, spurred a presidential declaration of emergency to stabilize the lake and develop a plan to provide an outlet (Sager and Chambers 1986). To determine a safe level for the lake, the USACE assumed that potential consolidation of the blockage deposit and erosion of the pyroclastic and debris avalanche deposits could lower the effective dam crest by about 5 m (~15 ft) elevation to 1059 m (3,475 ft) (Sager and Chambers 1986). Using this elevation as the threshold for failure, the USACE conducted a variety of analyses to determine lake levels that potentially could induce piping failure in the blockage and an analysis to determine the volumetric input and potential rise of lake level under an extreme hydrological event. A USACE analysis of piping failure (Sager and Chambers 1986, USACE 1983) concluded that a sustained, long-term lake level above 1055 m (3,460 ft) elevation could potentially lead to piping failure. Therefore, 1055 m was deemed the maximum safe lake level. A “normal operating level” for the

lake was determined with the intention that it have sufficient capacity for short-term storage of extreme hydrological events and moderate volcanic events. The capacity needed was based on analysis of the rare combination of a probable maximum flood event occurring immediately after a 100-year flood event (Sager and Chambers 1986). This combination of rare events, without a lake outlet, was determined to have the potential to raise the lake level by about 5.5 m (18 ft). The USACE further assumed that future volcanic events, such as lahars, pyroclastic flows, and lava flows, could raise the lake by up to 3 m (10 ft) (USACE 1983). Owing to these potential rises in lake level, the USACE adopted a 6.1-m (20-ft) lake rise as the necessary capacity to temporarily accommodate rare hydrological and moderate volcanic events, and recommended a safe operating elevation of 1049 m (3,440 ft) (Sager and Chambers 1986). Below this elevation, saturation of the debris-avalanche deposit was deemed to have only a remote chance of triggering failure through piping (Sager and Chambers 1986). Coincident seismic, volcanic, and hydrological events capable of raising lake level more than 6.1 m (20 ft) were deemed very remote and an acceptable risk within the recommended range of safe operating lake levels. Table 3-1 summarizes the significance of various lake elevations.

By August 1982, the lake had risen to elevation 1055.5 m (3,462 ft); Meyer and Carpenter (1983) projected that, under normal precipitation, the lake would overtop the blockage in or before December 1985. To lower and control the lake level, USACE installed barge-mounted pumps to pump lake water through a conduit buried across the debris blockage (Sager and Chambers 1986). The pumps were put into full operation and began drawing water from the lake in November 1982 at a rate of 5.1 $m^3 s^{-1}$ (180 cfs). The USACE evaluated options for providing a safe, permanent lake outlet while water was being pumped from the lake (Sager and Chambers 1986).

Consequences of a Breaching of the Blockage

Owing to concern about a possible breach of the blockage and recognizing that prehistorical releases of Spirit Lake had led to huge lahars, Dunne and Fairchild (1984) and Swift and Kresch (1983) modeled potential lahar hazards along the Toutle and Cowlitz River valleys from a hypothetical failure of the blockage. Both concluded that a breaching of Spirit Lake would be catastrophic. Swift and Kresch (1983) assumed an instantaneous breach and complete release of nearly 390 million m^3 (314,000 ac-ft) of water if the lake reached 1059 m (3,475 ft) elevation and piping failure occurred. They then assumed that the released flood water would erode and entrain nearly 2 billion m^3 of sediment along the flow path—mostly across the debris avalanche—and transform into a lahar. Starting from a location in the North Fork Toutle River valley just upstream from the confluence with Green River

Table 3-1—Definitions of elevations of Spirit Lake

Elevation		Level	Significance of elevation level	Reference
Meters	*Feet*[a]			
1080	3,543	Top of blockage	Elevation of physical low point along blockage crest	Glicken et al. (1989)
1071	3,513		Elevation of debris avalanche-pyroclastic deposits contact at critical point north	Glicken et al. (1989)
1069	3,506	Pyroclastic deposit base	Elevation of debris avalanche-pyroclastic deposits contact at critical point south	Glicken et al. (1989)
1064	3,490		Initial estimate of approximate elevation of debris avalanche-pyroclastic deposits contact	USACE (1983)
1059	3,475		Effective dam crest after assumed potential deposit consolidation	Sager and Chambers (1986), USACE (1983)
1058	3,470		Top of tunnel intake wall	Sager and Chambers (1986)
1056	3,462		Lake level on August 1, 1982	Glicken et al. (1989)
1055	3,460	Safe operating level	Maximum short-term safe level for lake based on estimates of potential for seepage erosion failure	Sager and Chambers (1986), USACE (1983)
1049	3,440	Normal operating level	Normal long-term safe operating level of lake that allows for temporary rises of 6.1 m (20 ft) during rare hydrological events or moderate volcanic events	Sager and Chambers (1986), USACE (1983)
1039	3,408		Lake level on May 21, 1980	Glicken et al. (1989)
975	3,200		Approximate average pre-1980 lake level	Glicken et al. (1989)

[a] Elevations reported in National Geodetic Vertical Datum of 1929.

(see fig. 2-7), they used a one-dimensional hydraulic model with assumed effective friction coefficients for a sediment slurry to route the lahar downstream. Based on this model, they concluded that peak discharge near Kid Valley, about 8 km (5 mi) upstream of the confluence of the North and South Fork Toutle Rivers, could be 72 500 $m^3 s^{-1}$ (~2.5 million cfs) and as much as 39 000 $m^3 s^{-1}$ (~1.4 million cfs) at the mouth of Toutle River. At the confluence of the Cowlitz and Columbia Rivers (fig. 2-7), discharge was forecast to be as great as 31 000 $m^3 s^{-1}$ (~1 million cfs). Predicted flow depths within the inundation boundaries are 18 m (60 ft) at Castle Rock; 9 to 12 m (30 to 40 ft) at Toutle, Silver Lake, Kelso, and Longview, and 4.5 to 6 m (15 to 20 ft) at Toledo. Such a catastrophic event would likely lead to loss of life and to significant (>$1 billion) economic damages.

The model by Swift and Kresch (1983) represents an extreme-case scenario of the full release of Spirit Lake and massive sediment entrainment, but the results mimic reality. Scott (1988b) estimated that peak discharge of the largest of the Pine Creek–age lahars inferred to be related to breaching(s) of an ancestral Spirit Lake

may have been about 200 000 m^3 s^{-1} (7 million cfs) at Kid Valley, with a peak flow depth of 35 m (115 ft) (see figs. 2-20 and 2-21). Mapping of the maximum heights of deposits of those Pine Creek-age lahars by K.M. Scott and R.J. Janda[1] and Chan (2008) showed that deposits are found along the North Fork Toutle, South Fork Toutle, Toutle, and Cowlitz Rivers at altitudes similar to those predicted by Swift and Kresch for a lahar caused by a hypothetical breaching of the modern lake. Thus, as unimaginable as the predicted inundation limits and potential discharges of lahars from a modern breach may be, lahars of that magnitude and related to a breaching of an ancestral Spirit Lake have happened in the Toutle-Cowlitz River system.

Ground-Water Conditions Within the Blockage

Ground water within the Spirit Lake blockage results from infiltration of rainfall and snowmelt, movement of ground water from the volcano, and seepage of surface runoff from Johnston Ridge and the channel draining the volcano's crater (Bergfeld et al. 2008, Glicken et al. 1989, Wynn et al. 2016). Water levels within a limited network of piezometers installed in the debris blockage were monitored from September 1982 to October 1984. As late as 1984, measured water levels showed the development of a ground-water mound within the blockage (Glicken et al. 1989). To the west of the blockage crest, ground water flowed toward North Fork Toutle River. To the east, it flowed toward Spirit Lake. Ground water may also discharge to the fan of pre-1980 volcanic deposits that underlie the debris-avalanche deposit. By late 1984, ground-water had risen locally into the blast and ash cloud deposits mantling the debris-avalanche deposit. Limited piezometer data collected subsequently (last collected in 2013; see footnote 1) showed that the mound of ground water identified in the blockage by Glicken et al. (1989) may still reside locally within the ash cloud deposit.

A geophysical (controlled-source audio-magnetotelluric, or CSAMT) survey (Wynn et al. 2016) revealed a shallow aquifer near the Spirit Lake blockage with a depth as shallow as 10 m (~30 ft) below ground; that aquifer extends no deeper than about 50 m (~160 ft) below ground. A simple model of depth to ground water indicates that the top of the shallow aquifer approaches the bed of the North Fork Toutle River downstream of the confluence with Coldwater and Castle Lake outlet channels (Wynn et al. 2016) (fig. 3-5). The CSAMT survey also detected a deeper

[1] **Scott, K.M.; Janda, R.J.** Unpublished map. On file with: Jon Major, USGS Cascades Volcano Observatory, 1300 SE Cardinal Court, Bldg. 10, Suite 100, Vancouver, WA 98683.

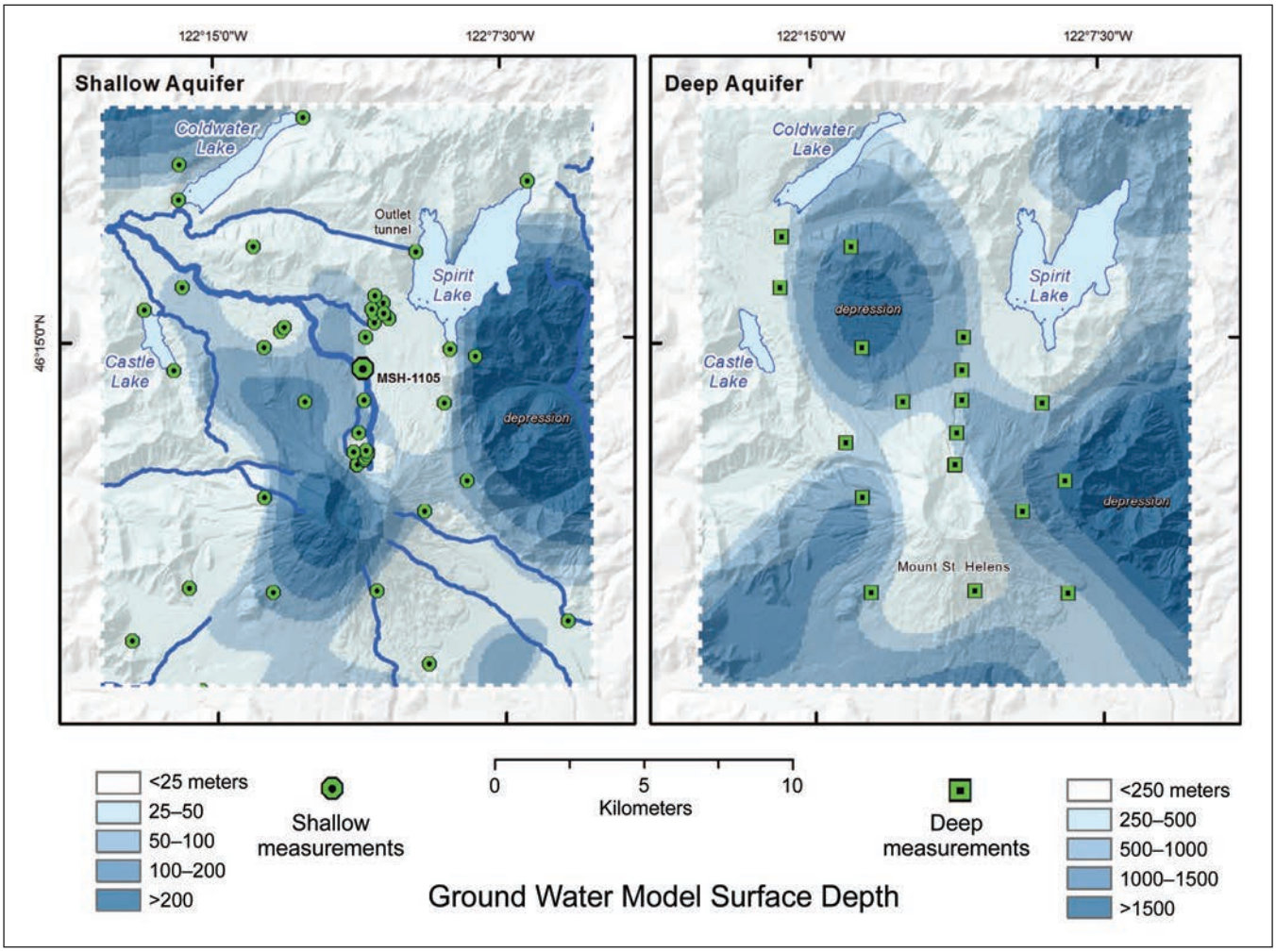

Figure 3.5—Map of depth to ground water in shallow aquifer around Mount St. Helens and within debris-avalanche deposit based on geophysical surveys. From Wynn et al. (2016).

regional aquifer at a depth of 500 to 1000 m (1,650 to 3,300 ft). Ground-water seepage from the blockage into Spirit Lake was estimated to be less than 1 percent of the mean annual rate of filling of Spirit Lake (Glicken et al. 1989). Thus, the ground-water gradient within the blockage is low, and ground-water input to the lake from the blockage is a minimal contributor to lake volume.

Chapter 4: History and Operations of the Spirit Lake Tunnel

Background and Context

The U.S. Army Corps of Engineers (USACE) implemented an emergency pumping operation in November 1982 to stabilize the level of Spirit Lake (Britton et al. 2016, Glicken et al. 1989, Sager and Chambers 1986). Once it was stabilized, they determined a permanently safe lake level (see chapter 3) and evaluated alternatives for a permanent outlet (Britton et al. 2016, Sager and Chambers 1986). Ultimately, the USACE settled on boring a 2600-m (8,500-ft) long tunnel extending from the west side of Spirit Lake through Harry's Ridge and into the valley of South Coldwater Creek (fig. 3-1). Sager and Chambers (1986) provided a description of the design and construction of the outlet tunnel and intake structure. The tunnel became operational in May 1985. After the tunnel was constructed, the USACE transferred ownership to the U.S. Forest Service.

Tunnel Background and Hydraulic Design

Required tunnel hydraulic capacity was determined by routing a probable maximum flood event preceded by a 100-year return interval flood through the lake basin. The total volume of these two rare floods is 69 million m^3 (56,000 ac-ft) (see chapter 5). To prevent the lake from rising above the elevation deemed the maximum safe operating elevation—1055 m (3,460 ft)—peak outflow through the tunnel needed to be 15.6 $m^3 s^{-1}$ (550 cfs) (Sager and Chambers 1986). Thus, the normal operating lake level and outflow capacity of the tunnel were designed so that such an unusual suite of hydrological events could be accommodated temporarily without exceeding the maximum safe lake level.

Long-term operating criteria adopted for tunnel performance require that flow through the tunnel not exceed 75 percent of the tunnel height (i.e., the tunnel must operate under an atmospheric and not pressurized condition); the normal lake elevation should be about 1049 m (3,440 ft) with lake level fluctuation limited to about 1.5 m (5 ft) during normal flood events; and the intake gate regulating flow into the tunnel remaining fully open at 1.22 m (4 ft) (Britton et al. 2016, Sager and Chambers 1986). Based on these operating criteria, the tunnel was designed to have a diameter of 3.3 m (10.8 ft). This design diameter was deemed capable of passing the required flow capacity as well as allowing for minor offsets during construction and variations in tunnel roughness (Britton et al. 2016, Sager and Chambers 1986).

Tunnel Geology

The tunnel passes through bedrock that bounds the western edge of Spirit Lake. It penetrates volcanic rock grouped into two major lithologic units: Tertiary-age (36 to 27 million years old) predominantly volcanic tuffs (a general term for consolidated pyroclastic rock), which is overlain by basalt and basaltic andesite lava flows (Britton et al. 2016, Evarts and Ashley 1993) (fig. 4-1). The bedrock has been regionally deformed; the section through which the tunnel passes strikes roughly north-south normal to the tunnel orientation and dips about 30° to 40° eastward. Subvertical faults and shear zones are abundant in the Johnston Ridge–South Coldwater Creek area but show evidence of only minor (≤10 m; ≤30 ft) offset (Evarts and Ashley 1993). Many of the faults are filled or crossed by Tertiary dikes showing that they are old; none show evidence of recent movement. The volcanic rocks in the area have been overprinted by burial metamorphism, and volcanic glass and minerals have been replaced by smectite and various other clays. Many faults and shear zones in the area show evidence of low-temperature, shallow-level hydrothermal alteration and mineralization (Evarts and Ashley 1993).

Lithology and discontinuities along the tunnel were mapped in detail (1:120 scale) during construction. Britton et al. (2016) describe the generalized tunnel geology as:

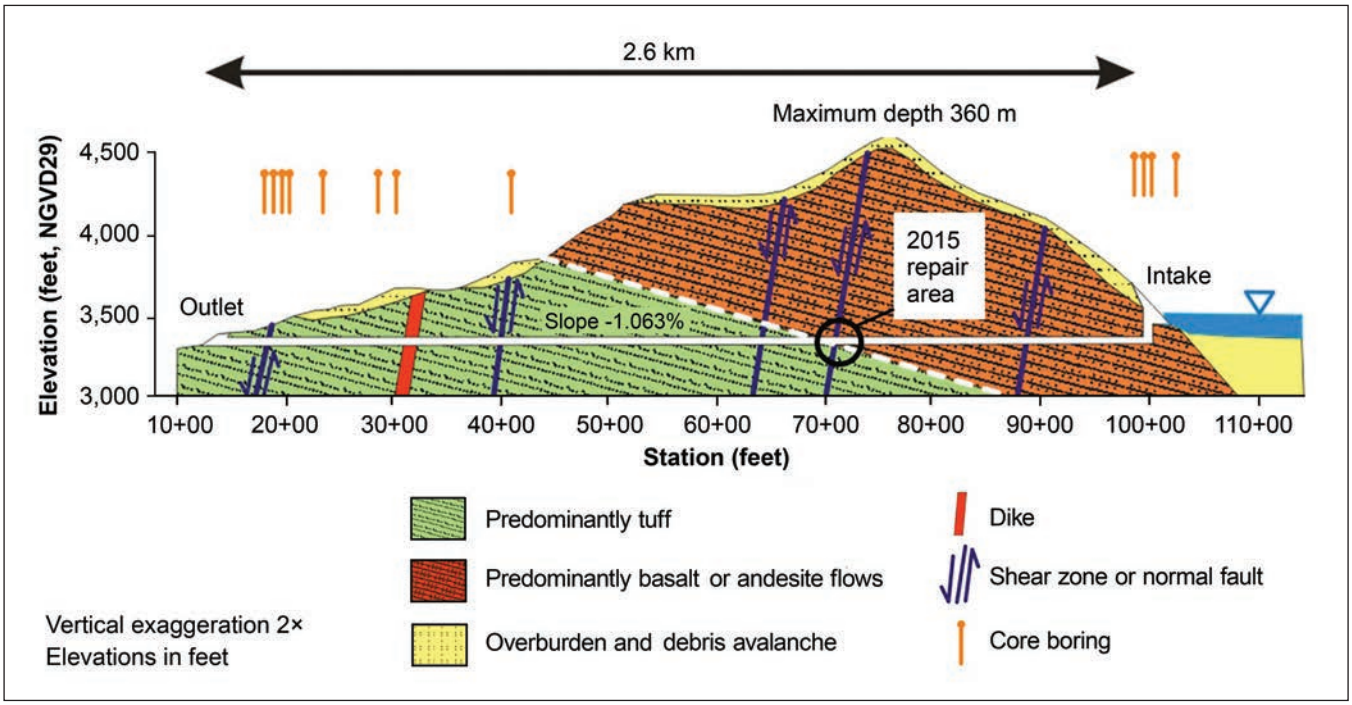

Figure 4-1—Schematic depiction of geology of bedrock along tunnel alignment (from Britton et al. 2016).

> The western two-thirds of the tunnel penetrates a sequence of tuffaceous rock types. The tuffs…have strengths of 34 MPa to 100 MPa (710–2,100 ksf). Interbedded lava flows range from less than 30 m (100 ft) to greater than 100 m (330 ft) thick, with strengths between 100 MPa and 250 MPa (2,100–5,200 ksf). The eastern one-third of the tunnel penetrates a sequence of predominantly basaltic and andesitic lava flows with minor amounts of interbedded volcanic tuffs. The geologic contact between the two units is composed of soft, decomposed tuffs.

Twelve total, and five major, shear zones and faults were encountered along the tunnel (Britton et al. 2016). These faults and shear zones varied in width from 1 m (3 ft) to nearly 20 m (65 ft). They consist of highly fractured rock in various stages of decomposition and plasticity. Most of the shear zones cross the tunnel steeply nearly normal to its centerline. The two most significant shear zones, dubbed the Julie and Kathy L. shear zones, are in volcanic tuffs decomposed to weak rock and swelling clays (Britton et al. 2016). They form a 90-m (300-ft) long shear-zone complex near the geologic contact between the volcanic tuffs and basaltic andesite lava flows and lie under the maximum rock overburden (fig. 4.1). The two most significant shear zones within that complex are 15 m (~50 ft) and 20 m (65 ft) wide. The tunnel boring machine used to construct the tunnel had difficulty gripping the rock in this shear-zone complex, and the soft clay encountered caused deviation of the vertical alignment of the tunnel (Britton et al. 2016). A substantial inflow of ground water (4700 lpm; 1,200 gpm) was encountered when the Julie and Kathy L. shear-zone complex was penetrated, but that inflow subsided to a few lpm within days. Elsewhere, only small inflows (20 lpm; 5 gpm or less) were encountered locally from rock fractures.

Tunnel Construction

All but 70 m (225 ft) of the downstream tunnel was excavated using a tunnel boring machine (TBM) (Britton et al. 2016, Sager and Chambers 1986). The distal 70 m was excavated using a drill-and-blast method. The TBM bored the tunnel to a diameter of 3.4 m (11 ft). Three types of support systems were used to anchor the tunnel, depending upon rock quality. In “good rock” (55 percent of the tunnel), no supports were used. In “fractured rock” (35 percent of tunnel), the walls and roof were covered with a minimum of 5 cm (2 in) of reinforced shotcrete. In “sheared rock” (10 percent of the tunnel), a steel rib set–shotcrete support system was placed along the walls and roof (285 degrees of the tunnel circumference). The floor along the length of the tunnel was lined with pre-cast or cast-in-place concrete (Sager and Chambers 1986).

The steel rib-set support system was designed based on rock loads estimated using the modified Terzaghi rock-load classification system (e.g., Britton et al. 2016, Hoek and Brown 1980, Sager and Chambers 1986). Based on rock quality and squeezing ground encountered in the worst shear zones and the classification system used, the original tunnel design called for 150-mm (6-in) wide steel ribs having 250 MPa (36 ksi) yield strength. Owing to constructability issues with the TBM used, the contractor proposed, and the USACE accepted, using 100-mm (4-in) wide steel ribs having 250 MPa (36 ksi) yield strength. Standard rib spacing was to be 1.2 m (4 ft), but spacing could be as little as 0.3 m (1 ft) in zones of squeezing ground (Britton et al. 2016, Sager and Chambers 1986). Where needed, drains were installed 1.5 m (5 ft) into the tunnel roof.

The greatest difficulty during tunnel construction occurred when the TBM encountered the 90-m (~300-ft) wide Julie and Kathy L. shear-zone complex (Britton et al. 2016). Within that shear-zone complex steel rib sets were spaced as close as 0.6 m (2 ft) including through a 20 m (65 ft) long section of very highly sheared tuff adjacent to, but downstream of, the contact with basaltic andesite. The contact between the major bedrock units dips upstream in the tunnel. As a result, “good rock” in the basaltic andesite on the upstream side of contact was reached in the tunnel roof before the contact was reached in the tunnel floor. The contractor stopped placing steel ribs along the highly sheared zone once the roof contact was reached. Thus, a section of sheared volcanic tuff along the tunnel walls and floor was left unsupported by steel ribs upstream of the vertical projection of the contact in the tunnel roof. In that unsupported zone, a few steel struts were installed and the floor covered with cast-in-place concrete (Britton et al. 2016, Sager and Chambers 1986).

Tunnel Performance

Since the tunnel became operational in 1985, it has been inspected annually to gauge its integrity. Some inspections resulted in minor patchwork repairs to correct distressed shotcrete, particularly within the Julie and Kathy L. shear-zone complex (Britton et al. 2016). During an inspection in October 1992, significant distress within a 30-m (100-ft) long section of the Julie and Kathy L. shear-zone complex was discovered. Large sections of shotcrete had pulled away from the tunnel walls, the floor had heaved and cracked the precast flooring, and rib sets had buckled and sheared. Owing to this magnitude of distress, indicative that squeezing ground was affecting the full tunnel diameter, a repair plan was devised and funding secured, and in late 1995 (and in 1996), the repairs were implemented. The repair consisted of removing distressed shotcrete and heaved material, and installing a more robust

rib set–shotcrete support system (Britton et al. 2016). Thirty-four full-circular, 200-mm (8-in)-wide steel rib sets having 350 MPa (50 ksi) yield strength were installed within the distressed section. The original rib sets had been installed using both 0.6-m (2-ft) and 1.2-m (4-ft) spacing. After excavating material between the original rib sets, the new rib sets were installed and covered with either reinforced shotcrete or cast-in-place concrete (Britton et al. 2016). The original rib sets were left in place.

Although there have been no signs of additional movement along the section of tunnel repaired in 1995 and 1996, the repair slightly constricted the tunnel (Britton et al. 2016). This constriction in combination with the deviated vertical alignment effected during original construction produced unacceptable flow depth at full flow capacity. Thus discharge through the tunnel had to be reduced. This reduced capacity slightly increased the risk of an unusual hydrologic event raising the lake level higher than the maximum safe operating level. But this minimal increase in "flood" risk balanced against a safe, but lower, tunnel outflow capacity of 10 $m^3 s^{-1}$ (350 cfs), which would prevent tunnel pressurization, was deemed acceptable (Britton et al. 2016).

Subsequent to the 1996 repair, floor heave was noted along the upstream end of the Julie and Kathy L. shear-zone complex in the vicinity of the contact between major rock units. Over a span of several years, the floor heaved approximately 0.6 m (2 ft) but then stabilized (Britton et al. 2016). Despite this heave, the tunnel still passed its reduced discharge without violating flow depth criteria. During an inspection in October 2014, an additional 0.5 m (1.5 ft) of floor heave was discovered; the tunnel walls and roof showed no distress. A followup inspection in April 2015 revealed an additional 0.1 m (0.3 ft) of floor heave (Britton et al. 2016) (fig. 4.2). As a result, the tunnel diameter had been reduced to about 2 m (7 ft), far below its design of 3.4 m (11 ft). A hydraulic routing analysis showed that flow capacity within the tunnel would have to be restricted further to 7 $m^3 s^{-1}$ (250 cfs) to avoid violating flow depth criteria (Britton et al. 2016). Because this reduced level of flow capacity to prevent pressurization would significantly increase the potential for an unsafe rise in lake level during an unusual hydrological event, another major repair was required.

The tunnel was closed, and repairs commenced in January 2016. The repair consisted of excavating the heaved material and installing the same full-circle, 200-mm (8-in) wide steel rib sets that were used in the 1996 repair, spaced at 0.6 m (2 ft). Steel lagging was placed between rib sets and the volume between the ribs, lagging, and excavated ground filled with non-shrink grout; ribs and lagging

Figure 4-2—Location where tunnel floor had heaved. Note offset in tunnel floor from where person is standing to water flow in foreground (from Britton et al. 2016).

were then covered with shotcrete (Britton et al. 2016). During the 2016 repair, wall and roof rock were excavated back so that the larger, more robust rib sets would not constrict tunnel diameter as they had following the 1996 repair. Following the repair, tunnel flow capacity was restored to at least 10 $m^3 s^{-1}$ (350 cfs). Though this still requires a restriction on headgate opening capacity, the slightly increased risk of raising lake level above the maximum safe operating level during an unusual hydrological event balanced against outflow that does not pressurize the tunnel is deemed acceptable (Britton et al. 2016).

The USACE anticipates that other sections of the Julie and Kathy L. shear-zone complex will deform in the future. But owing to the positive performance of the 1996 repair, it does not anticipate having to repair again the sections already rehabilitated. It expects that the same full-circle, wide steel rib sets used in the 1996 and 2016 repairs can be deployed throughout that shear zone complex to provide a successful rehabilitation that will require less maintenance and intervention (Britton et al. 2016).

Chapter 5: Hydrology and Potential Hydrologic Loading of the Spirit Lake Outlet

Background and Context

The hazard posed by Spirit Lake is fundamentally about water. Understanding where that water comes from, the relationship between water storage and lake level, and the circumstances under which it could initiate a breach of the blockage are critical to evaluating the current condition of the lake and possible future alternatives for its management. Here we describe the hydrology of the Spirit Lake watershed; estimate the magnitude, duration, and volume of extreme hydrologic events; and define the hydrologic risk potential posed by the hydrology of the system. In addition, we evaluate the hydrologic consequences of the largest possible floods in Spirit Lake for a range of plausible alternative outlets; results of this analysis are then incorporated into the assessment of risk (see chapter 8). Much of this material draws from a recent U.S. Army Corps of Engineers (USACE) analysis (USACE 2016a), but we also use other sources and attempt to synthesize a comprehensive evaluation of the hydrologic drivers that could lead to catastrophic flooding, and their uncertainties.

Analysis of the hydrology of Spirit Lake basin and placing it into historical and statistical context are inevitably constrained by the sparse data available. The Natural Resources Conservation Service has operated a SNOTEL site at Spirit Lake (Site 777) since October 4, 1983, providing precipitation, temperature, and snowpack data. Other nearby SNOTEL sites and their inception dates are Sheep Canyon (Site 748; October 1, 1980); Swift Creek (Site 1012; August 13, 2002) and June Lake (Site 553; December 11, 1980). The closest weather site that predates the 1980 eruption was 40 km (25 mi) away at Glenoma, Washington. Streamflow measurements are similarly sparse, and there are no streamflow gauges on any streams draining into Spirit Lake. The closest U.S. Geological Survey (USGS) gauges currently operating downstream are on the North Fork Toutle River below the sediment retention structure near Kid Valley, Washington (site 14240525) and the lower Toutle River at Tower Road near Silver Lake, Washington (site 14242580) (see sites FTP and TOW in fig. 2-7). The USGS has operated a gauge that records the elevation of Spirit Lake near the tunnel intake since October 29, 1987 (site 14240304). This gauge plus the known elevation-volume curve for Spirit Lake allows for calculating inflows to the lake on a daily basis based on the change in lake elevation. Sparse meteorological, streamflow, or lake level information in this area from before the eruption constrains analysis to the roughly three decades since the eruption and limits estimates of the frequency and magnitude of storms and discharge events.

Climate and Precipitation Patterns in the Spirit Lake Watershed

The regional and local climates determine the pattern of precipitation. The position of high- and low-pressure systems over the North Pacific largely controls the climate of the Pacific Northwest. During fall and winter, the Aleutian low and Pacific high move southward; their interaction produces west to southwesterly flow of moisture-laden air, resulting in cool and wet winters. During the spring and summer, the Aleutian low weakens and moves northward, and high pressure dominates the region, resulting in a west to northwesterly flow of dry and relatively cool air. Most precipitation, therefore, occurs in winter (November–March) with relatively little summer moisture.

The precipitation regime in the Spirit Lake basin includes both rain and snow, as elevations in the basin range from 1050 m (3,450 ft) to 2545 m (8,355 ft). Average annual precipitation from 1981 to 2010 at the Spirit Lake SNOTEL site is 2260 mm (90 in) and ranges from 1335 to 3535 mm (50 to 140 in). Estimated average precipitation for the 47 km^2 (18 mi^2) basin as a whole is 3175 mm (125 in) (PRISM Climate Data 2016, USACE 2016a). Over the period of record at the Spirit Lake SNOTEL site, peak snow-water equivalent (SWE) has ranged from 60 to 935 mm (~2.5 to 37 in), 5 to 26 percent of annual precipitation. Peak SWE typically occurs in March or April, and the snowpack melts off quickly through May and June.

There are no large rivers feeding Spirit Lake; instead, numerous small creeks and gullies drain into the lake from all sides. Slopes immediately adjacent to the lake are steep and lack substantial vegetation, resulting in rapid runoff during storms. Very short rainfall to runoff response was most pronounced immediately following the 1980 eruption owing to the new ash blanket with very low hydraulic conductivities (Leavesley et al. 1989). Over the intervening years since the eruption, rainfall-to-runoff timescales have been slowed by drainage network development and increased permeability of the hillslope material (Major and Yamakoshi 2005). Runoff generally follows the normal annual precipitation pattern and is highest from November through February and lowest from August through September.

Effects of Hydrologic Events and Floods Across a Range of Scales

From the standpoint of hydrologic loading, we are interested in the volume of water that can be delivered to the lake in a specific amount of time, and the corresponding rise in lake level. The absolute elevation of the lake, and hence the risk of a breakout flood, is related to two factors: the volume(s) of water delivered by

hydrologic events and the elevation of the lake at the time of these events. Although the volumes associated with individual events and corresponding lake volume and elevation change can be calculated, the starting elevation for any particular event cannot be known and must be treated probabilistically.

We consider three distinct classes of hydrologic events: (1) "normal" annual flow volumes resulting from seasonal patterns of precipitation and snowmelt, (2) large historical floods, and (3) the estimated probable maximum flood (PMF). Each of these classes of hydrologic phenomena has different antecedent conditions, inflow volumes, and potential lake elevation changes associated with it.

In comparing the effects of events of different magnitudes on the potential risk of blockage failure, it is important to recognize that the absolute discharge (volume per unit time) and peak flow associated with any event are less important than the total volume of the event, as the latter directly influences the change in the lake's volumetric storage and level. We, therefore, consider the total volumes associated with these different types of events.

To provide a useful reference for understanding event volumes, we related them to the volume-elevation curve for Spirit Lake. The data for this relationship were developed by the USACE in 1983 (USACE 2016a) and recently checked against 2009 LiDAR for the upper elevations (fig. 5-1). For consistency, we use the original (1983) data; differences between these data and the newer LiDAR ranged from 0.2 to 1.0 percent. We linearly interpolate to extend the volume-elevation relationship to the estimated base of the pyroclastic deposits along the crest of debris blockage (1069 m; 3,506 ft; see chapter 3).

The USGS gauge that records lake level provides critical data for understanding the risk of blockage failure from hydrologic processes (fig. 5-2). We draw two conclusions from this plot. First, lake levels have been consistently higher since 2004, in part because of the tunnel intake gate restriction (75 percent of its full 4-ft opening) to minimize the risk of flow depth in the tunnel exceeding design depth (see chapter 4). Second, it is clear that high stands of the lake that come close to exceeding 1055 m (3,460 ft), the designated maximum safe operating elevation, occur only during periods of extended closure for tunnel repair. Otherwise, lake level is maintained 5 to 6 m (15 to 20 ft) below this threshold elevation.

The record of fluctuating lake levels along with the known elevation-volume curve for Spirit Lake makes it possible to calculate inflows to the lake on a daily basis since October 29, 1987 (fig. 5-3). The inflow derives from a water balance between changes in lake volume and the calculated outflow through the tunnel based on the tunnel's stage-discharge relation. Full details for how inflows were calculated are contained in USACE (2016a).

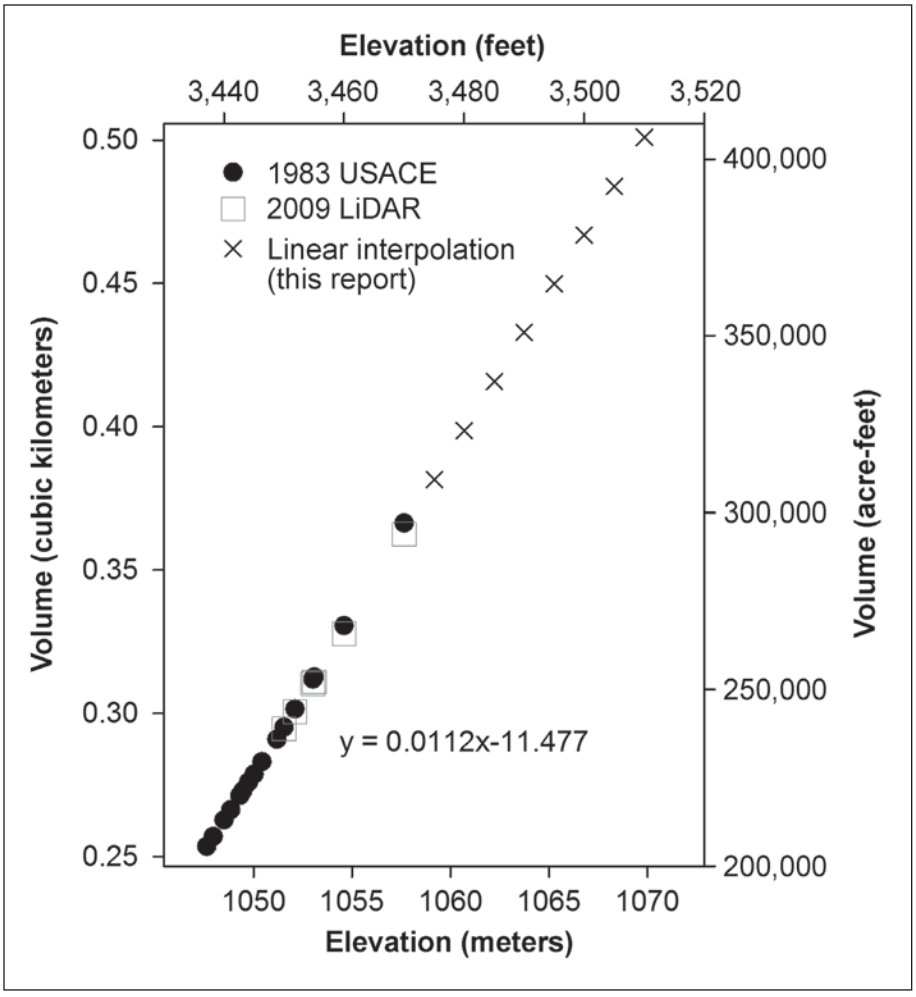

Figure 5-1—Elevation-volume curve for Spirit Lake. Original 1983 design values (solid circles) and 2009 LiDAR-derived data (open squares) both from USACE (2016a). Equation for linear interpolation (X) of volumes for higher elevations given in SI units. Elevations reported in NGVD29.

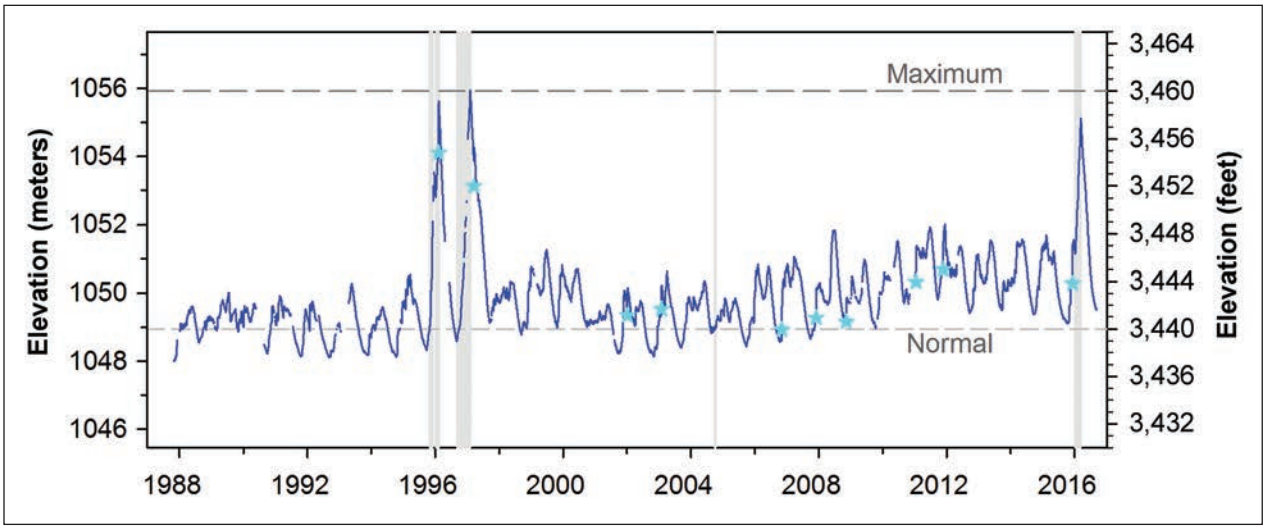

Figure 5-2—Daily water-surface elevation of Spirit Lake from October 1987 through September 2016 from U.S. Geological Survey gauge at Tunnel at Spirit Lake, Washington (14240304) with normal operating level and maximum elevation for safe operation. Gray vertical bars indicate periods of extended tunnel closure, and stars indicate the timing of the 10 largest 1-day inflows during the period of record (USACE 2016a).

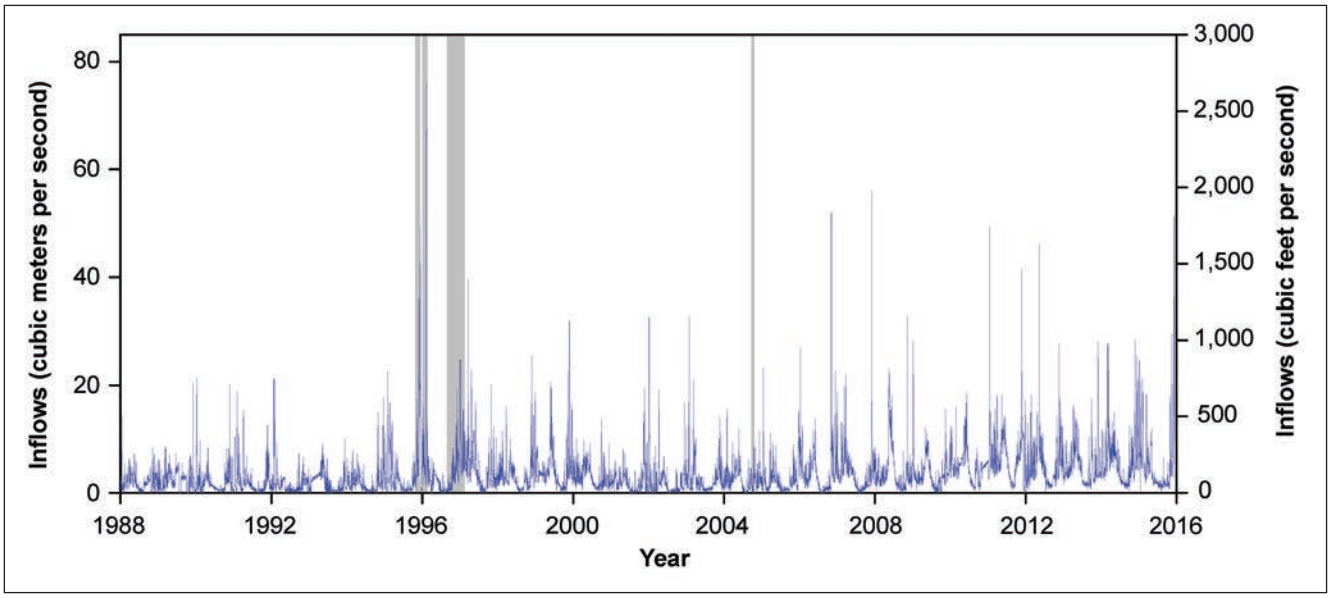

Figure 5-3—Reconstructed inflows to Spirit Lake, from USACE (2016a). Gray vertical bars indicate periods of extended tunnel closure.

The USACE considers 11.3 $m^3 s^{-1}$ (400 cfs) to be the average inflow to Spirit Lake (USACE 2016a). The tunnel is designed to pass a maximum 15.6 $m^3 s^{-1}$ (550 cfs) outflow. To place this inflow into a volumetric perspective, a flow of 11.3 $m^3 s^{-1}$ (400 cfs) corresponds to a volume change of ~987 000 $m^3 day^{-1}$ (800 ac-ft day^{-1}). From the linear trend of the elevation-volume curve (fig. 5-1), 30 cm of elevation change corresponds to 3.5 million m^3 (2,870 ac-ft per one foot of elevation change);

thus, at "normal" flow and without any outlet, the lake would rise on average 30 cm (1 ft) every 3.5 days. In very rough terms, if lake outflow was blocked, it would take approximately 230 days for the lake to rise from its normal operating elevation (1049 m; 3,440 ft) to the base of the pyroclastic deposits along the blockage crest (1069 m; 3,506 ft), and about 160 days to rise from the highest recorded lake stand at 1055.5 m (3,462 ft) to 1069 m (3,506 ft). This reveals an important fact about the Spirit Lake outlet system: under "normal" inflows, a complete failure of the existing outlet would not result in an instantaneous flood but rather would require the lake to fill over an additional 5 to 8 months before a breakout flood was imminent. This lag time from outlet failure to blockage breaching likely would allow for intervention (i.e., pumping operations following the 1980 eruption) to remove or minimize the risk of catastrophic lake release. In other words, unlike an instantaneous failure of a constructed dam, a total failure of the outlet at Spirit Lake under normal flow conditions is best characterized as having the potential for a "slow-onset disaster."

Loading Resulting From Large and Extreme Historical Floods

We also consider the potential for the lake to fill and fail under exceptional hydrologic conditions, such as the large regional floods that occurred in 1996–1997 (Colle and Mass 2000). Such large floods are typically "rain-on-snow" events, where very high rainfall intensities combine with unusually warm air temperatures and moist winds to melt snowpack rapidly, contributing large volumes of snowmelt-derived water to the rainfall totals (Harr 1981). For example, at June Lake in southwestern Washington during the February 1996 flood, approximately 1000 mm (39 in) of runoff available water was generated from over 725 mm (28.5 in) of precipitation with the remainder snowmelt (Colle and Mass 2000, USACE 2016a).

Almost all large floods in this region occur during the rainy season (November to March) with substantially smaller peaks during the snowmelt season (April to June). The top five maximum daily inflows for the snowmelt season range from 19.3 to 22.9 $m^3 s^{-1}$ (680 to 810 cfs), with the maximum on record at 46.2 $m^3 s^{-1}$ (1,630 cfs) (May 2012). For the rainy season, the top five inflows range from 41.7 to 56.1 $m^3 s^{-1}$ (1,470 to 1,980 cfs), with the 1996 flood (flood of record) a significant outlier (79 $m^3 s^{-1}$; 2,790 cfs). The largest recorded storm inflows are on the order of four to six times the "normal" flow of 11.3 $m^3 s^{-1}$ (400 cfs) (table 5-1). Analysis of the hydrographs from individual inflow events gives an indication of the average duration and volume for large storms.

Total inflow volumes during floods are roughly an order of magnitude (10×) larger than "normal" daily inflow volumes. Using the calculated rate of rise of 3.5

Table 5-1—Event discharges, durations, and volumes

Event type	Peak flow	Duration	Total event volume
	$m^3 s^{-1}$ (cfs)	*Days*	*km^3 (ac-ft)*
Average annual	11.3 (400)	N/A	0.010 (800)
Annual peaks[a]	*low [mean] high* 32.6 [43.0] 56.1 (1,150 [1,520] 1,980)	*low [mean] high* 8 [13] 25	*low [mean] high* 0.007 [0.015] 0.029 (5,910 [12,220] 23,600)
Flood of record (1996)	79.0 (2,790)	8	0.020 (15,800)
Probable maximum flood	1,218.5 (43,000)	9	0.069 (56,000)

N/A = Not applicable.

[a] From ranking of annual peak events (USACE 2016a). Nine largest events during the period of record, excluding flood of record.

million m^3 per 30 cm of lake rise (2,870 ac-ft per foot of lake elevation rise), a large flood event could raise the lake level about 1.5 to 2 m (5 to 6 ft) (fig. 5-1).

A composite flow frequency curve developed from the reconstructed inflow record reveals the full range of flows of different durations (fig. 5-4) (USACE 2016a). Although separate rain and snowmelt season curves were developed, we show only the rain curve here as it represents larger flows. Peak flows are approximately twice the 1-day flow for the same recurrence interval.

A detailed probabilistic analysis was conducted to assess the frequencies of lake elevations at different levels depending on the starting elevation of the lake and the storm magnitude (USACE 2016a). Monte Carlo simulation was used to establish different probabilities of starting lake elevations at the time of different events; the probability of the flow event was derived from the 10-day flow frequency curve (fig. 5-4). The 10-day event represents the flood because this event was empirically determined to have the best correlation with lake-level change (USACE 2016a). The results of this analysis allowed for confidence limits to be applied to the resulting pool-stage frequencies and make it possible to establish a level of risk for exceeding the maximum safe operating elevation (fig. 5-5).

A flood of the type recorded in the historical record (not the PMF) resulting in a lake rise that reaches the maximum safe operating elevation has an annual exceedance probability of approximately 0.001. Annual exceedance probability, also referred to as annual probability or exceedance probability, is the probability of an event of a specified magnitude occurring in a given year. The probability that this type of flood will cause the lake to rise to the level necessary to induce seepage erosion in the pyroclastic deposits is many orders of magnitude less. An

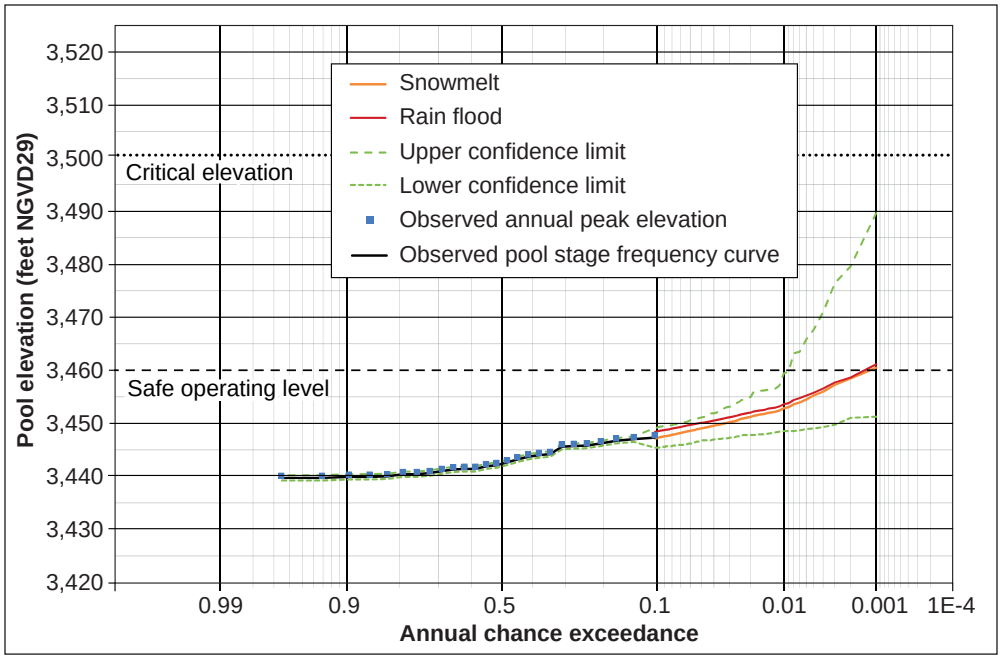

Figure 5-5—Pool-stage frequency curve for current operating conditions based on Monte Carlo simulation. Source: USACE (2016a).

important caveat for this analysis, however, is that the starting lake elevations were treated probabilistically. In reality, although high stands of the lake near maximum safe operating level are rare from a population or percentage of time perspective, they occur commonly during tunnel maintenance and repair. Lake levels near maximum safe operating level have occurred three times in the 32 years since the tunnel opened. More precisely, the tunnel has been closed for 285 days since it was opened. This represents approximately 2 percent of the 32 years of operation. In fact, it is **only** during maintenance and repair episodes that the lake has reached this level since the tunnel became operational. Thus the results of this analysis need to be seen through the lens that events (e.g., high lake levels) that are rare in the aggregate are relatively common when special circumstances apply (e.g., tunnel maintenance and repair).

In summary, all high lake levels occurred during periods of extended tunnel closure, or put another way, all extended closures promoted high lake levels. Inflows during historically large floods can promote high lake stands if they occur during times of closure. The highest lake levels in 1995 and 1996 occurred when large storms or extended wet periods accompanied times of tunnel closure. But large storms are not required to raise the lake level to the safe operational threshold. During times of closure, average inflows can also raise the lake level. Large floods that have occurred when the tunnel has not been closed have not resulted in high lake stands.

Loading Resulting From the Probable Maximum Flood

The probable maximum flood (PMF) is the largest flood that could conceivably occur at a particular location, and here represents the most extreme hydrologic loading that could occur in the Spirit Lake watershed. To understand the potential impact of a PMF, we consider how lake level might rise for the range of starting elevations and outflow rates associated with the existing tunnel and plausible alternative outlets.

Deriving the PMF generally takes into consideration (1) the probable maximum precipitation (PMP), (2) maximum basin snowmelt, (3) minimum surface losses, and (4) a unit hydrograph that reflects characteristic basin runoff. In generating the PMF for Spirit Lake, the USACE (1983) used the best available data to estimate the worst-case scenario for a flood-generated rise in lake level. The protocol included a method of estimating PMP, a method subsequently revised by the National Weather Service in 1994. The revision generally results in a downward adjustment of PMP values for the region. The PMF generated in 1983 and used without revision by the USACE (2016b) may be conservative, as the PMP is the single most influential factor driving the PMF.

The hydrograph used in the 1983 routing analysis began at an average January lake level, had an antecedent condition of saturated ground, and consisted of a double event. The 9-day duration event includes a 100-year flood followed by the PMF, and the analysis assumes outflow through a tunnel having a peak discharge of 15.9 $m^3 s^{-1}$ (560 cfs). This exceedingly rare combination of events had an estimated volume of 69 million m^3 (56,600 ac-ft) and produced a 5.5-m (18-ft) rise in lake level. Following this PMF, Spirit Lake requires 6 months to return to normal lake level assuming average inflow and outflow conditions. The original outlet design allowed for 6.1 m (20 ft) of freeboard to accommodate rare hydrological events temporarily without exceeding the maximum safe operating lake level (see chapter 3).

The current risk assessment does not update the PMP/PMF analysis, but it does generate new routing scenarios that apply the current standard of practice in defining the PMF to each of the alternative conditions evaluated. Rather than using the 100-year flood followed by the PMF, the new routing begins with a peak inflow that is half of the PMF, followed 5 days later by the PMF. This updated protocol results in a significant increase in flow over the original scenario. The shape of the hydrograph for the updated PMF is identical to that developed in the 1980s (fig. 5-6).

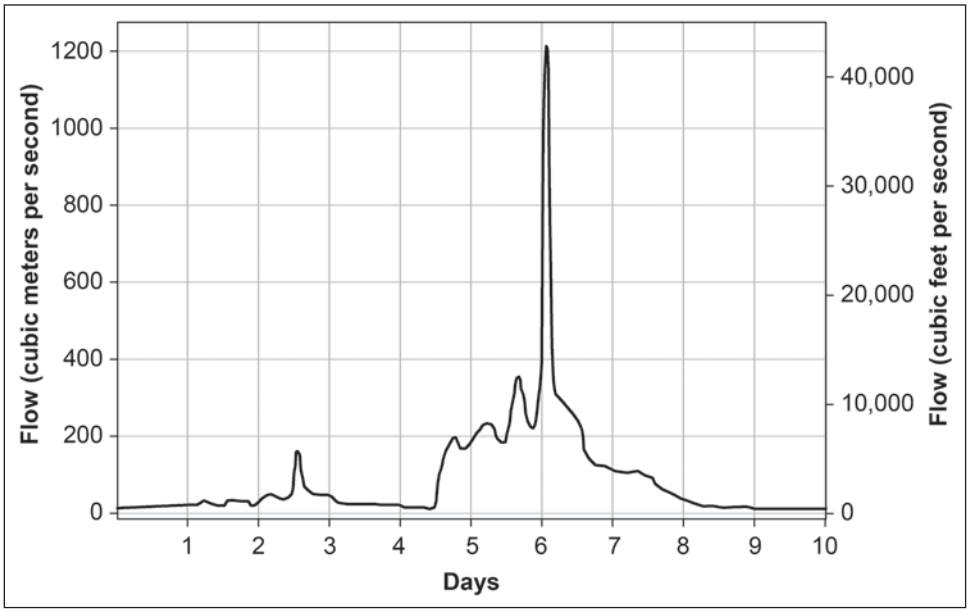

Figure 5-6—Hydrograph of the rainy season (November–March) Probable Maximum Flood . Source: USACE (2016a).

The PMF has a peak discharge of 1219 $m^3 s^{-1}$ (43,000 cfs) and an event volume of 69 million m^3 (56,000 ac-ft) (fig. 5-6). To place this flow into context, this is about 15 times the maximum 1-day peak flow and 3.5 times the volume of the February 1996 storm of record as reconstructed from the lake level record (table 5-1). For a drainage area of 47 km^2 (18 mi^2), a peak flow of 1219 $m^3 s^{-1}$ (43,000 cfs) represents an upper outlier on a curve of the largest floods ever measured from all gauges within the continental United States (O'Connor et al. 2002).

A key analysis (USACE 2016a) compared the PMF routing under different starting assumptions and conceptual outlet alternatives. "Routing" in this context refers to calculating the rise in lake level that includes the hydraulic effects of different outlets. That is, the inflow to the lake over time was reduced by the outflow through the tunnel using different gate openings, through hydraulically equivalent buried conduits, and through a conceptual open channel; these alternatives are described in greater detail in chapter 8 (USACE 2016a):

- Alternative 1—Existing tunnel and intake.
- Alternative 2—Major rehabilitation of the existing tunnel and intake.
- Alternative 3—A conduit shallowly buried across the debris blockage fed by a permanent pumping facility.

- Alternative 4—A gravity-fed conduit more deeply buried across the debris blockage.
- Alternative 5—An open channel across the debris blockage.

In calculating the hydrologic loading associated with the PMF, these five alternatives can be collapsed into three hydraulically equivalent alternatives:

- Existing restricted condition (Alternative 1), which reflects the currently hydraulically constricted tunnel with a 3-ft (1-m) gate opening.
- Rehabilitated tunnel or alternative conduit outlet (Alternatives 2 through 4), which provide full outflow capacity (15.6 $m^3 s^{-1}$ [550 cfs]).
- Riverine channel that drains the lake (Alternative 5).

Two different initial conditions of lake elevation were employed in the analysis: a normal pool elevation (1049 m [3,440 ft]; Scenario 1); and a lake elevation raised to 1052 m (3,450 ft) as a result of an antecedent flood equal to one-half the PMF (Scenario 2). Analyses also were done for the tunnel closed by repair or failure (Alternative 1b); in these analyses there is no lake outflow. The results (USACE 2016a) are shown in table 5-2 and figs. 5-7 through 5-10.

Table 5-2—Probable maximum flood routing scenarios of alternative conditions

	Starting elevation		Peak elevation		Distance below SOL[a]		Distance below pyroclastic deposit base[b]		Peak outflow		Recession time to NOL[c]
	Meters	*Feet*	*Meters*	*Feet*	*Meters*	*Feet*	*Meters*	*Feet*	$m^3 s^{-1}$	*cfs*	*Months*
Alternative 1a (gate open)											
Scenario 1	1048.8	3,440	1054.8	3,459.7	0.1	0.3	14.1	46.3	10.0	353	8+
Scenario 2	1051.6	3,449.4	1056.9	3,466.5	-2.0	-6.5	12.0	39.5	11.4	403.3	8+
Alternative 1b (gate closed)											
Scenario 1	1048.8	3,440	1063.0	3,486.5	-8.1	-26.5	5.9	19.5	0	0	—
Scenario 2	1051.9	3,450.3	1065.3	3,494.2	-10.4	-34.2	3.6	11.8	0	0	—
Alternatives 2–4											
Scenario 1	1048.8	3,440	1054.3	3,458.2	0.6	1.8	14.6	47.8	13.0	458.2	6
Scenario 2	1051.6	3,449.1	1056.6	3,465.5	-1.7	-5.5	12.3	40.5	15.3	540.2	7
Alternative 5											
Scenario 1	1048.8	3,440	1052.8	3,453.2	2.1	6.8	16.1	52.8	137.8	4,863	6
Scenario 2	1050.1	3,444.3	1053.4	3,455.2	1.5	4.8	15.5	50.8	176.6	6,233	7

— = No data.

[a] SOL = safe operating level (SOL) = 1054.9 m (3,460 ft).

[b] Pyroclastic deposit base = 1068.9 m (3,506 ft).

[c] NOL = normal operating level = 1048.8 m (3,440 ft).

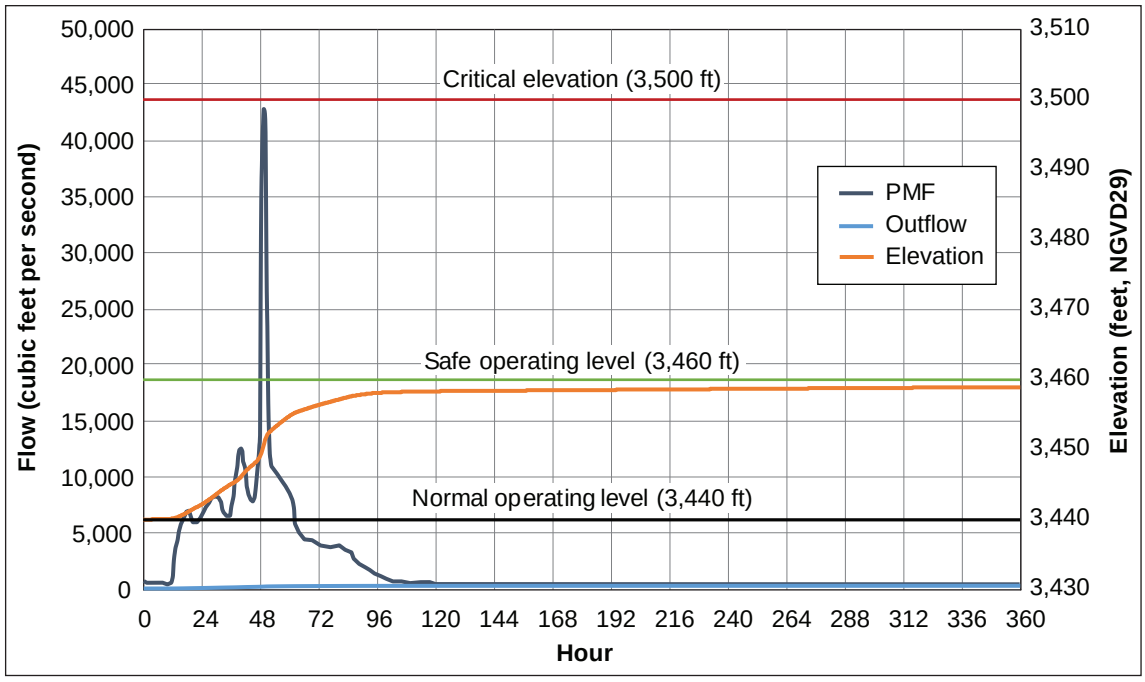

Figure 5-7—Probable maximum flood (PMF) routing Scenario 1, Alternative 1. Outflow refers to discharge from the existing tunnel with the gate open. Source: USACE (2016a).

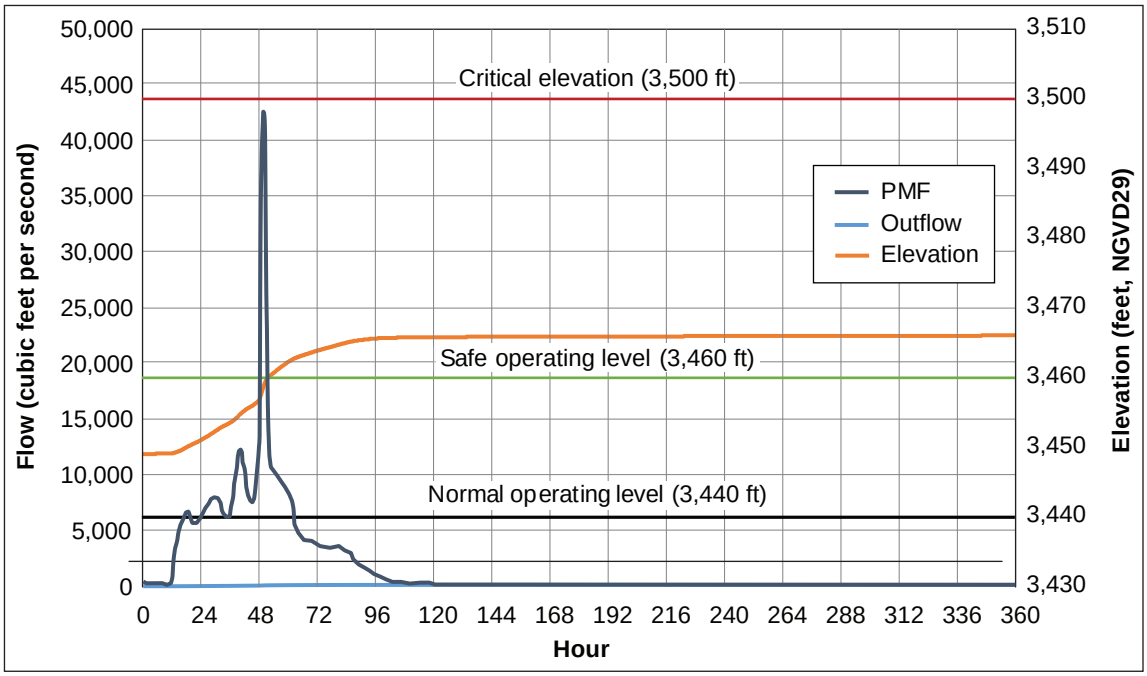

Figure 5-8—Probable maximum flood (PMF) routing Scenario 2, Alternative 1. Outflow refers to discharge from the existing tunnel with the gate open. Source: USACE (2016a).

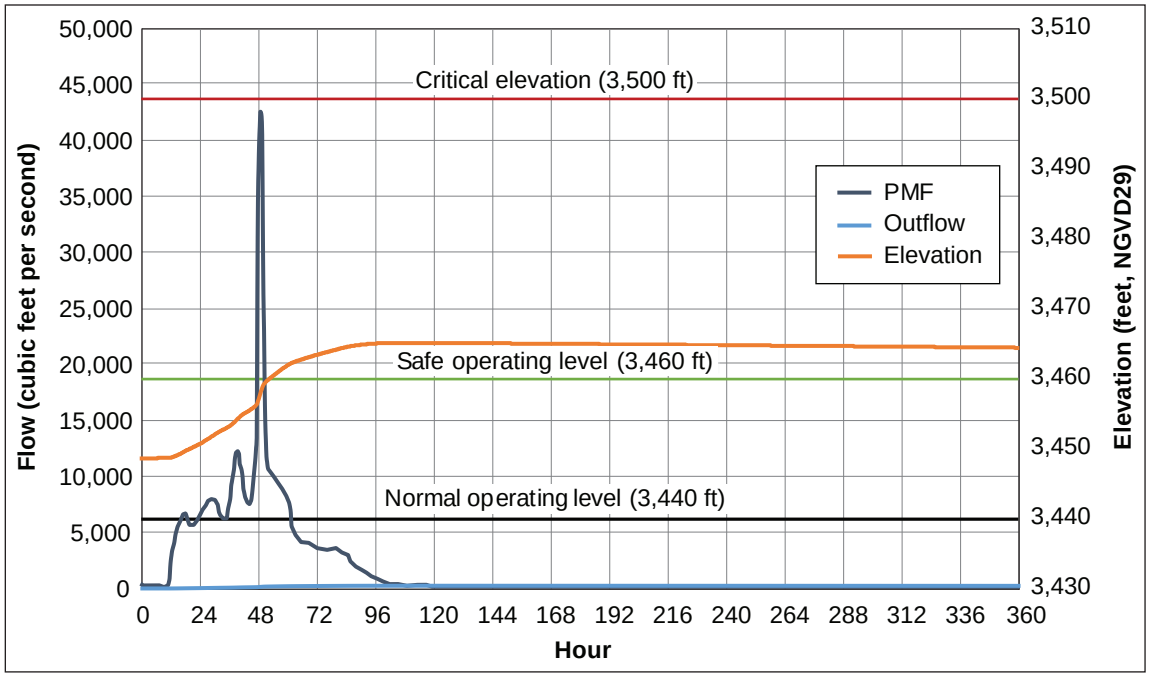

Figure 5-9—Probable maximum flood (PMF) routing Scenario 2, Alternatives 2 through 4. Outflow refers to discharge from the tunnel and augmented drainage infrastructure. Source: USACE (2016a).

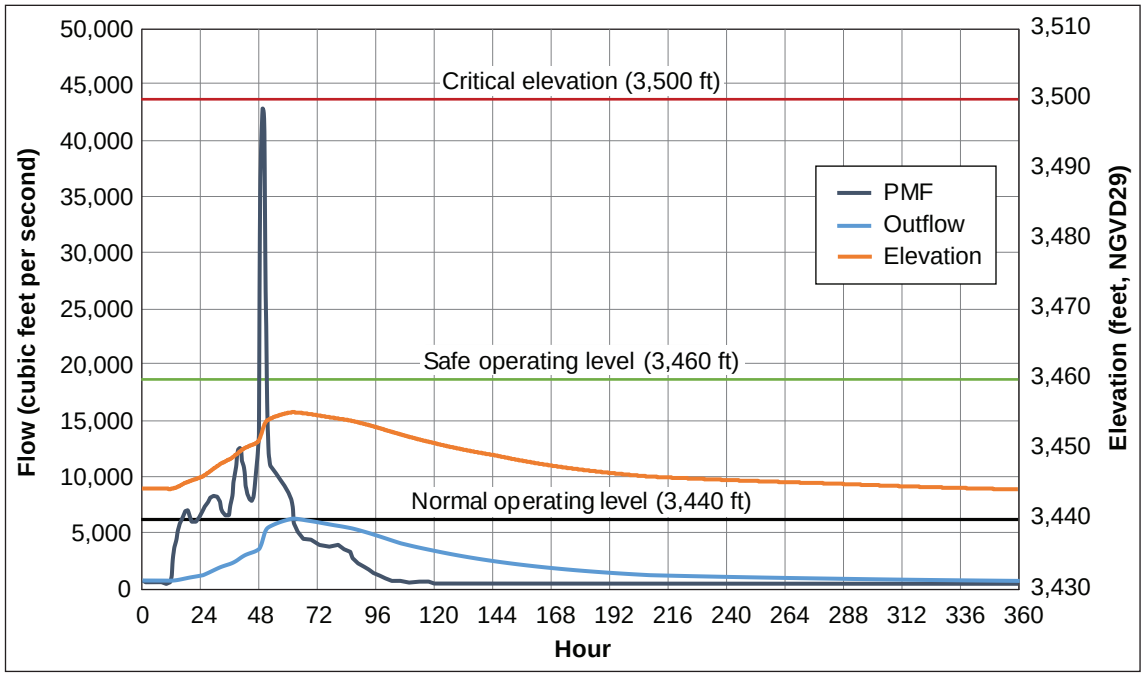

Figure 5-10—Probable maximum flood (PMF) routing Scenario 2, Alternative 5. Outflow refers to discharge from the open channel. Source: USACE (2016a).

This analysis reveals several key points. First, although a PMF is a highly unlikely event, under existing outlet conditions it has the potential to raise the lake elevation above the established maximum safe operating elevation for prolonged periods of time (weeks to months) (fig. 5-8; table 5-2). This is particularly the case when the lake is already at a high level, owing either to antecedent conditions (i.e., Scenario 2) or to extended tunnel closure. If a PMF occurred when the lake was already at a high level (1051 to 1055 m; 3,450 to 3,460 ft) and the tunnel was closed, lake elevation would rise to nearly the contact between the debris avalanche and pyroclastic deposits and a catastrophic failure could be imminent. As previously noted, lake elevations up to the maximum safe operating level have occurred three times in the past 30 years during tunnel closure. Hence, Spirit Lake is at maximal risk from PMF-scale hydrologic loading when the lake is artificially elevated. Indeed, this is the **only** circumstance when the hydrologic loading could result in rapid (days) failure of the blockage.

Second, in the event of an extremely large PMF-scale flood, the outflow capacity of the tunnel (maximum capacity is 15.6 $m^3 s^{-1}$ [550 cfs]) does not allow the lake to drain rapidly (figs. 5-7 and 5-8). Essentially, the volume of water involved in a PMF is orders of magnitude larger than can be passed by the tunnel swiftly. Even with the tunnel at full outflow capacity, the lake would require about 6 to 8 months to drawdown to the normal operating level.

The open channel alternative (Alternative 5) is less constrained than the “pipe” options (Alternatives 1 through 4) for releasing water from the lake (figs. 5-9 and 5-10). In the channel, discharge scales with lake elevation, and the lake level drains down from precarious levels faster (fig. 5-10).

A PMF-routing analysis was not conducted using a starting elevation at the maximum safe operating level (SOL), a condition that simulates lake level following an extended closure for tunnel repair. But the results from lower starting elevations indicate that an even higher probability of reaching the pyroclastic-deposits contact would apply to Alternatives 1 through 4 under that higher initial condition of SOL. The consequence of a higher starting elevation for the open channel alternative is less clear as the outflow would scale with the flood inflow, making high stands much less likely and drainage following a PMF much more rapid (fig. 5-10). The open channel alternative is therefore much less sensitive to initial conditions of lake level.

The PMF routing shows that the existing outlet infrastructure is potentially hydrologically unsafe or inadequate under some scenarios. Even with a tunnel or other pipe-like outflow operating at full capacity, lake level exceeds maximum safe operating level under any scenario in which lake level is elevated by at least a few

meters above normal operating level. But there is medium to low confidence in this assessment owing to the high degree of uncertainty in the PMP and PMF (USACE 2016a).

Summary

A detailed analysis of the hydrology of the Spirit Lake basin reveals both the soundness and vulnerabilities of the current infrastructure for releasing water from the lake and ensuring that a catastrophic breakout flood does not occur. Unlike constructed dams in which a failure of the infrastructure could lead to a near-instantaneous reservoir release, a complete failure or blockage of the existing tunnel will not result in an instantaneous outbreak flood. Instead, under most circumstances, many months are required for the lake to fill to a level that will induce breaching of the blockage. Presumably, this lag time would allow for intervention to reduce the risk of catastrophic failure.

The current tunnel outlet has worked well to pass both normal and historically large storm events. Over the 32 years that the tunnel has operated, lake levels have never exceeded 1055 m (3,460 ft), the designated maximum safe operating elevation. This elevation is conservative and based on current knowledge a potential failure of the debris blockage is remote unless lake level approaches or exceeds 1069 m (3,506 ft). Even a succession of very large storms would be unlikely to raise the lake to this critical elevation, but they reduce its capacity to accommodate additional stormflow significantly.

Despite the overall successful performance of the existing tunnel, this hydrological analysis revealed that the risk of a breakout flood is significantly heightened after extended closure for repair. The highest lake levels over the past 32 years have been associated with three periods of tunnel closure. During these three periods, lake levels approached the maximum safe operating level. A PMF routing analysis revealed that dangerously high lake levels can occur if a PMF-type event happens while the lake is artificially elevated. Although a PMF event has a very low likelihood of occurrence (annual probability ≤ 0.001) the combination of a PMF and high antecedent lake level could be catastrophic. There is a moderate to high degree of uncertainty about the absolute magnitude of the PMF; additional analysis may reduce this uncertainty.

Chapter 6: Pacific Northwest Seismicity and Potential Seismic Loading of Spirit Lake Outlet

Background Context

The Pacific Northwest lies along the Western U.S. continental margin, where the Juan de Fuca oceanic plate subducts obliquely beneath the North American continental plate. Subduction occurs along the 1100-km- (680-mi-) long Cascadia subduction zone, which extends from northern California to Vancouver Island, Canada. The Juan de Fuca plate subducts at a rate of about 4 cm yr^{-1} (1.6 in yr^{-1}). As a result of subduction and clockwise rotation of crustal blocks (fig. 6-1) (McCaffrey et al. 2007, Wells and McCaffrey 2013), the region is subject to three principle types of earthquakes: great megathrust earthquakes formed when the locked interface between the two plates releases suddenly, deep earthquakes formed within the subducting oceanic plate where it dehydrates and endures tension under flexure downdip of the locked interface, and crustal earthquakes resulting from stresses induced by block rotation and plate interactions. Historical earthquakes in the Pacific Northwest (since Euro-American settlement began in the early 1800s) have occurred on crustal faults or within the subducting slab; there have been no great megathrust earthquakes. Earthquake magnitudes, durations, and recurrence depend on the style of earthquake and where it originates; response to an earthquake at any specific site depends on the distance to the earthquake's hypocenter, pathway conditions, and specific site conditions.

Neither a probabilistic seismic hazard analysis (PSHA) nor site-specific seismic response analysis has been conducted for the Spirit Lake outlet project. However, various regional seismic studies have been conducted. The analysis of possible seismic hazard presented here relies upon a general understanding of the type, magnitude, and approximate frequency of regional earthquakes and the latest update of the U.S. Geological Survey (USGS) National Seismic Hazard Maps for the Western United States (Peterson et al. 2014, 2015).

The updated seismic hazard analysis for the Western United States considers both fault-based sources and seismicity-based random background earthquakes, which account for unknown faults. The analysis assumes that future, damaging earthquakes will occur largely near past earthquake locations or along known faults having evidence of past surface rupture (Petersen et al. 2014). Fault-based models are based on slip rates, earthquake magnitudes, and dates of offset, or on several measurements of geodetic strain rates across the region. Future seismicity-based background earthquakes are based largely on statistical analyses of a catalog of 5,622 earthquakes greater than or equal to magnitude (M) 3.5 that occurred between 1850 and 2012.

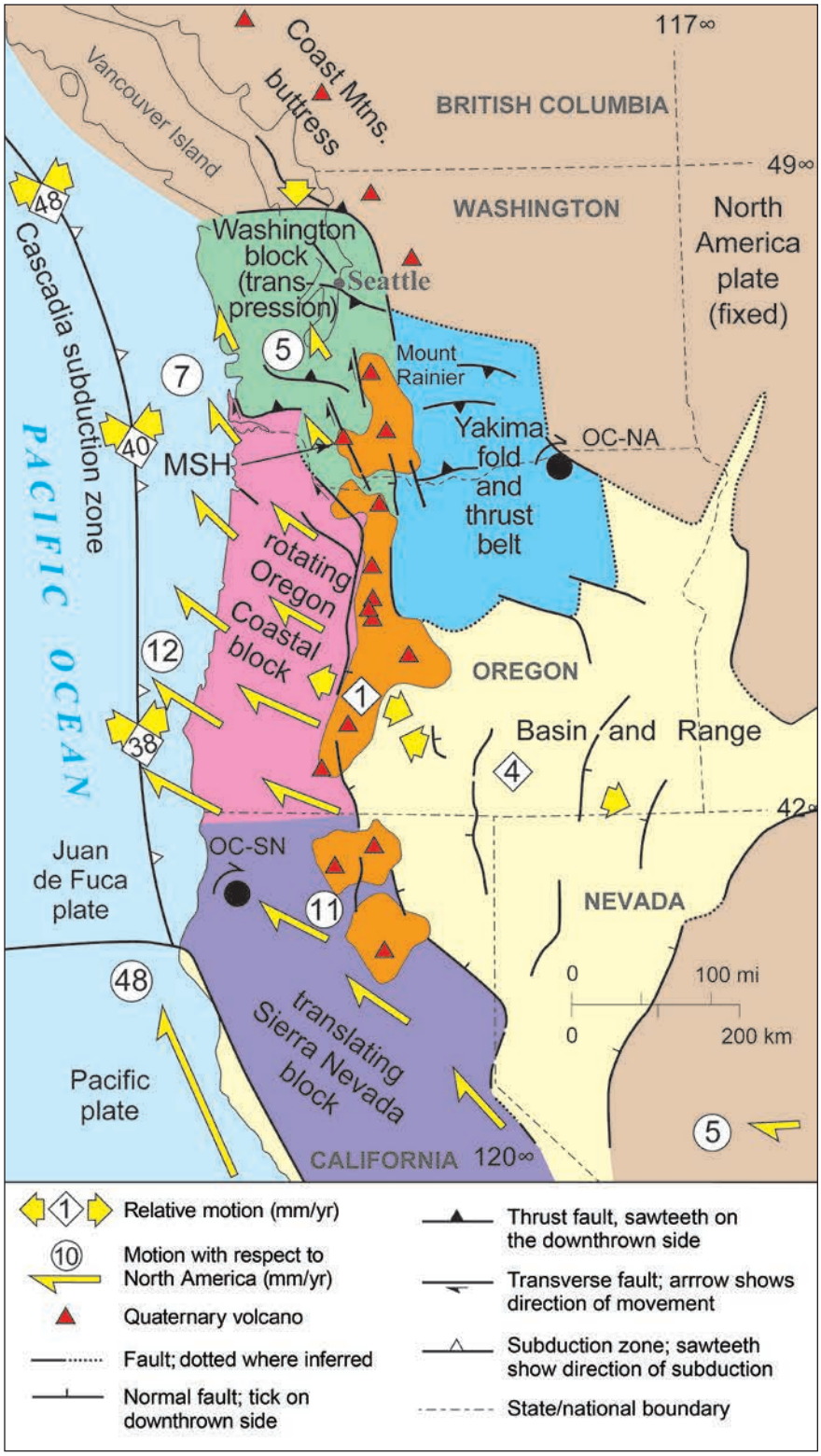

Figure 6-1—Tectonic setting of Cascadia, showing location of Cascadia subduction zone and microplate rotations. The Cascadia subduction zone is responsible for great megathrust earthquakes and deep intraslab earthquakes. Regional crustal block rotation causes north-south compression, uplift, and faulting, which are responsible for crustal earthquakes. MSH = Mount St. Helens. Source: Pringle (2008), modified from Wells et al. (1998, 2002).

Seismic Sources

Cascadia Megathrust Earthquakes

Cascadia megathrust earthquakes are long-duration (several minutes) subduction-zone events having magnitudes greater than M8.0. They are infrequent events that have happened, on average, about every 300 to 550 years over the past 10,000 years (Atwater and Hemphill-Haley 1997, Goldfinger et al. 2012, Petersen et al. 2014). Although geologic evidence remains under some debate, it is thought that these megathrust earthquakes typically rupture the full length of the subduction zone, resulting in ~M9 earthquakes, more often than as serial partial-zone ruptures generating M8+ earthquakes over a span of years or decades (Goldfinger et al. 2012; Kelsey et al. 2002, 2005; Nelson et al. 2006; Williams et al. 2005). The most recent megathrust earthquake along the Cascadia subduction zone, estimated to have been M8.7–9.2, occurred on January 26, 1700 (Atwater et al. 2005; Satake et al. 1996, 2003). Overall, the Cascadia subduction zone is locked mainly offshore, but in central Oregon the locked zone extends inland (McCaffrey et al. 2007). Modern geodetic measurements are consistent with strain accumulating above the locked zone (Flück et al. 1997, Gomberg et al. 2010, McCaffrey et al. 2007, Wang et al. 2003). The largest historical event thought originally to have occurred along the subduction zone interface was the 1992 M7 Mendocino earthquake along northern California (Oppenheimer et al. 1993), though subsequent analysis infers it to be from a blind crustal thrust fault above the plate interface (McCrory et al. 2012).

The geometry of the subducting Juan de Fuca plate is spatially variable along the Cascadia subduction zone (McCrory et al. 2012). In western Washington, the slab subducts very shallowly and forms a broad arch before dipping more steeply at about the longitude of Olympia (McCrory et al. 2012) (fig. 6-2). At that longitude (-123°), the plate is at a depth of about 40 km (25 mi). At the longitude of Seattle and Tacoma (-122°), plate depth is about 60 km (35 mi). In southwestern Washington and through Oregon, the plate dips more steeply and more uniformly (fig. 6-2). Plate depth beneath Spirit Lake is about 60 to 65 km (35 to 40 mi).

Because the response to an earthquake at any specific site depends on the distance to the earthquake's hypocenter and specific site conditions, the location of the downdip edge of rupture of the locked interface during a Cascadia megathrust earthquake is of potential concern for the Spirit Lake project. This location greatly affects ground motions at a site, and influences ground-motion models used for seismic hazard analysis. The precise location of the downdip edge of rupture is uncertain and differs among models used (Petersen et al. 2014). In general, the map distance from the downdip limit of a possible subduction-zone rupture to Spirit

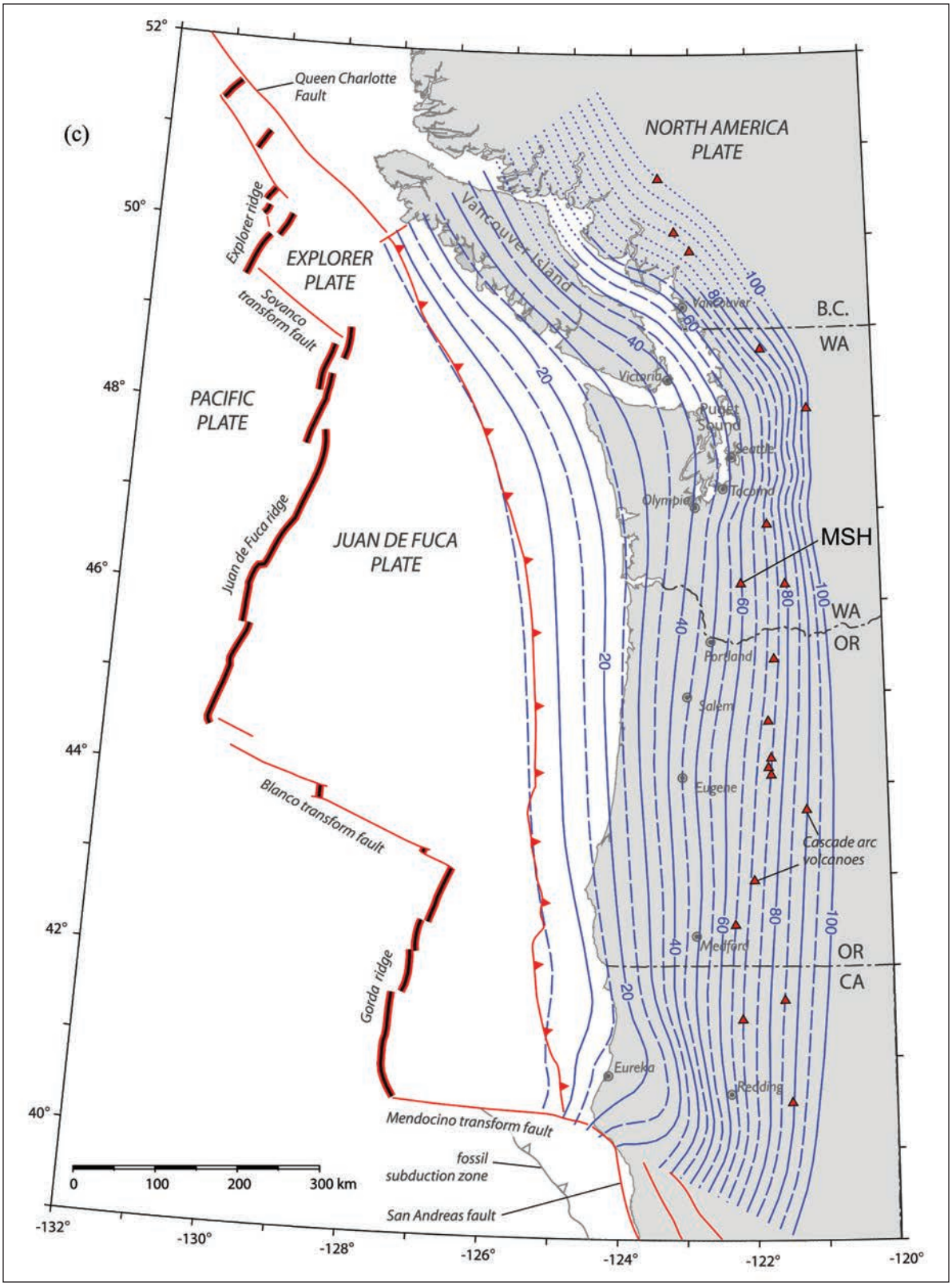

Figure 6-2—Map showing model of oceanic slab subduction. Solid lines denote depth contours in 10-km (6-mi) increments; long dashed lines denote supplemental depth contours in 5-km (3-mi) increments, and short dashed lines denote extrapolated contours. MSH = Mount St. Helens. Source: McCrory et al. (2012).

Lake ranges from about 90 to 200 km (55 to 125 mi) (fig. 6-3). At Spirit Lake, ground motions from a Cascadia megathrust earthquake likely would be strong, and shaking would likely last many tens of seconds to perhaps several minutes. Earthquake potential along the Cascadia subduction zone was very poorly understood in the early 1980s. Neither the design of the present outlet infrastructure nor the stability analysis of the debris blockage (Youd et al. 1981) considered a Cascadia megathrust earthquake.

Annual exceedance probabilities of great megathrust earthquakes along the Cascadia subduction zone vary spatially and with rupture scenario (Petersen et al. 2014). Full rupture, rather than partial rupture, has a higher exceedance probability (annual probability = 0.0019), with M8.6–9.3 dominating exceedance probabilities (fig. 6-4, table 6-1). Various models show that the greatest exceedance probabilities lie north of latitude 44° (fig. 6-5); the Spirit Lake outlet project lies at latitude 46.3°.

Deep Intraslab Earthquakes

Deep earthquakes generated within the subducting oceanic plate (called intraslab earthquakes) are smaller in size and shorter in duration, and occur more frequently than do the megathrust earthquakes. In western Washington, they typically occur at depths ranging from 30 to 50 km (20 to 30 mi) (fig. 6-6) (McCrory et al. 2012), commonly have magnitudes ranging from >M4 to about M7.5, and typically recur about once per decade. Intraslab earthquakes are nearly nonexistent from about Olympia, Washington, south to the Oregon-California border (fig. 6-6) (McCrory et al. 2012). Several earthquakes larger than M4 and having depths greater than 35 km (>20 mi) have occurred since the mid-20th century (Flück et al. 1997). The three largest of these deep earthquakes are the 1949 Olympia (M6.7; depth 50 km [30 mi]), the 1965 Puget Sound (M6.7; depth 60 km [35 mi]), and the 2001 Nisqually (M6.8; depth 50–55 km [30–35 mi]) earthquakes (Dewey et al. 2002, International Seismological Centre 2017, Petersen et al. 2002, USGS 2017). These largest intraslab earthquakes appear to be restricted along a kink in slab geometry (fig. 6-7), which apparently concentrates stress and strain accumulation (McCrory et al. 2012). Under southwestern Washington and Oregon, the slab appears to dip and slip smoothly with depth downdip of the locked interface and generates few intraslab earthquakes, though lack of these types of earthquakes there remains an anomaly (McCrory et al. 2012). Petersen et al. (2014) indicated that deep intraslab earthquakes of M7.2–7.5 in western Washington have a mean recurrence of 1,562 years (annual probability of 0.00064), and those of M7.2–8.0 have a mean recurrence of 1,010 years (annual probability of 0.00099) (table 6-2). Deep intraslab earthquakes were known about in the early 1980s, and such earthquakes were considered in the original design of the present outlet project.

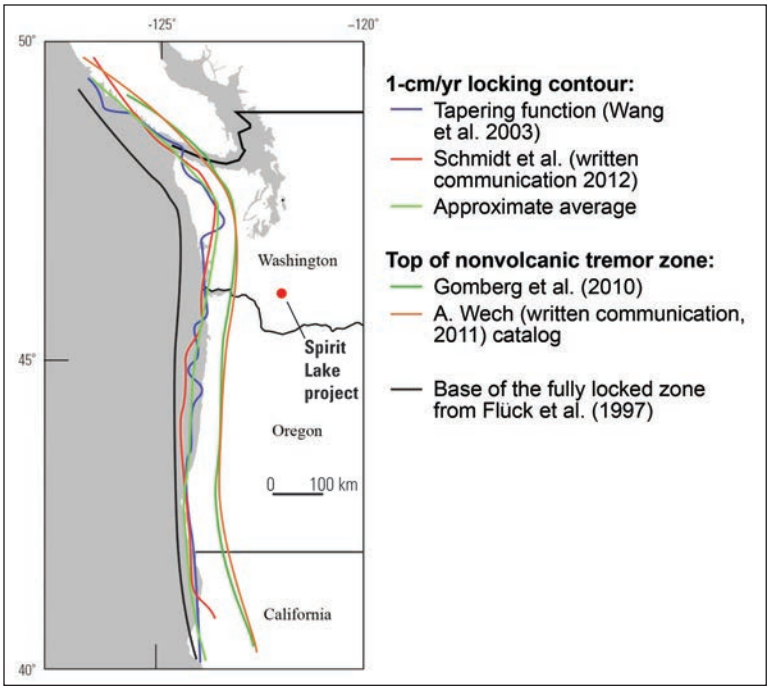

Figure 6-3—Possible locations of down-dip edge of Cascadia subduction zone rupture. Source: Petersen et al. (2014).

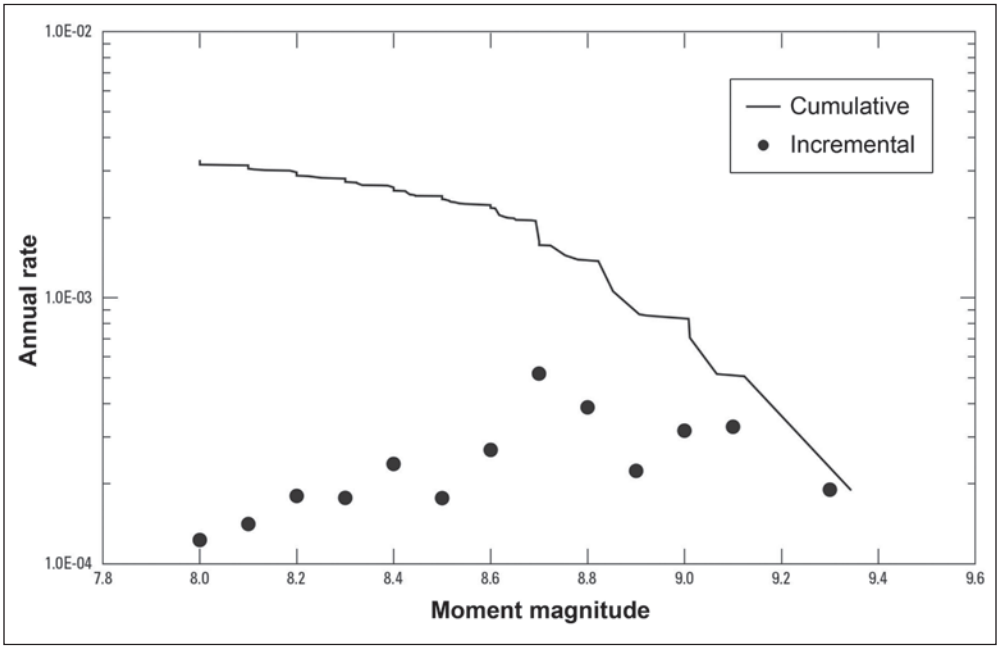

Figure 6-4—Total cumulative and binned incremental magnitude-frequency distributions for all rupture scenarios for the Cascadia subduction zone. Source: Petersen et al. (2014).

Table 6-1—Event rates for Cascadia subduction zone

	Rupture cases	M_w	Mean rate for individual rupture (per year)	Weight
Characteristic (segmented)	Full Cascadia subduction zone[a] (all four segments)	8.6–9.3	0.0019	1.0
	Partial rupture Case B[b] (southern three segments)	8.4–9.1	0.00021	
	Case C[b] (southern two segments)	8.3–8.9	0.00047	0.5
	Case D[b] (southernmost segment)	8.1–8.8	0.00052	
	Northern zone	8.3–8.9	0.001	0.1
Gutenberg-Richter (floating rupture)	Full Cascadia subduction zone[c]	8.0–8.7	0.0012	0.1
	Southern zone[d]	8.0–8.7	0.0012	0.4

[a] Full Cascadia subduction zone, southern three segments, southern two segments, and southernmost segment rupture cases correspond to Goldfinger et al. (2012), cases A, B, C, and D, respectively. The northern zone extends from the northernmost edge of Case B to the northern end of Cascadia subduction zone.

[b] Rates were determined in a way that maintains the relative rates observed by Goldfinger et al. (2012) while honoring the logic tree rate discussed in Petersen et al. (2014). See Petersen et al. (2014) for details.

[c] Rate is scaled from logic tree presented in Petersen et al. (2014).

[d] Rupture floats over the southern part of Cascadia subduction zone only.

M_w = earthquake magnitude.

Source: Peterson et al. (2014).

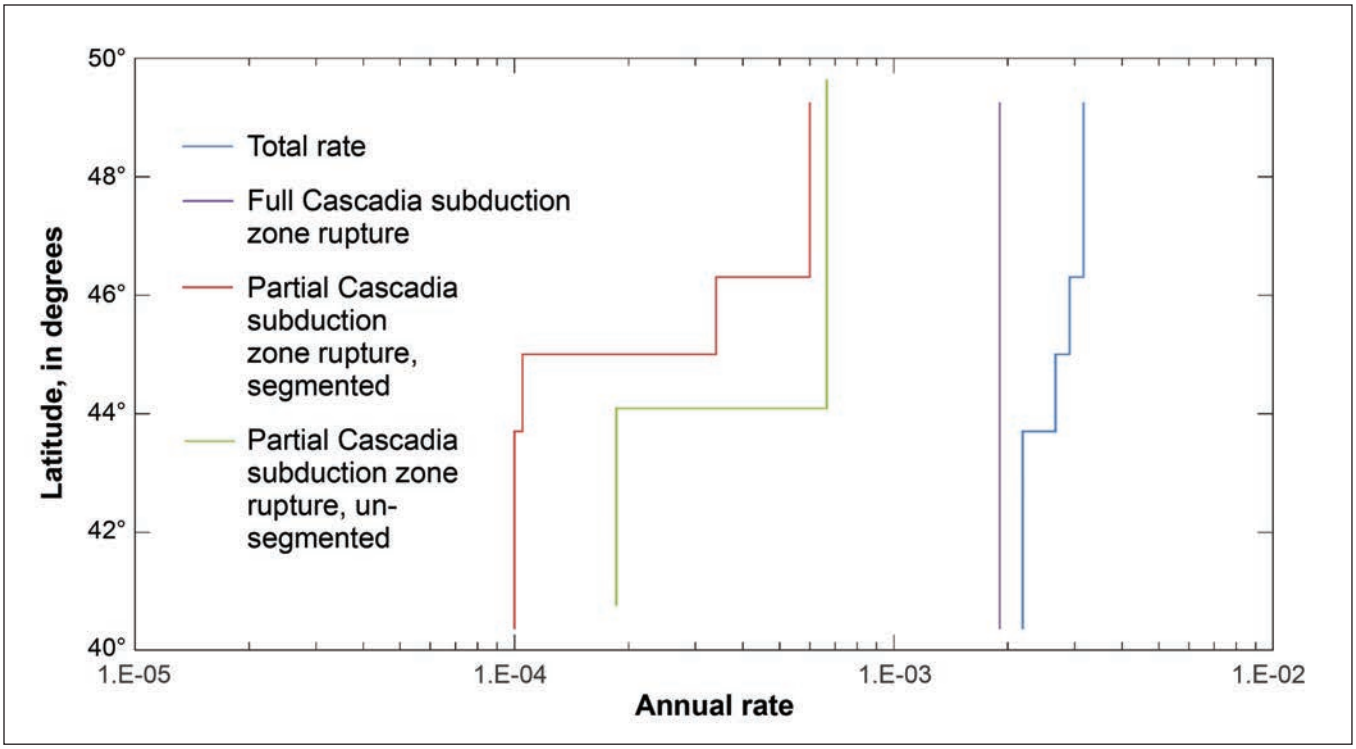

Figure 6-5—Variation of earthquake rates as a function of longitude along the Cascadia subduction zone. Source: Petersen et al. (2014).

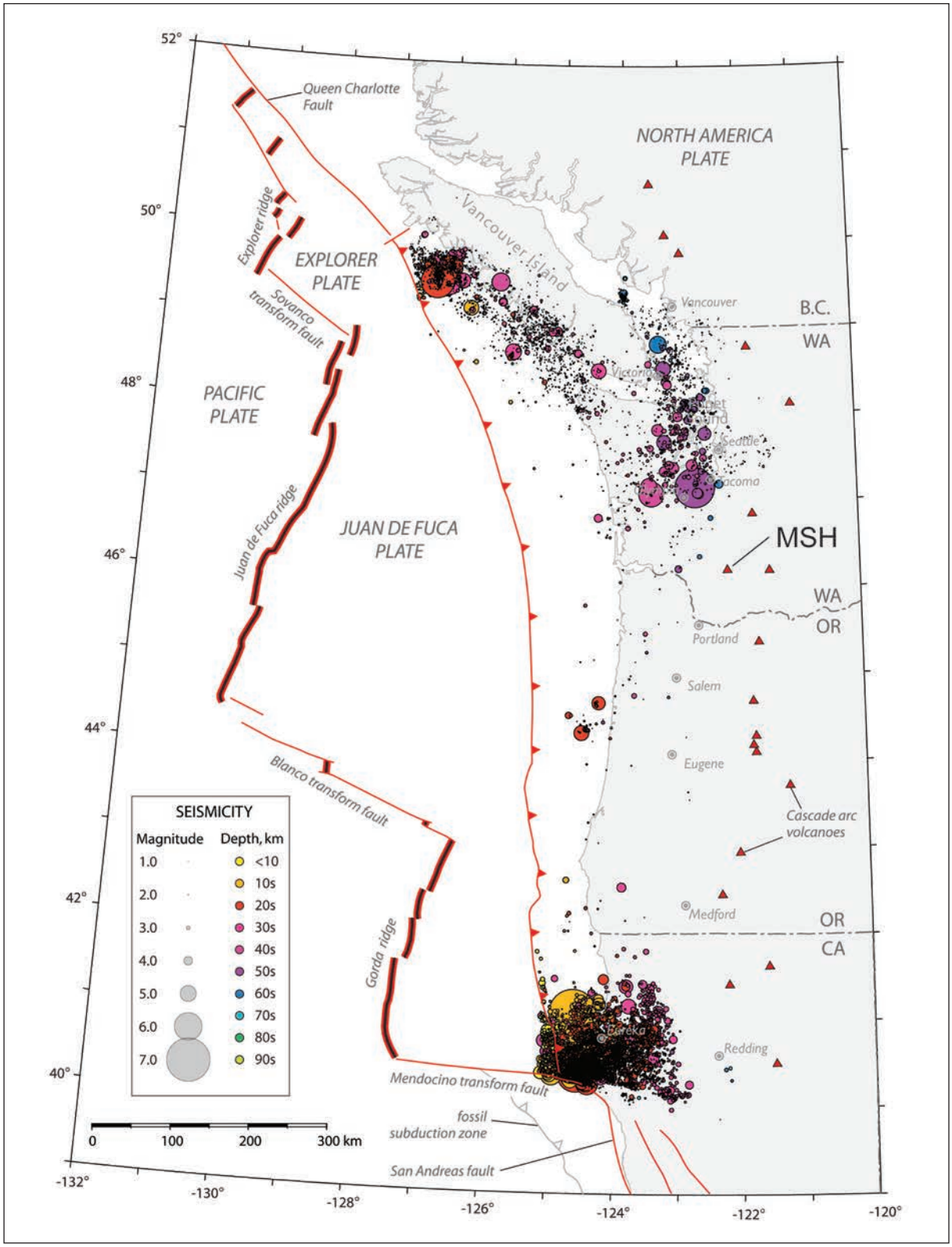

Figure 6-6—Map showing distribution of epicenters of deep intraslab earthquakes beneath the Cascadia subduction zone boundary colored by depth range. MSH = Mount St. Helens. Source: McCrory et al. (2012).

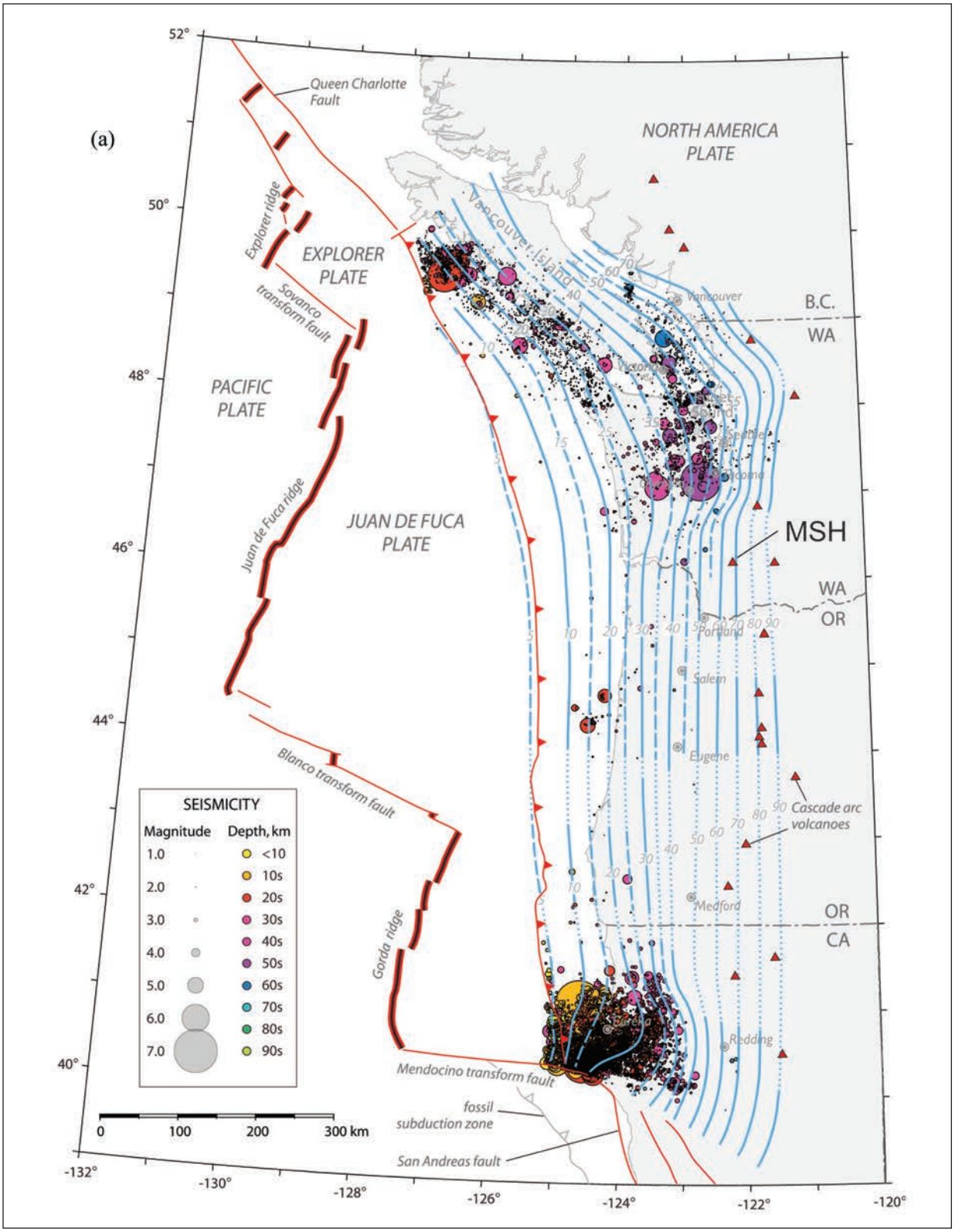

Figure 6-7—Map showing hand-contoured model of the Juan de Fuca slab surface and deep intraslab seismicity located beneath the modeled surface. Solid lines denote depth contours in 10 km (6 mi) increments; long dashed lines denote supplemental depth contours in 5-km (3-mi) increments, and short dashed lines denote extrapolated contours. MSH = Mount St. Helens. Source: McCrory et al. (2012).

Table 6-2—Benioff zone (deep intraslab) earthquake rates

Region	2008 mean annual rate	2008 mean return time	2014 mean annual rate	2014 mean return time	Mean annual rate for M_w 7.2–7.5	Return time	Mean annual rate for M_w 7.2–8	Return time
		Years		*Years*		*Years*		*Years*
Northwest California	0.0441	22.7	0.0273	36.6	0.00021	4,762	0.00037	2,703
Western Oregon	0.004	250	0.00374	267	0.00013	7,692	0.00016	6,250
Western Washington	0.1153	8.7	0.1357	7.4	0.00064	1,562	0.00099	1,010

M_w = earthquake magnitude.

Source: Peterson et al. (2014).

Shallow Crustal Earthquakes

Shallow crustal earthquakes (<30 km; 20-mi depth) are also smaller in magnitude, shorter in duration, and occur more frequently than do the megathrust earthquakes. They have magnitudes and frequencies somewhat similar to deep intraslab earthquakes. They occur along crustal faults or as random seismicity not associated with any known surface faults. They result mainly from margin-parallel shortening (roughly north-south compression) that owes to rigid block rotation rather than compression in the direction of plate convergence (Hyndman et al. 2003). The most frequent crustal earthquakes are ≤M5.5, but crustal earthquakes up to M7.5 are thought possible. There have been no very large (>M7) historical crustal earthquakes recorded. The three largest historical crustal earthquakes (~M7) in the general region occurred in north-central Washington in 1872, and on Vancouver Island in 1918 and 1946 (Hyndman et al. 2003). Extrapolation of the statistics of smaller crustal events and assessment of geodetic and geological deformation rates indicate that crustal earthquakes have the following approximate recurrence intervals: ~1.3 years for M≥4, ~10 years for M≥5, ~50 years for M≥6, and ~400 years for M≥7 (Hyndman et al. 2003). Relative motions of the Oregon, western Washington, and Vancouver Island crustal blocks indicate permanent shortening that causes these upper crustal earthquakes across the Puget region is ~4 mm yr^{-1} (McCaffrey et al. 2007). This shortening is likely distributed over several faults.

Numerous faults are present in the Cascade Range, but most are of Tertiary age and not active. During design of the Spirit Lake outlet tunnel, a few small faults were mapped in detail, and during construction five major faults were crossed and mapped (see chapter 4). However, there is no evidence that the faults crossed by the tunnel are active (Evarts and Ashley 1993). A query of the USGS Quaternary Fault database (accessed March 11, 2016) (USACE 2016a) shows no known active faults

in the vicinity of the Spirit Lake project. That database shows that the nearest fault with recent (<15,000 years) geological movement is the Portland Hills fault located 65 km (40 mi) to the southwest of Spirit Lake.

Clearly, there is much yet to be learned about shallow crustal seismicity in the region. There are many landslide-dammed lakes and large rockslides in Washington that are dated and may be associated with earthquakes, but none are yet associated with mapped faults (e.g., Pringle et al. 1998, Schuster et al. 1992, Suter et al. 2013).

St. Helens Seismic Zone

Despite a lack of known active faults in the Spirit Lake vicinity, there is a fairly defined and extensive zone of diffuse seismicity that trends in a north-south direction. This zone of seismicity, known as the St. Helens seismic zone (SHZ), is a ~100-km (~60-mi) long north-south striking zone of crustal earthquakes that stretches from about 30 km (20 mi) south of Mount St. Helens to about 60 km (~40 mi) north (Weaver and Smith 1983). It is defined by small- to moderate-magnitude earthquakes ranging from about M2.5 to 5.5 and is characterized by nearly vertical right-lateral strike-slip motion (fig. 6-8). North of Mount St. Helens, the seismogenic zone of the SHZ occurs at about 15 km (10 mi) depth; south of the volcano the seismogenic zone is shallower and above 10 km (6 mi) depth (Weaver et al. 1987).

The largest known earthquake along the SHZ is the February 14, 1981, M5.5 Elk Lake earthquake (Grant et al. 1984). Expansion of the regional seismic network in the Mount St. Helens area as a result of the 1980 eruptive activity showed the SHZ to be very active south of Cowlitz River (Weaver and Smith 1983). Although seismicity is diffuse and not located along a single fault plane, Weaver and Smith (1983) interpreted the distribution of seismicity to result from a concentration of small active faults or concentrated crustal seismic zone; Grant et al. (1984) inferred the SHZ north of Mount St. Helens to consist of a series of short, parallel fault zones. Weaver and Smith (1983) empirically estimated that a M7 earthquake could be associated with a rupture of half the length of the seismic zone. They emphasize, however, there is as yet no geologic evidence for the kinds of slip required for an earthquake of this magnitude had such magnitude earthquakes recurred over geologic time. They state that absent any reliable method to estimate the maximum magnitude earthquake capable by the SHZ, crustal earthquakes of moderate to large magnitude along this zone should be considered possible.

The Spirit Lake outlet tunnel is located along the eastern edge of the SHZ. One concern is that a moderately large earthquake (M6 to 7) on this seismic zone could activate displacement along faults that cross the tunnel. The SHZ was neither well understood nor considered during the original design of the Spirit Lake outlet

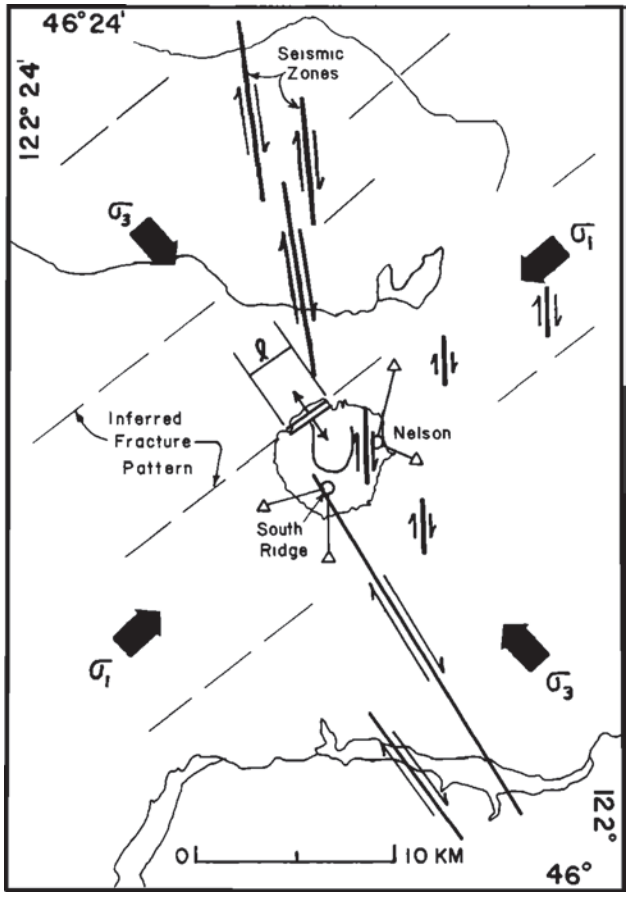

Figure 6-8—Model of crustal spreading at Mount St. Helens. North-striking bold lines depict segments of the St. Helens seismic zone; arrows show slip direction. Bold arrows indicate directions of regional minimum (σ3) and maximum (σ1) principal stresses. Source: Weaver et al. (1987).

project. The updated seismic hazard analysis maps by Petersen et al. (2014, 2015) do not consider this seismic zone.

The present failure-mode analysis considers the SHZ to be a significant seismic source. The U.S. Army Corps of Engineers (USACE) developed an approximate earthquake magnitude-frequency relationship for this zone from a catalog of historical seismicity (Advanced National Seismic System—ANSS) (USACE 2016a). Earthquakes located within 5 km (3 mi) of Mount St. Helens were excluded to reduce contamination resulting from events related to volcanic activity. Extrapolated results of the compiled relationship indicate an earthquake of M6.5 to 7 might have a mean recurrence of 300 to 1,000 years (annual probability of 0.001–0.003) (fig. 6-9). These results are broadly consistent with recurrence intervals for regional shallow crustal earthquakes estimated by Hyndman et al. (2003).

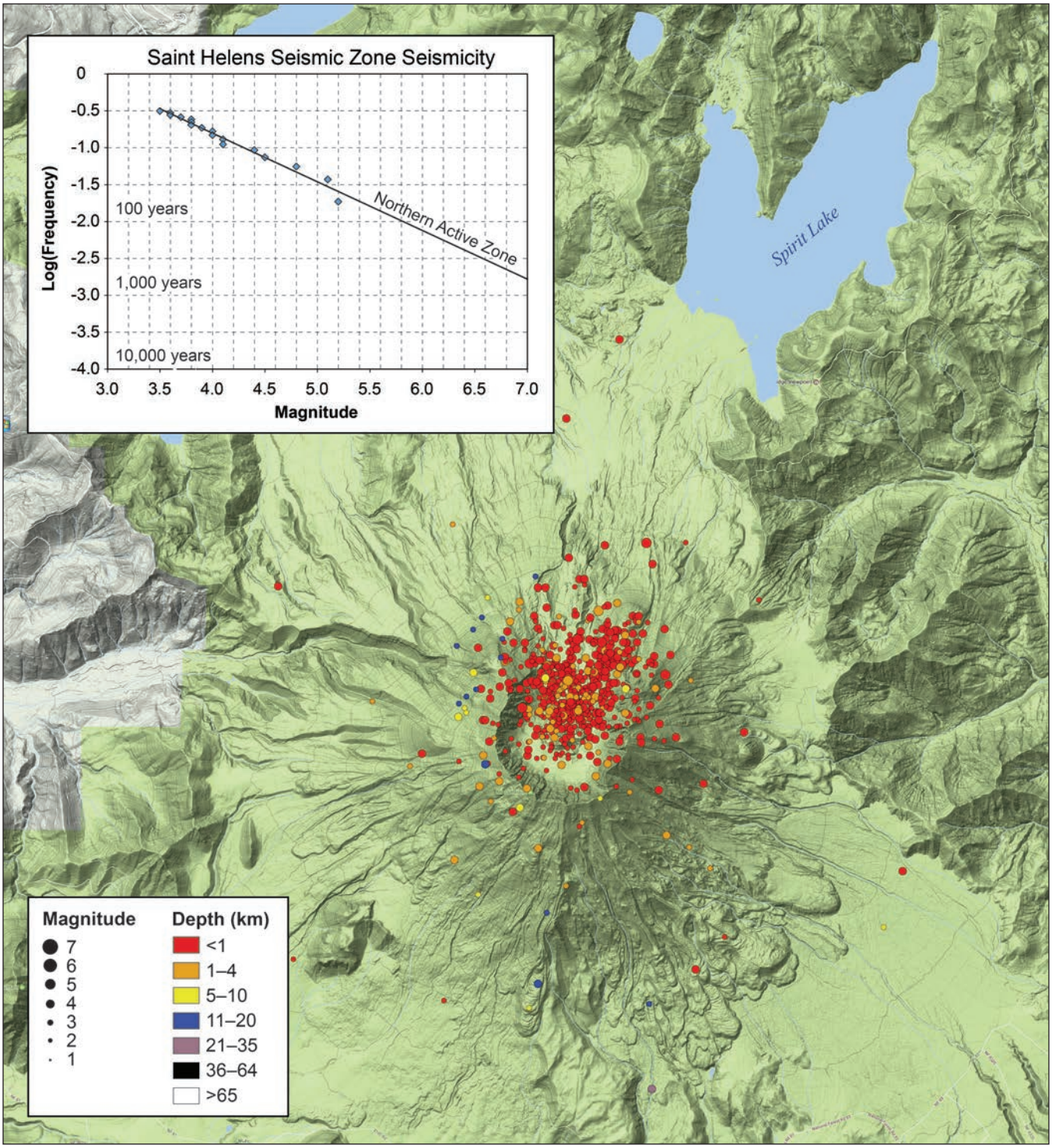

Figure 6-9—Locations of and magnitude-frequency relations among earthquakes greater than M3.5 in Mount St. Helens region. Source: USACE (2016a).

Volcanic Earthquakes

Independently of tectonically sourced earthquakes, magma migration and volcanic eruptions also trigger earthquakes. In general, volcanic earthquakes typically occur in swarms, have maximum magnitudes that are smaller than earthquakes commonly associated with tectonic events (typically <M5), and increase in numbers before eruptions (McNutt 1996). During the buildup to the 1980 eruption of Mount St. Helens, thousands of earthquakes ranging from M2 to 3.5 occurred as magma migrated upward into the edifice; the largest earthquake had M4.2 (Endo et al. 1981). The onset of eruption on May 18, 1980, was accompanied by a M5.2 earthquake, which likely represented onset of the large rockslide–debris avalanche (Kanamori et al. 1984). Moderate to large earthquakes (>M5) can be associated with volcanic activity, especially caldera collapse. The 1912 caldera-collapse eruption of Mount Katmai, Alaska, the largest eruption of the 20th century, included several ≥M6 earthquakes, the largest M7 (Abe 1992). Earthquakes as large as M5.7 accompanied caldera collapse during the 1991 eruption of Mount Pinatubo (Power et al. 1996).

The Spirit Lake outlet project lies within 8 km (5 mi) of Mount St. Helens, and thus volcanic earthquakes were considered a potential threat to the project. But uncertainty clouds the maximum magnitude event that should be considered. Given the volcanic history of Mount St. Helens and seismicity associated with eruptions worldwide, volcanic earthquakes in the region of the Spirit Lake project are likely to be no larger than M6 to 7, and most likely to be <M6. The failure-mode analysis presented here considers a volcanic earthquake of M6.5.

Seismic Considerations and Evaluations of Blockage and Outlet Infrastructure

Original Seismic Design Standards and Evaluations

The tunnel intake structure was designed with deep intraslab and volcano seismicity considered. The concrete, gravity intake structure, keyed into bedrock, was designed based on seismic zone 4 and uses a seismic coefficient of 0.2 (Sager and Chambers 1986). The intake structure is founded on stratified and jointed volcanic bedrock. No shear-wave-velocity measurements are available for this bedrock, but based on description, it best classified as Site Class “B” Rock (table 6-3). Seismicity was not specifically considered in the design of the outlet tunnel or the bolting of the slopes above the intake structure. Within the tunnel, original rock design conditions for the support system were assumed to be “moderately to very blocky and

Table 6-3—Site classification (e.g., Dobry et al. 2000)

Site class	Shear wave velocity, v_s	Blow count[a] N or N_{ch}	Shear strength, s_u
	Feet per second (meters per second)	*BPF*	*Pounds per square foot (kilopascals)*
A. Hard rock	>5,000 (>1500)	N/A	N/A
B. Rock	2,500–5,000 (760–1500)	N/A	N/A
C. Very dense soil and soft rock	1,200–2,500 (360–760)	>50	>2,000 (>100)
D. Stiff soil	600–1,200 (180–360)	15–50	1,000–2,000 (50–100)
E. Soft clay soil	<600 (<180)	<15	<1,000 (<50)

N/A = not applicable.

[a] BPF = blows per foot. Number of blows needed to drive a standard penetration tool 1 foot into soil using a standard hammer.

seamy," (class 4–5 of Terzaghi's classification system). In squeezing ground, rock conditions were assumed to be "squeezing rock, moderate to great depth," (class 7–8) (Britton et al. 2016, Sager and Chambers 1986; see also chapter 4).

Spirit Lake Debris Blockage Seismic Evaluation

A PSHA has not been performed for either the Spirit Lake outflow tunnel or the debris blockage. But Youd et al. (1981) conducted an initial assessment of seismic stability of the debris blockage. They concluded the debris blockage was stable under forces from the types of probable earthquakes known about at the time. Youd et al. (1981) stated:

> In the event of a nearby earthquake of magnitude 5 or greater, some settlement of the debris-avalanche blockage could occur due to compaction. In a large event, settlement could be as much as a couple of meters. Lateral spreading of parts of the blockage could also occur, but lateral displacement of the entire mass would not be likely to exceed a few meters even in a large event. These displacements would not reduce the ability of the blockage to hold back the water in Spirit Lake unless water in the lake was at the critical overtopping level. Locally, ground displacements could be much greater during an earthquake but those displacements would not affect the overall stability of the blockage. Consideration was given to the possibility of liquefaction and massive downstream flow failure of the blockage. Past experience indicates that such flows do not develop on slopes less than 5 percent (Youd 1978, p. 48). The slope of the North Fork Toutle River valley is about 2.5 percent, and the average general slope on the blockage is about

3.0 percent. These gentle slopes effectively eliminate potential for flow failure under all but the most severe hydrologic conditions. If the blockage were to become completely saturated, flow failure might be possible on the steeper slopes near the crest of the blockage. Again, flow failure would be possible on some steeper local slopes.

Although Youd et al. (1981) concluded that the debris blockage was stable under likely earthquake loading, the assessment was conducted in the absence of any knowledge of Cascadia megathrust earthquakes and only limited knowledge of the SHZ. The performance of the debris blockage under strong, long-duration ground shaking represents a gap in our knowledge.

Seismic Design to Consider for Updated Assessment of Spirit Lake Outflow Project

Seismic Design Criteria

U.S. Army Corps of Engineers design guidelines utilize an operating basis earthquake (OBE) and a maximum design earthquake (MDE) (USACE 2016b). The OBE is considered to be an earthquake that has a 50-percent probability of exceedance in 100 years (a 144-year return period event based upon the Poisson equation $p_t = 1\text{-}e^{-Pt}$) (Wang and Ormsbee 2005). Such an earthquake is estimated from a site-specific PSHA. The MDE is the maximum level of ground motion for which a structure is designed or evaluated.

For "critical" structures, which are part of a high-hazard project and whose failure will result in loss of life, the MDE represents the expected ground motions that could be produced by the maximum credible (or considered) earthquake (MCE). The MCE is defined as the greatest earthquake magnitude that can reasonably be expected to be generated by a specific seismic source. The MCE determination includes both the expected maximum magnitude and the source-to-site distance. The MCE is an informed judgment based on seismological and geological evidence from a deterministic seismic hazard analysis. The expected ground motion from the MCE may be produced either by an individual seismic source or by a composite of several seismic sources that could produce different shaking levels for different ground motion frequencies. The MCE is typically associated with the 84^{th}-percentile expected ground motion for major active faults and may be associated with the median (50^{th} percentile) expected ground motion for potentially active faults (with slip rates of ~0.1 mm yr^{-1} or less). The result of a 2,475-year PSHA (2-percent probability of exceedance in 50 years) is commonly used in the international building code to estimate the approximate peak ground acceleration of the MCE event.

Seismic Hazard Curve

Specific peak horizontal ground accelerations (PGA) for the Spirit Lake outlet project have not been determined. A mean PGA-frequency curve was generated by the USACE (USACE 2016a) using the regional seismic hazard analysis for the Western United States (Petersen et al. 2014, 2015) (data available from http://earthquake.usgs.gov/hazards/products/conterminous/2014/data/) (fig. 6-10). In this curve, there is considerable uncertainty for annual exceedance probabilities less than 0.0001. Peak ground accelerations corresponding to annual exceedance probabilities for common design criteria were interpolated from this mean curve (table 6-4).

Seismic Hazard Deaggregation

Probabilistic seismic hazard analysis combines the probabilities of all earthquake scenarios having different magnitudes and distances from a site with predictions of resulting ground motion intensity to determine seismic hazard at a site (Lin and Baker 2011). PSHA also incorporates uncertainties in ground motion predictions by using multiple ground motion prediction models (Lin and Baker 2011). Seismic hazard deaggregation is used to identify the relative contributions of different earthquakes to the exceedance probability of a given ground acceleration level. The USGS provides a web application that performs seismic deaggregation. But at the time this failure mode analysis study was conducted (see chapter 8), USGS had not yet published a web application to perform seismic hazard deaggregation using the updated regional PSHA (Petersen et al. 2014). Thus, a deaggregated seismic hazard for the peak ground accelerations in the Spirit Lake region (USACE 2016a) is based on an earlier regional PSHA (Petersen et al. 2008). The deaggregation assumes an average shear-wave velocity of 760 m s^{-1} (2,500 fps) for the upper 30 m (100 ft) of crust. Based on this older deaggregation result, the primary contributors to seismic hazard at the Spirit Lake project site are M5.0–6.5 events at a distance <20 km (<12 mi) (Mount St. Helens volcano, St. Helens seismic zone, and random background seismicity). However, deep intraslab earthquakes (M5.5 to 7.0) at distances of 80 to 120 km (50 to 75 mi) and Cascadia megathrust earthquakes (M8–9) at distances of 90 to 200 km (55 to 125 mi) should also be considered potential contributors to seismic hazard owing to their longer duration of shaking and at present unknown potential impacts on the debris blockage.

Table 6-4—Peak horizontal ground acceleration (PGA) summary

Earthquake	USACE-defined annual exceedance probability criteria	Recurrence interval	PGA (g)
		Years	
Operating basis earthquake (OBE)	0.0069	144	0.10
Maximum design earthquake (MDE) for "non-critical" structures	0.0011	910	0.27
International Building Code common "maximum considered earthquake"	0.0004	2,475	0.40
Maximum considered earthquake for "critical" structures	0.0001	10,000	0.66

USACE = U.S. Army Corps of Engineers.

Source: Peterson et al. (2014).

Chapter 7: Volcanic Processes, Risks, and Probabilities Affecting the Spirit Lake Outlet

Aside from hazards posed by hydrological events and regional earthquakes, eruptions of Mount St. Helens pose additional hazards to drainage infrastructure at Spirit Lake. A volcanic center has existed in the Mount St. Helens region for at least 300,000 years (Clynne et al. 2005, 2008), and over the past 4,000 years the volcano has been frequently active. Here, we provide a synopsis of the more recent major eruptive history, the volcanic processes responsible for eruptive products, and a very simplistic attempt at assessing possible frequencies of eruptions and eruptive products.

Synopsis of Recent Eruptive History

Mount St. Helens is a highly explosive volcano and the most frequently active volcano in the Cascade Range (Mullineaux 1996). It has produced abundant tephra falls (deposits of which are called airfall tephra, ash fallout, or tephra fallout), pyroclastic density currents (flows and surges), lava domes, lava flows, lahars, and debris avalanches. The volcano has a long history of eruptions driven by evolved, silicic magmas, but in the past few millennia has had a history of more complex eruptions that involve both mafic and silicic magmas (Clynne et al. 2005, 2008; Crandell 1987; Mullineaux 1996).

The eruptive history of Mount St. Helens is divided into various "eruptive stages" that lasted for millennia and include periods of dormancy lasting from centuries to millennia (fig. 2-2). Each "eruptive stage" is subdivided into "eruptive periods" that commonly lasted decades to centuries. The most recent "eruptive stage" of Mount St. Helens began about 4,000 years ago. This is called the Spirit Lake stage. The following eruptive periods have occurred during this eruptive stage (Clynne et al. 2005, Mullineaux 1996):

Smith Creek eruptive period (3,900 to 3,300 years ago). During this period, Mount St. Helens was very explosive and erupted mostly volcanic ash. This eruptive period had two primary phases of activity (3,900 to 3,850 years ago and 3,500 to 3,300 years ago). The second period of activity produced the largest volume Holocene eruption of Mount St. Helens. Actual volume of this eruption is not well constrained, but is estimated to have been about 3 to 10 times as voluminous as the 1980 eruption (Carey et al. 1995; Clynne et al. 2005; M.A. Clynne, written communication 2016[1]). During this eruptive period, huge lahars swept down the Toutle River and Lewis River valleys, likely reaching the Columbia River (Major and Scott 1988; Scott 1988a, 1989).

[1] **Clynne, M.A. 2016.** Written communication. Research geologist, U.S. Geological Survey, 345 Middlefield Road, Mail Stop 910, Menlo Park, CA 94025. mclynne@usgs.gov.

Pine Creek eruptive period (2,900 to 2,500 years ago). During this eruptive period, the volcano erupted ash, produced pyroclastic flows, dacite lava domes, and two relatively small debris avalanches off the north flank (Clynne et al. 2005, Hausback and Swanson 1990). Repeated collapses of lava domes produced broad fans of volcanic debris as much as 200 m (650 ft) thick on the south flank. Similar deposits also smothered the North Fork Toutle River valley. During this period, the largest lahars known from Mount St. Helens (≥1 billion m^3) swept the Toutle River valley (Scott 1988b) (figs. 2-19 through 2-21). These lahars are inferred to have formed as a result of a breaching(s) of an ancestral Spirit Lake, likely blocked by the debris avalanches off the north flank.

Castle Creek eruptive period (2,500 to 1,800 years ago). The Castle Creek eruptive period marked a significant transition in magma chemistry. Most of the eruptive products prior to Castle Creek time were of dacite or silicic andesite composition. This period began erupting mafic andesite and basalt compositions. The Castle Creek eruptive period produced many lava flows and domes, pyroclastic flows, and tephra fall deposits. Andesite lava flows descended all flanks of the volcano about 2,500 years ago. After a centuries-long lull, renewed volcanism around 2,200 years ago produced andesite lava flows on the north flank, as well as dacite lava flows and lava domes, pyroclastic flows, ash falls, and lahars. Activity in this eruptive period culminated with eruptions of fluid basalt lava flows that poured down all flanks of the volcano as far as 13 km (8 mi). The Cave Basalt to the south, which erupted about 1,900 years ago, was the most recent and farthest traveled of those lava flows. The lavas erupted during the Castle Creek period changed the shape of the volcano from a cluster of dacite lava domes into a more classic cone shape (fig. 2-2).

Sugar Bowl eruptive period (850 to 900 CE). Eruptive activity during this period produced lava domes on the flanks of the edifice, ash falls, lahars, and directed explosions. Two small “lateral blasts” associated with emplacement of the Sugar Bowl dome on the northeast flank were directed toward Spirit Lake and affected an area about one-tenth the size of that of 1980 blast pyroclastic density current (Crandell and Hoblitt 1986). The deposits extend up to 30 km (20 mi) from the volcano.

Kalama eruptive period (1479 to 1720). This eruptive period produced large-volume dacite tephra falls, pyroclastic flows, lava domes, lahars, and andesite lava flows. Many thick andesite lava flows descended all flanks of the volcano between about 1510 and 1570. These flows traveled 4 to 6 km (2.5 to 4 mi) from the center of the volcano. The volcano attained its pre-1980 form during this eruptive period.

Notably, two large explosive phases occurred in close temporal proximity. The early Kalama eruptive phase began with a large dacite explosive eruption in 1479 and followed in 1482 with another violent explosive phase. Over the following decades, lava domes that grew in the volcano's summit crater were disrupted by explosive eruptions. In the early to mid-1500s, the volcano erupted andesitic products, including thick lava flows on all flanks, culminating in the Worm Complex lava flows on the south flank. Late Kalama phase eruptions from about 1620 to 1750 produced the dacitic Summit Dome; during growth, it shed volcaniclastic debris down all flanks (Yamaguchi and Hoblitt 1995).

Goat Rocks eruptive period (1800 to 1857). This short-lived eruptive period produced dacite tephra fallout, an andesite lava flow (Floating Island flow) that descended the north flank of the volcano, and the north-flank Goat Rocks dacite lava dome (Hoblitt et al. 1980)—associated eruptions of which were observed (fig. 2-3) intermittently over a few decades (Yamaguchi et al. 1995). Growth of the Goat Rocks dome produced small lahars. The last significant eruption before 1980 occurred in 1857.

Significance of Recent Eruptive History

Since late Pine Creek time (about 2,500 years ago), the volcano has variously erupted dacite, andesite, and basalt, sometimes all within the same eruptive period. Hence, the chemistry of magmatic products fluctuates during eruptive episodes, so we cannot assume that eruptions of more effusive products (andesite, basalt) portend less explosive activity, or that more explosive dacite eruptions cannot eventually lead to effusive activity that can produce long-traveled lava flows.

It is clear from the past 4,000 years that the volcano has frequently produced many large lahars capable of traveling long distances along river valleys and depositing many-meters-thick layers of sediment along channels. It has also frequently erupted medium- to long-travel-distance lava flows (4 to 15 km; 2.5 to 10 mi) that have descended all flanks of the volcano.

Unless a new vent opens on the flanks of the volcano, the present geometry indicates future eruptive activity will be focused in the north-facing crater and areas north of the volcano will be at highest risk of impact from volcanic processes and associated eruptive products shed (with the exception of tephra falls having impact zones dependent on wind direction). The frequency of eruptions over the past 4,000 years, and common production of tephra falls, pyroclastic flows, lahars, and lava flows, indicate a high probability that the area immediately north of the volcano can (and will) be affected by these processes.

Estimates of Volcanic Process Frequency

Although Mount St. Helens has erupted more than 100 times in the past 40,000 years—documented by more than 100 recognizable tephra fall deposits (Mullineaux 1996)—the geological record of its eruptions is incomplete. Thus, any attempt to estimate the frequency or annual probability of an eruption, let alone of a specific volcanic process, is fraught with significant uncertainty. Furthermore, eruptions cluster in time and are interspersed with periods of dormancy. Therefore, estimates of annual exceedance probabilities can vary greatly depending on the period chosen for averaging. For example, the probability of an eruption ≥0.1 km^3 (130 million yd^3) at Mount St. Helens averaged over the past 15,000 years is ~0.0008 (12 events), but that interval included ~7,000 years of dormancy. Over the past 4,500 years, the probability of that size eruption is ~0.002 (nine events), but that interval included several 300- to 600-year dormant intervals. Over the past 500 years, the probability of that size eruption is ~0.008 (four events), a period that included two dormant intervals of 50 to 100 years (Hoblitt and Scott 2011). Given its eruptive history over the past 4,500 years, and especially over the past 500 years, one can argue that Mount St. Helens is in a period of increased eruptive frequency (Hoblitt and Scott 2011).

A few Cascades volcanoes have produced enormous volumes of tephra fallout (tens of cubic kilometers of magma) during caldera-forming eruptions over the past million years (Hildreth 2007, Hoblitt and Scott 2011). The most recent such event occurred at Mount Mazama (Crater Lake) about 7,700 years ago (Bacon 1983) and deposited about 30 cm (12 in) of tephra fallout 500 km (300 mi) from the vent. Analyses of magma accumulation within the Mount Mazama system conclude that it will be thousands of years before sufficient magma accumulates to produce another caldera-forming eruption (Bacon et al. 1997). From the character of eruptions over the past few thousands of years, Mounts Rainier, Adams, and Hood are judged presently incapable of such violent activity (Hildreth 2007, Hoblitt and Scott 2011). Therefore, Mount St. Helens is the only volcano considered capable of providing any significant volcanic loading on the Toutle River watershed.

Here, we make a very broad and simplistic assessment of probabilities of volcanic loading as a function of volcanic process and distance from the volcano (table 7-1). The probabilities depicted are based on estimates of approximate size and frequency of volcanic processes and products, with an emphasis of occurrence in the past few millennia. In general, our simplistic analysis indicates annual exceedance probabilities of some volcanic process affecting the crater or proximity of the volcano (<8 km; < 5 mi) is high—ranging from about 0.1 to 0.001. At distances

Table 7-1—Assumed semiquantitative volcanic loading

	Distance <5 km		Distance 5–8 km		Distance >8 km	
	Impact within or near crater		Impact capable of reaching Spirit Lake		Impact capable of reaching Spirit Lake and beyond	
Eruptive process	**Geologic record**	**~Probability**	**Geologic record**	**~Probability**	**Geologic record**	**~Probability**
Tephra fall[a]	Several explosive eruptions that deposited tephra fallout several centimeters to more than 1 m thick	0.01	Several explosive eruptions that deposited tephra fallout several centimeters to more than 1 m thick	0.01	Several explosive eruptions that deposited tephra fallout several centimeters to more than 1 m thick	0.01
Lava dome[b]	Extensive dome building activity within the past 4,500 years; 1980–2008: two dome complexes	0.01	A lava dome is unlikely to erupt near Spirit Lake, but dome collapses in the crater could generate pyroclastic flows that melt snow and ice and generate water floods or lahars	$<10^{-5}$ that an erupted lava dome will directly affect the project	A lava dome is unlikely to erupt near Spirit Lake, but dome collapses in the crater could generate pyroclastic flows that melt snow and ice and generate water floods or lahars	$<10^{-5}$ that an erupted lava dome will directly affect the project
Lava flow[c]	Several	0.01	Several flows affected all flanks in past 2,500 years	0.001	Three groups of basalt lava flows erupted between 2,000 and 1,800 years ago; some traveled more than 12 km from the volcano	0.001
Pyroclastic flow[d]	Many; several during 1980 eruptions	0.01	Many; several during 1980 eruptions	0.002	Many flows, but few on north side that have traveled more than about 8 km; associated ash clouds could travel more than 8 km	0.001
Laterally directed surge[e] (highly energetic pyroclastic density current)	Three are known: two ~900 CE; one in 1980	0.002	Three are known: two ~900 CE; one in 1980	0.002	Three are known: two ~900 CE; one in 1980	0.002
Debris avalanche[f]	Four are known: two ~20 ka; two from 2.5 to 3 ka; one in 1980	<0.001	Four are known: one ~20 ka; two from 2.5 to 3 ka; one in 1980	<0.001	Four are known: one ~20 ka; two from 2.5 to 3 ka; one in 1980	<0.001
Lahar[g] (volcanic debris flow)	~40 in Toutle River valley in past 50 ka	0.1	~40 in Toutle River valley in past 50 ka	0.1	~40 in Toutle River valley in past 50 ka	0.01

[a] We have rounded the annual probability of explosive eruptions over the past 500 years as discussed in Hoblitt and Scott (2011) to the nearest order of magnitude to estimate the annual probability of occurrence of tephra fall greater than about 5 to 10 cm near the volcano. See also Mullineaux (1996).

[b] Numerous lava domes have been erupted throughout the history of Mount St. Helens, and are associated with all known eruptive periods (Clynne et al. 2005, 2008; Crandell 1987; Hoblitt et al. 1980; Mullineaux 1996). The annual probability of an eruption producing a lava dome is assumed to be similar to that for an eruption that produces tephra fallout.

[c] Many lava flows are associated with eruptive period, and are especially well documented over the past few millennia after the volcano began erupting more complex mixtures of andesite, basalt, and dacite (Clynne et al. 2005, Hoblitt et al. 1980).

[d] Both explosive and effusive eruptive phases have produced pyroclastic density currents (both flows and surges). The geologic record documents numerous deposits of pyroclastic flows (Crandell 1987).

[e] All three surges were directed to the north. The two surges ~900 CE affected an area about one-tenth the size of the 1980 event (Crandell and Hoblitt 1986).

[f] Three debris avalanches into the North Fork Toutle River valley (two ~2.5 to 3 ka; one in 1980) have blocked Spirit Lake outlet (Glicken et al. 1989, Hausback and Swanson 1990). A fourth descended the west-southwest flank about 20 ka (Clynne et al. 2005). The debris avalanches 2.5 to 3 ka ultimately induced breaching of Spirit Lake and formation of very large lahars (volcanic debris flows) (one about 10^9 m^3) down the Toutle River valley (Scott 1988b). But given the current edifice geometry, it is unlikely that a large sector of the volcano will fail in a massive debris avalanche. Therefore, the annual probability of this type of event is certainly <0.001.

[g] Large lahars (>1 to 10 million m^3) are commonly clustered during periods of active eruption, but smaller lahars (<1 million m^3) capable of traveling at least a few kilometers are frequent not only during active eruptive phases, but can also be generated by meteorological events during phases of dormancy (e.g., Major et al. 2005; Scott 1989). The number of lahars listed is based on known deposits of large lahars. The higher annual probability (0.1) combines all lahars; the lower annual probability (0.01) assumes only large lahars generated during active eruptive phases.

>8 km (5 mi) from the volcano, annual exceedance probabilities are somewhat lower, but still relatively high (0.01–0.001).

The nature of the volcanic process dictates the degree of impact on drainage from Spirit Lake. Tephra fallout, for example, though having a relatively high occurrence probability (~0.01), will have relatively little impact on most outlet options (see chapter 8) except perhaps for that employing a pumping barge. A tunnel, buried conduit, or open channel are unlikely to be severely impaired by tephra fallout. In contrast, lahars, pyroclastic flows, lava flows, and volcanically induced floods have a much greater potential to impair outlet infrastructure but generally have a lower annual exceedance probability of affecting that infrastructure at the relevant distances from the volcano. Yet, they still have approximate annual exceedance probabilities >0.001, with lahars of varying sizes having potential annual exceedance probabilities in the range 0.01 to 0.1. (See additional discussion of lahar probabilities in chapter 2.) Owing to the current geometry of the volcano, it is unlikely that a large sector will fail in a massive debris avalanche. Therefore, the annual exceedance probability of that type of volcanic event is likely very much less than 0.001.

Chapter 8: Risk Assessment of Alternatives for the Spirit Lake Outlet

When the 1980 debris avalanche buried the upper North Fork Toutle River valley, Spirit Lake became a closed basin with no outlet. In this mountain setting, there are a limited number of practical approaches for allowing water to drain from the lake. The risks associated with the principal approaches are evaluated in this section. Possible lake outlets include:

- A tunnel through bedrock that bypasses the blockage (the existing outlet).
- A conduit buried within the blockage into which water is pumped or drains naturally.
- A channel across the debris blockage.

There is no risk-free way to get water out of the lake. Each alternative strategy has inherent risks associated with the flood, earthquake, volcano, and derivative geomorphic (e.g., landslide, erosion) hazards associated with this region of substantive topographic relief in an active volcanic arc subject to intense and focused storms (table 8-1). Here, we examine possible vulnerabilities of each outlet alternative to processes that may be caused by the three major regional hazards and their geomorphic derivatives. We do this to estimate the probability (likelihood) that a specific event will cause an outlet to stop passing water and consequently lead to a catastrophic release of Spirit Lake. We do not link the outlet alternatives to any specific outcomes (such as remaining below some cost constraint or remaining below some stated threshold for probability of breaching), nor do we rank-order the alternatives according to some expected outcome value. The sole purpose is to identify potential failure modes of each alternative and the likelihood that they will lead to release of lake water.

Potential Failure Mode Analysis

Potential risks to the existing infrastructure of the Spirit Lake outflow project, and some possible alternatives, were assessed using a U.S. Army Corps of Engineers (USACE) standardized dam-safety risk-assessment procedure. That procedure involves identifying potential failure modes based on an evaluation of infrastructure capabilities. Normally, this risk-assessment procedure is applied to constructed dams. Here, it is applied to the Spirit Lake outflow project even though the debris blockage is not an engineered structure and is not classified as a dam in the USACE National Inventory of Dams. For the Spirit Lake outflow project, “failure” is defined as a breaching of the debris blockage and an uncontrolled release of the lake. Unlike constructed dams, where infrastructure failure can lead to an immediate, uncontrolled release of an impounded reservoir, failure of the Spirit Lake outflow project

Table 8-1—Summary of principal risk-driving events related to major natural hazards

Hydrological hazards:
Typical wet season: average storms; average discharge peaks; normal inflow to lake
Atypical wet season: unusual storms; historical floods (e.g., 1996); abnormal inflow to lake
Probable maximum flood-type extreme event
Seismic hazards:
Shallow crustal earthquakes <M5 to M7.5 (?), shaking durations of a few to many seconds, epicenter distance from Spirit Lake possibly <20 km (<10 mi)
Deep intraslab earthquakes M4 to M7.5, shaking durations seconds to tens of seconds, epicenter distance from Spirit Lake ≥80 km (50 mi)
Megathrust earthquake M8 to M9+, shaking duration tens of seconds to several minutes, epicenter distance from Spirit Lake 90 to 200 km (55 to 125 mi)
Volcanic hazards:
Lahar
Tephra fall
Pyroclastic flow
Lava flow
Geomorphic hazards (derivatives of hydrological, seismic, and volcanic hazard events):
Landslides
Shallow seated debris flows, slumps, rockfalls
Deep-seated, large-volume mass wasting
Channel avulsion across debris avalanche deposit
Channel incision
Knickpoint development and migration
Sediment transport

is a two-step process. First, the infrastructure that provides an outlet for the lake must fail and prevent water from draining safely. Then, the lake must rise to a level capable of breaching the debris blockage. Hence, failure of outlet infrastructure at Spirit Lake in most instances does not lead to immediate or even imminent release of lake water. The potential failure mode analysis (PFMA) therefore considered not only assessment of the potential modes by which the outlet infrastructure might hypothetically fail, but also the potential that the lake will rise to its breaching elevation range (1059 to 1069 m; 3,475 to 3,506 ft; see table 3-1) without successful intervention to stabilize and lower lake level. There are, however, possible scenarios attached to a channel across the blockage which could lead swiftly to an uncontrolled lake release without having to raise lake level. Though not formally evaluated using the PFMA procedure, we highlight possible geomorphic risks associated with a channel that potentially could allow a breaching of the blockage without having to raise lake level.

The PFMA was conducted by a team of subject-matter experts from several federal agencies (table 8-2). The team's perceptions of project capabilities and vulnerabilities were informed based on existing data. No new data were collected to inform assessment of potential failure modes.

The PFMA consists of evaluation of the existing infrastructure that provides lake drainage and four conceptual alternative outlet structures:

- Alternative 1—Existing tunnel and intake.
- Alternative 2—Major rehabilitation of the existing tunnel and intake.
- Alternative 3—A conduit shallowly buried across the debris blockage fed by a permanent pumping facility.
- Alternative 4—A gravity-fed conduit more deeply buried across the debris blockage.
- Alternative 5—An open channel across the debris blockage.

The team identified and evaluated potential failure modes by various loading methods (hydrologic, seismic, volcanic, geomorphic, and operational [component malfunction or operation and maintenance challenges]). They performed evaluations of risk for alternatives 2 through 5 on conceptual-level "designs" only—no

Table 8-2—Risk assessment team

Name	Office	Discipline
Silas Sanderson	U.S. Army Corps of Engineers (USACE), Portland District	Geotechnical engineer (facilitator)
Chris Budai	USACE, Portland District	Geologist (Spirit Lake project manager)
Jeremy Britton	USACE, Portland District	Geotechnical engineer (PA team leader)
David Scofield	USACE, Portland District	Geotechnical engineer
Angela Duren	USACE, Portland District	Hydrologic engineer
Logan Negherbon	USACE, Portland District	Hydraulic engineer
Michelle Sanders	USACE, Portland District	Intern (note taker)
Nick Hanson	USACE, Portland District	Structural engineer
Louis Landre	USACE, Portland District	Economist
Justin Hall	U.S. Bureau of Reclamation, Denver	Geotechnical engineer/tunnel engineer
Jon Major	U.S. Geological Survey, Cascades Volcano Observatory	Research hydrologist
Gordon Grant	U.S. Forest Service, Pacific Northwest Research Station	Research hydrologist
Jonathan Berry	U.S. Forest Service, Pacific Northwest Region	Geotechnical engineer

specific engineering designs were evaluated. Furthermore, for alternatives 3 through 5, the team assumed that the tunnel was no longer operational. In other words, there is no outlet redundancy for any scenario considered. We assume that any alternative will have a functional lifetime of at least 50 years, a nominal lifespan for many USACE projects.

The team first developed a list of potential failure modes, then identified those modes deemed to be the most relevant and likely risk drivers. Excluded from further evaluation were failure modes considered to be irrelevant or unlikely. Appendix 1 provides the rationale for exclusion of potential failures modes.

Risk Assessment Methodology

The risk assessment includes a consideration of the likelihood of breaching of the blockage and an uncontrolled release of Spirit Lake, as well as potential consequences should breaching occur. The likelihood of a release of lake water is a function of the likelihood that the posited loading process will occur, the likelihood it will cause the outlet to fail and allow the lake level to rise, and the likelihood that an intervention to prevent breaching of the blockage will be unsuccessful. After estimating the joint probability of this chain of events for each potential failure mode, the likelihood that a failure (lake release) will occur was broadly categorized (table 8-3). The team also assigned a level of confidence to the failure likelihood (table 8-4).

Basic Failure Modes

Hypothesized failure modes for the various outlet structures considered provide four basic ways of preventing water from leaving the lake and one mechanism for releasing lake water (fig. 8-1). Water can be prevented from leaving the lake by rendering the tunnel infrastructure, a pumping station, or an intake to a buried conduit inoperable, or by blocking an open channel. In each of these scenarios, ultimate failure occurs when the lake rises to an elevation that initiates internal seepage erosion through the Spirit Lake blockage. These are the principal outcomes and ultimate failure formally evaluated. The alternative to having the lake rise and breach the blockage is to have some geomorphic process (such as knickpoint migration) induce upstream-migrating erosion from the downslope side of the blockage crest, which consequently breaches the blockage and releases lake water. Though such a geomorphically driven failure mode was not formally evaluated, we highlight how this might happen.

Table 8-3—Failure likelihood categories

Failure likelihood	Description
Remote	Annualized likelihood of failure is more remote than 1/1,000,000. Several events must occur concurrently or in series to cause failure, and most, if not all, have negligible likelihood such that the failure likelihood is negligible.
Low	Annualized likelihood of failure is between 1/1,000,000 and 1/100,000. The possibility of failure cannot be ruled out, but there is no compelling evidence to suggest it will occur or that a condition or flaw exists that could lead to initiation.
Moderate	Annualized likelihood of failure is between 1/100,000 and 1/10,000. A fundamental condition or flaw is known to exist; indirect evidence suggests failure is plausible; and key evidence is weighted more heavily toward "less likely to fail" than "more likely to fail."
High	Annualized likelihood of failure is between 1/10,000 and 1/1,000. A fundamental condition or flaw is known to exist; indirect evidence suggests failure is plausible; and key evidence is weighted more heavily toward "more likely to fail" than "less likely to fail."
Very high	Annualized likelihood of failure is between 1/1,000 and 1/100. There is direct evidence or substantial indirect evidence to suggest a failure has initiated or is likely to occur in the near future.
Failure progression likely	Annualized likelihood of failure is between 1/100 and 1/10. Performance suggests failure is initiating and likely to progress in the near future.
Failure progression observed	Annualized likelihood of failure is greater than 1/10. Performance confirms progression toward failure is occurring.

Source: USACE (2014b).

Table 8-4—Confidence categories

Confidence level	Description
Low	The team is not confident in the order of magnitude for the assigned category, and it is entirely possible that additional information would change the estimate.
Moderate	The team is relatively confident in the order of magnitude for the assigned category, but key additional information might possibly change the estimate.
High	The team is confident in the order of magnitude for the assigned category, and it is unlikely that additional information would change the estimate.

Source: USACE (2014b).

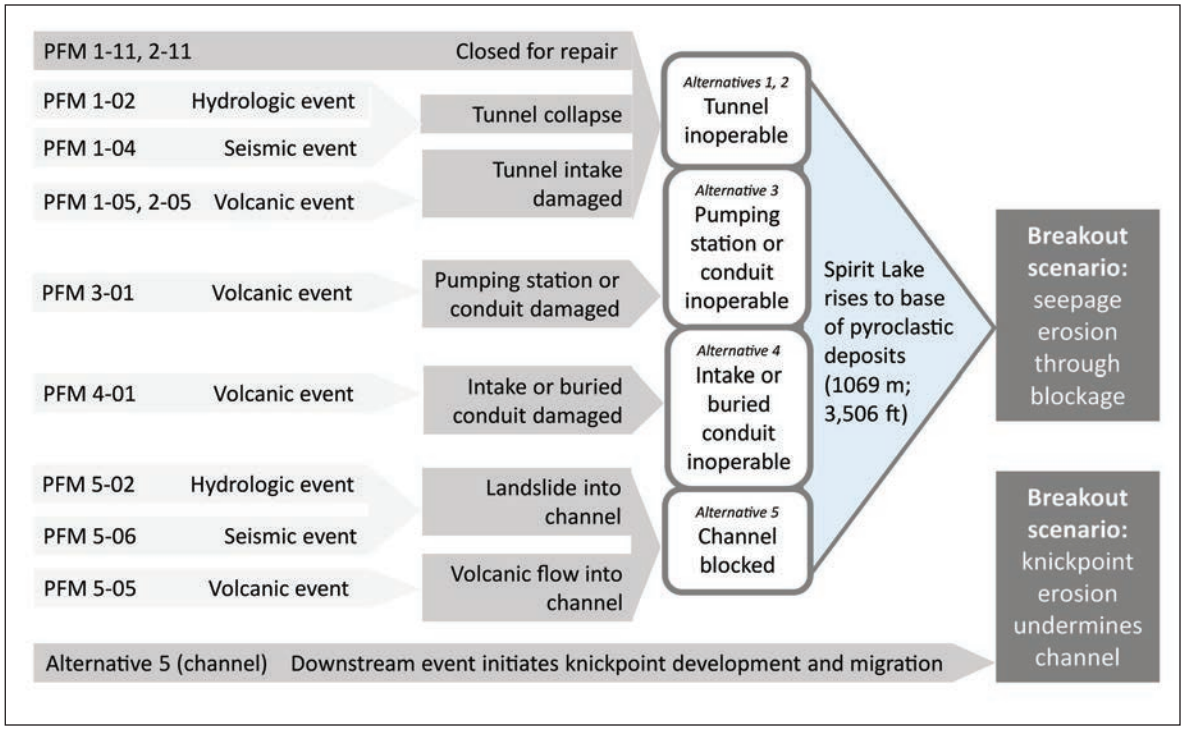

Figure 8-1—Schematic depiction of potential failure modes, outcome of failure mode on infrastructure, and ultimate potential consequence of outlet system failure.

Consequences of Breaching of the Blockage and Release of Spirit Lake

A breaching of the blockage and release of Spirit Lake would be catastrophic (Dunne and Fairchild 1984, Scott 1988b, Swift and Kresch 1983). Released lake water would entrain sediment, increase flow volume severalfold, and transform into a massive lahar. Toutle, Silver Lake, Castle Rock, Lexington, Toledo, and Kelso-Longview are the population centers within the path of such a lahar. Inundation depths are predicted to be about 18 m (60 ft) at Castle Rock and Lexington, 9 to 12 m (30 to 40 ft) at Kelso and Longview, and 4 to 6 m (15 to 20 ft) at Toledo; discharges are predicted to be tens of thousands of cubic meters per second (millions of cubic feet per second) (Swift and Kresch 1983). The estimated transit time of the lahar from breach inception to inundation of population centers is about 10 hours to Castle Rock, 14 hours to Toledo and Lexington, and 16 hours to Kelso-Longview. Swift and Kresch (1983) did not quantify the loss of lives, but note that it is likely.

The impact of a lahar resulting from a breaching of Spirit Lake blockage would be vastly greater than the impacts sustained by the lahars produced during the May 18, 1980, eruption, and those lahars had significant economic impact. There is

geological evidence of massive lahars (~10^9 m^3) sweeping the Toutle-Cowlitz river system from breaching(s) of an ancestral Spirit Lake (Scott 1988b). The inundation limits of a lahar spawned by a hypothetical catastrophic breaching of current Spirit Lake (Swift and Kresch 1983) match reasonably well mapped inundation limits of those ancestral lahars (K.M. Scott and R.J. Janda[1]; Chan 2008).

Because breaching of the blockage is not immediate upon failure of a drainage outlet, there should be time to prepare and evacuate communities in advance of catastrophic breaching. Emergency management systems are highly developed, and there is a heightened sense of awareness of the danger that exists. Therefore, life loss in the event of a breaching may be minimized. Owing to predicted depths of inundation, economic damages would be substantial—in the billions of dollars. Economic losses include direct damage to structures (both residential and commercial), economic damages to materials stored within commercial buildings, severe damage to and disruption of land-based (Interstate 5 and rail) and navigational (Columbia River) corridors, loss of commerce, and extensive and expensive reconstruction costs. Fisheries would likely be compromised or destroyed, potentially for years to decades. Extensive and expensive dredging would be expected to last for years.

Analyses of Risk Associated With Outlet Alternatives

We turn now to risk associated with each alternative outlet evaluated. The alternatives are broadly classified into two categories: pipe-style infrastructure or a channel, each of which would provide egress of lake water. The existing tunnel and a conduit buried across the blockage represent pipe-style infrastructure, and we evaluate these first. For each alternative outlet, we briefly define a hypothesized failure mode that is considered to be a potentially significant risk driver, then describe conditions under which it might promote catastrophic breaching of the blockage. We then summarize briefly relevant information from prior chapters of this report to provide context for the outlet and hypothesized failure mode, and discuss the potential for intervention to prevent breaching of the blockage. We conclude each assessment by classifying the likelihood (and confidence) that the posited failure mode will result in a breaching of the blockage and release of lake water.

[1] **Scott, K.M.; Janda, R.J.** Unpublished map. On file with: Jon Major, USGS Cascades Volcano Observatory, 1300 SE Cardinal Court, Bldg. 10, Suite 100, Vancouver, WA 98683.

Alternative 1—Existing Tunnel and Intake

The team identified 12 potential failure modes (PFM) for the existing outlet infrastructure (table 8-5). Most PFMs were judged to not pose significant risk. Here, we evaluate four failure modes deemed key risk drivers for the existing infrastructure.

Each potential failure mode results in damage to the tunnel or intake infrastructure, which renders them inoperable and allows the lake level to rise. There are three principal ways that the existing infrastructure may fail to pass water: internal failure of the tunnel; a failure of the intake, blocking flow into the tunnel; or closure of the tunnel during repairs. The following hypothetical failure scenarios examine these possibilities.

Hypothetical failure mode scenario PFM 1-02—
A probable maximum flood event induces tunnel failure. Consequently, lake level rises to the elevation that induces internal seepage erosion and breaching of the blockage.

For this failure mode, a succession of extreme hydrologic events occurs and inflow to the lake greatly exceeds outflow. Rapid and exceptional volumetric input raises the lake from its normal operating level (1049 m; 3,440 ft) to an elevation that overtops the intake wall (1058 m; 3,470 ft) (Sager and Chambers 1986) (see table 3-1). Uncontrolled flow into the tunnel damages support infrastructure, erodes weak rock, and induces tunnel blockage. With the tunnel inoperable, the lake level rises to an elevation that initiates internal seepage erosion through the Spirit Lake blockage, and the blockage breaches and releases all or a large proportion of the lake.

***Context*—**Hydrological analysis shows input volumes associated with storms that caused large historical floods are insufficient to raise the lake to a threatening level. However, an exceedingly rare hydrological event, the probable maximum flood, can raise the lake to a threatening level, especially if the lake is already elevated above its normal operating level. Analysis detailed in chapter 5 examined the change in lake storage caused by a probable maximum flood event that was preceded by another exceptional hydrological event having an inflow equivalent to half the probable maximum flood. In total, this exceptional sequence of events delivers 69 million m^3 (56,000 ac-ft) of water to the lake over a span of several days. Under existing outflow capacity, the lake would rise to nearly the maximum safe operating level (1055 m; 3,460 ft) if the starting elevation is the normal operating level (1049 m; 3,440 ft). However, if the average starting elevation is only a few meters higher, the lake could rise and overtop the intake structure. If the intake wall is overtopped, flow into the tunnel is uncontrolled.

Table 8-5—Potential failure modes hypothesized for alternative 1: existing infrastructure

Potential failure mode ID	Potential failure mode description	Potential significant risk driver[a]	Failure likelihood (confidence) category
PFM 1-01	Probable maximum flood event overtops intake structure and induces tunnel failure. Lake rises to elevation that overtops debris blockage.	N	
PFM 1-02	Probable maximum flood event overtops intake structure and induces tunnel failure. Lake rises to elevation of contact between debris avalanche and overlying pyroclastic deposits. Seepage erosion within pyroclastic deposits leads to failure of debris blockage.	Y	Remote (low)
PFM 1-03	Earthquake causes significant displacement along faults crossing tunnel, which leads to tunnel blockage or failure. Lake rises to elevation that overtops debris blockage.	N	
PFM 1-04	Earthquake causes significant displacement along faults crossing tunnel, which leads to tunnel blockage or failure. Lake rises to elevation for internal seepage erosion.	Y	Remote (moderate)
PFM 1-05	An eruption triggers a lahar that flows into Spirit Lake and generates a debris-laden wave that damages intake structure and blocks flow into tunnel. Lake rises to elevation for internal seepage erosion.	Y	Remote (moderate)
PFM 1-06	Landslide or rockfall from hillslope above tunnel intake damages infrastructure and blocks flow into tunnel.	N	
PFM 1-07	Earthquake induces liquefaction of debris blockage.	N	
PFM 1-08	Earthquake damages intake structure, which allows uncontrolled flow into tunnel. Tunnel subsequently fails.	N	
PFM 1-09	Localized failure of tunnel lining leads to partial collapse and reduction of tunnel capacity.	N	
PFM 1-10	Slope failure by any mechanism blocks tunnel outlet portal. Tail water accumulation in tunnel creates hydraulic shock that induces tunnel failure.	N	
PFM 1-11	Extended closure during major tunnel repair leads to precarious lake level and is followed by hydrological event that results in uncontrolled flow into tunnel. Tunnel subsequently fails.	Y	Moderate (low)
PFM 1-12	Extended closure during major repair leads to precarious lake level followed by an earthquake.	N	

[a] The rationale for not considering potential failure modes to be significant risk drivers is provided in appendix 1.

The tunnel crosses several zones of weak rock and squeezing ground that are erodible, and some supports remain undersized (Britton et al. 2016). Uncontrolled flow into the tunnel will likely induce pressurized flow and cause tunnel damage.

The debris-avalanche deposit consists entirely of rocks from the Mount St. Helens edifice. It is composed predominantly of heterogeneous gravelly sand but contains rocks meters in diameter (Glicken et al. 1989). The texture of the deposit is extremely variable because rock from the mountain is highly shattered, and larger fragments become blended into finer grained matrix over spatial scales of many hundreds of meters (thousands of feet). It is mantled by deposits from the blast pyroclastic density current (the blast deposit) and pumiceous pyroclastic flow and ash cloud deposits from several later flows. The blast deposit is heterogeneous and consists of friable, fragmental rock debris larger than coarse sand overlain by silt- to sand-sized debris composed of ground-up bits of rock. Its thickness across the Spirit Lake blockage ranges from a few centimeters to as much as 12 m (40 ft) (Glicken et al. 1989). The ash cloud deposit is composed mainly of pumiceous sand (40 to 60 percent) and silt (40 to 60 percent), and across the blockage it ranges from <1 to 12 m (<3 to 40 ft) thick (Glicken et al. 1989). It is highly erodible and exhibits evidence of internal seepage erosion that developed within a few years of the 1980 eruption (fig. 3-3). An initial blockage-stability analysis performed by Youd et al. (1981) assumed that pyroclastic deposits were mainly a thin mantle atop the debris-avalanche deposit; their analysis thus focused on stability of the debris avalanche and assumed that the most likely potential failure mode was overtopping of the blockage. Subsequent field analyses determined that the pyroclastic deposits were much thicker, and that internal erosion within those deposits, not blockage overtopping, was the most likely potential mode of blockage failure.

Potential for intervention—If the tunnel fails, there may be opportunity for intervention to prevent the lake from reaching an elevation that breaches the blockage. Under average inflow conditions (11.3 $m^3 s^{-1}$; 400 cfs), it will take about 4 months to raise the lake from the level that overtops the intake structure to the base of the pyroclastic deposits along the blockage crest (1069 m; 3,506 ft; Glicken et al. 1989; see table 3-1). But internal seepage erosion of the uppermost part of the debris avalanche deposit could begin before the lake reaches that elevation. Under greater inflow conditions, intervention time is less. In the 1980s, the USACE installed a pumping system to lower and stabilize the lake level before the tunnel was constructed (Sager and Chambers 1986). Depending upon weather, site conditions, and implementation time, it could take months before pumping operations to reduce and stabilize the lake level could begin. Once seepage erosion through the blockage is observed, intervention would be problematic. Prevention of uncontrolled flow into

the tunnel may be possible but would require a pre-engineered solution, and implementation of the solution may be difficult.

Likelihood of blockage breaching and release of the lake—The likelihood that this failure mode will lead to a breaching of the blockage and release of the lake is **REMOTE**, although the team has **LOW confidence** that this is the proper classification.

This failure mode requires a succession of significant hydrologic events each having an annual probability of less than 0.001 (see chapter 5) to induce uncontrolled flow into the tunnel. It then requires a few months for the lake to rise to an elevation that could breach the blockage under average inflow conditions. This lag time from outlet failure to potential breaching of the blockage may afford the opportunity for successful intervention. Assuming the intake infrastructure can be accessed, intervention to prevent uncontrolled flow into, and failure of, the tunnel may be possible. This hypothetical failure mode is subject to substantial hydrological and geological uncertainty.

Hypothetical failure mode scenario PFM 1-04—
An earthquake induces tunnel failure. Consequently, the lake level rises to the elevation that induces internal seepage erosion and breaching of the blockage.

For this failure mode, a major earthquake (assumed M6.5–7) occurs along the St. Helens seismic zone (SHZ) at a distance of <10 km (<6 mi). The earthquake displaces one or more of the major faults that cross the tunnel sufficiently to reduce flow capacity. Restricted capacity induces a flow depth that exceeds safe operating design. Flow depth in excess of design depth damages support infrastructure, erodes weak rock, and renders the tunnel inoperable. With the tunnel inoperable, the lake level rises to an elevation that initiates internal seepage erosion through the Spirit Lake blockage.

Context—There has never been a historical earthquake of M6.5–7 along the SHZ; the largest historical earthquake is M5.5 (Grant et al. 1984). Furthermore, there is no geological evidence to suggest that an earthquake of the magnitude assumed for this failure mode has occurred along the SHZ. But in the absence of any reliable estimate of the maximum magnitude earthquake capable by the SHZ, a moderate- to large-magnitude earthquake should be considered possible (Weaver and Smith 1983). A regional seismic hazard analysis indicates that a crustal earthquake >M6 has a return interval of about 50 years, and one >M7 has a return interval of about 400 years (Hyndman et al. 2003). A USACE estimate of magnitude-frequency relations for the SHZ, extrapolated from a catalog of historical seismicity, suggests that an M6.5–7 earthquake on the SHZ might have a mean recurrence interval of 300 to

1,000 years (USACE 2016a), but geologic evidence argues otherwise (see chapter 6). An updated regional probabilistic seismic hazard analysis (Petersen et al. 2014) indicates that peak ground accelerations (PGA) having return periods of about 100 to 1,000 years range from about 0.1 to 0.3 g. The tunnel intake was built to a standard design PGA of 0.2 g (Sager and Chambers 1986).

The tunnel crosses through five major shear zones. Offset along any of these zones would restrict flow and also expose weak, erodible rock. An offset >2.75 m (10 ft) could completely close the tunnel (Britton et al. 2016, Sager and Chambers 1986). The 1.2 m (4 ft) of heave that prompted the most recent tunnel repair in 2016 did not result in tunnel failure; the tunnel remained operational but with a headgate opening restriction (Britton et al. 2016).

A historical M6.8 regional earthquake has occurred since the tunnel became operational. The epicenter for that deep intraslab earthquake (2001 Nisqually earthquake) was 100 km (65 mi) from Spirit Lake. No specific damage to the tunnel was observed as a result of that earthquake, nor was there any liquefaction or earthquake-induced settling observed on or within the debris blockage. Many small sand boils were observed in the soft sediment plain behind the sediment retention structure on the North Fork Toutle River.

Tunnels typically perform well during earthquakes. For example, Dowding and Rozen (1978) analyzed scores of tunnels subject to earthquakes. They found little to no damage at PGA <0.2 g, minor damage consisting of cracked tunnel linings for PGA ranging from 0.25 to 0.4 g, and more consistent minor damage but no collapse for PGA up to 0.5 g. Jing-Ming and Litehiser (1985) observed floor heave of 5 to 30 cm (2 to 12 in) in a tunnel following the 1976 M7.8 Tang-Shan earthquake.

Potential for intervention—Assuming mean annual inflow (11.3 $m^3 s^{-1}$; 400 cfs), there should be adequate time to repair any tunnel damage caused by an earthquake. It would take about 6 to 8 months to raise the lake from its normal operating elevation to an elevation that could breach the blockage. But any damage to the intake structure could present difficulties closing the headgate, which could compromise repair efforts and ultimately lead to undesirable lake rise. Pumping operations to stabilize the lake below the top of the intake wall would likely be initiated if the intake infrastructure was compromised.

Likelihood of blockage breaching and release of the lake—The likelihood that this considered failure mode will lead to a breaching of the blockage and release of the lake is **REMOTE**, and the team has **MODERATE confidence** that this is the proper classification.

A crustal earthquake of M6.5 to 7 is a moderate- to low-probability event (recurrence interval between 50 and 400 years). The largest known earthquake on the SHZ is an M5.5 event, and there is no geological evidence for a large earthquake ≥M7 on this seismic zone. The few reference examples of tunnel performance under earthquake loading indicate that tunnels perform well and generally do not fail even during large earthquakes. Historical constriction of the Spirit Lake tunnel by as much as 1.2 m (4 ft) resulted in only limited loss of capacity (Britton et al. 2016). Assuming that the area can be accessed after a seismic event, and assuming that the intake structure is not damaged, intervention to prevent hydraulic damage within the tunnel is possible. The coincidence of a seismic event and exceptional hydrological event that provides rapid and extraordinary inflow to the lake is considered improbable.

No site-specific probabilistic seismic hazard analysis has been completed. Performance under a long-duration Cascadia megathrust event (M9) is uncertain. Site response to such an earthquake could potentially damage the intake structure, though that infrastructure was designed with deep intraslab and volcano seismicity considered (Sager and Chambers 1986, USACE 2016a). The amount of time to respond to infrastructure failure after an earthquake may be adequate to implement pumping intervention to reduce and stabilize lake level. But a M9 Cascadia megathrust quake will significantly complicate intervention. The entire Pacific Northwest will be affected, with potentially catastrophic damages to major cities and regional infrastructure. Agency assets across the government will be stretched thin and triage mentality required. Consequently, intervention at Spirit Lake may have a low priority initially.

Hypothetical failure mode scenario PFM 1-05—
An eruption triggers a lahar that flows into Spirit Lake and generates a debris-laden wave that damages the intake structure and blocks flow into the tunnel. The lake rises to an elevation that induces internal seepage erosion.

For this failure mode, an eruption of Mount St. Helens melts snow and ice in the crater and generates a lahar of sufficient volume ($\geq 10^7$ m^3) and velocity to reach Spirit Lake and create a debris-laden water wave (or series of debris-laden waves) that damages the intake structure. This debris does not damage the tunnel directly, but rather it blocks flow into the tunnel. With the tunnel intake inoperable and lake outflow inhibited, the lake level rises to an elevation that initiates internal seepage erosion through the Spirit Lake blockage.

Context—The distance from the center of the volcano crater to the lake is about 8 km (5 mi). A lahar (or pyroclastic flow or lava flow) would need to be of sufficient

volume and velocity to rapidly displace water and generate large waves. An inflow volume of about 100 million m^3 (84,000 ac-ft) is required to statically raise the lake from its normal operating elevation at 1049 m (3,440 ft) to the top of the intake structure at 1058 m (3470 ft) (Sager and Chambers 1986). An eruption-triggered, snowmelt-induced lahar occurred in March 1982 (fig. 2-13) (Waitt et al. 1983). It had a volume of about 10 to 15 million m^3 (13 to 20 million yd^3) and a velocity of about 5 to 15 m s^{-1} (15 to 50 ft s^{-1}) coming off the flank of the mountain (Pierson 1999). Most of this lahar followed the path of the 1980 debris avalanche down the North Fork Toutle River valley, but a substantial fraction entered the lake. The change in elevation of the lake level owing to this event is unknown. In 1984, a ~1-million-m^3 lahar entered and raised the lake level about 3 cm (0.1 ft) (Pringle and Cameron 1999). Pyroclastic flows from future eruptions could be of similar volume and velocity to the 1982 lahar. Lava flows from future eruptions could be of similar or larger volume, but would likely flow more slowly.

The tunnel intake lies along the western shoreline of Spirit Lake approximately 1.5 km (1 mi) from where flows enter the lake. It is oriented perpendicular to the travel path of any invading flows or impact-induced waves. But wave pulses that reflect within the lake basin may be excited. These reflected waves could subsequently approach the tunnel intake directly. Within the lake, there is substantial log debris that could wash up onto or slam into the intake structure. Bathymetry near the intake could magnify wave height.

Potential for intervention—Renewed volcanic activity could hinder intervention. The intake structure may be compromised after this event owing to debris blockage or damage. The static lake level may be higher after a lahar than before, making it more difficult to maintain the safe operating level of the lake. Nevertheless, successful intervention may be possible.

Likelihood of blockage breaching and release of the lake—The likelihood that this failure mode will lead to a breaching of the blockage and release of the lake is **REMOTE**, and the team has **MODERATE confidence** that this is the proper classification.

Large lahars (>10 million m^3) are commonly clustered during periods of active eruption. But smaller lahars (<1 million m^3) that can travel at least a few kilometers are frequent. They are caused by both eruptions and heavy rainfalls. The annual probability of a lahar reaching Spirit Lake is about 0.1 (see chapter 7). There has been at least one lahar of order 10^7 m^3 since the 1980 eruption that has reached the lake. But the likelihood of having a sufficiently energetic volcanic flow of sufficient volume to induce a large enough wave to overtop or damage the intake structure is

a relatively low-probability event (≤0.01 annual probability). Successful intervention may be possible before the debris blockage is compromised. The geometry and configuration of the intake structure compared to the lake geometry make it unlikely that reflecting waves will cripple the intake structure. Inhibiting flow into the tunnel is more likely than tunnel failure, and therefore intervention may be more straightforward and implemented more quickly. The dynamic characteristics of lake waves caused by invasive volcanic flows are not well understood, though some research has been done (Walder and Watts 2003, Walder et al. 2006).

Hypothetical failure mode scenario PFM 1-11—
An extended closure during major tunnel repair leads to a precarious lake level and is followed by a hydrological event that results in uncontrolled flow into the tunnel; the tunnel subsequently fails.

For this failure mode, a major repair of the tunnel necessitates extended closure of the intake gate. Tunnel repairs are conducted during late fall and early winter owing to fisheries and environmental restrictions. With no outflow, the lake level rises. The rate of rise is determined by inflow from storms and snowmelt. Repairs (which may be delayed for various reasons) continue until the lake level approaches the maximum safe operating level (1055 m; 3,460 ft), at which time the intake gate is opened. Owing to existing hydraulic operating restrictions (Britton et al. 2016) and high inflows during storm events, the lake level cannot lower rapidly. Hence, the lake is at a high and vulnerable stand for several months (see chapter 5). Following reopening of the tunnel, a series of substantial storms occurs and the lake level rises and overtops the intake wall. Uncontrolled flow into the tunnel damages support infrastructure, erodes weak rock, and induces tunnel blockage. With the tunnel inoperable, the lake level rises to an elevation that initiates internal seepage erosion through the Spirit Lake blockage.

Context—A high lake stand owing to closure during a major repair exposes the outflow infrastructure to substantial vulnerability, especially during winter storm season when environmental restrictions dictate timing of repairs. The lake need fill with only about 37 million m^3 (30,000 ac-ft) of water to rise from the maximum safe operating elevation of 1055 m (3,460 ft)—an elevation approached during each major repair (fig. 5-2)—to the point that it overtops the intake infrastructure at 1058 m (3,470 ft) elevation (Sager and Chambers 1986). That inflow volume could be delivered by two to three major winter storms (which in the past have delivered an average of 12 to 15 million m^3 (10,000 to 12,000 ac-ft) of inflow over 7 to 15 days) (see chapter 5). Therefore, the lake could fill to an undesirable level that could compromise the tunnel before pumping intervention could begin or be effective. An

inflow of about 90 million m^3 (73,000 ac-ft) is needed to raise the lake level from 1058 m (3,470 ft) to an elevation that could induce seepage erosion and breaching of the blockage (1069 m; 3,506 ft). This volume of inflow can be provided by about a half dozen major storms, or less than two probable maximum flood (PMF) events.

Potential for intervention—Under average inflow conditions (11.3 $m^3 s^{-1}$; 400 cfs), it would take only about 35 days to raise the lake from its maximum safe operating level to a level that overtops the intake structure; the same change in lake level could be accomplished by two to three large storms. Therefore, intervention to prevent uncontrolled flow into the tunnel could be problematic. From the time the intake is overtopped, the lake could rise to the level to induce internal seepage erosion and cause consequent blockage failure in as little as a few months (see discussion for PFM 1-02). Depending upon weather, site conditions, and implementation time, it could take several months before pumping operations to reduce and stabilize the lake level could begin. Therefore, depending on the nature of storms that follow an extended closure, intervention may be unsuccessful. Once seepage erosion through the blockage is observed, intervention would be problematic. Prevention of uncontrolled flow into the tunnel may be possible, but would require a pre-engineered solution, and implementation of the solution may be difficult.

Likelihood of blockage breaching and release of the lake—The likelihood that this failure mode will lead to a breaching of the blockage and release of the lake is **MODERATE**, although the team has **LOW confidence** that this is the proper classification.

This failure mode requires a sequence of large storms coincident with or following an extended closure that raises the lake level to near the maximum safe operating level. Extended closures during prior major repairs have raised the lake level that high, and successions of large storms have occurred during single seasons. This potential failure mode is subject to substantial hydrological uncertainty, but it starts with the lake at its most vulnerable level. The likelihood of intervention is uncertain because the required lake-level rise to compromise the intake and then reach the critical threshold level for seepage erosion could happen swiftly (within a few months) under very wet hydrologic conditions.

Alternative 2—Major Rehabilitation of Existing Tunnel and Intake

This alternative assumes that the outlet infrastructure has been fully rehabilitated. Thus only two of the original four failure modes deemed key risk drivers for the existing infrastructure are evaluated (table 8-6). Engineering improvements are assumed to mitigate the risks posed by extreme hydrologic events and earthquakes.

Table 8-6—Potential failure modes hypothesized for alternative 2: rehabilitated infrastructure

Potential failure mode ID	Potential failure mode description	Potential significant risk driver[a]	Failure likelihood (confidence) category
PFM 2-01	Probable maximum flood event overtops intake structure and induces tunnel failure. Lake rises to elevation that overtops debris blockage.	N	
PFM 2-02	Probable maximum flood event overtops intake structure and induces tunnel failure. Lake rises to elevation of contact between debris avalanche and overlying pyroclastic deposits. Seepage erosion within pyroclastic deposits leads to failure of debris blockage.	N	
PFM 2-03	Earthquake causes significant displacement along faults crossing tunnel, which leads to tunnel blockage or failure. Lake rises to elevation that overtops debris blockage.	N	
PFM 2-04	Earthquake causes significant displacement along faults crossing tunnel, which leads to tunnel blockage or failure. Lake rises to elevation for internal seepage erosion.	N	
PFM 2-05	An eruption triggers a lahar that flows into Spirit Lake and generates a debris-laden wave that damages intake structure and blocks flow into tunnel. Lake rises to elevation for internal seepage erosion.	Y	Remote (moderate)
PFM 2-06	Landslide or rockfall from hillslope above tunnel intake damages infrastructure and blocks flow into tunnel.	N	
PFM 2-07	Earthquake induces liquefaction of debris blockage.	N	
PFM 2-08	Earthquake damages intake structure, which allows uncontrolled flow into tunnel. Tunnel subsequently fails.	N	
PFM 2-09	Localized failure of tunnel lining leads to partial collapse and reduction of tunnel capacity.	N	
PFM 2-10	Slope failure by any mechanism blocks tunnel outlet portal. Tail water accumulation in tunnel creates hydraulic shock that induces tunnel failure.	N	
PFM 2-11	Extended closure during major tunnel repair leads to precarious lake level and is followed by hydrological event that results in uncontrolled flow into tunnel. Tunnel subsequently fails.	Y	Moderate (low)
PFM 2-12	Extended closure during major repair leads to precarious lake level followed by an earthquake.	N	

[a] The rationale for not considering potential failure modes to be significant risk drivers is provided in appendix 1.

Full design diameter (3.4 m; 11 ft) and proper tunnel alignment are assumed to be restored so that there are no hydraulic constrictions; the problematic weak zones have been fully shored with properly sized, rated, and spaced supports; and the intake infrastructure has been upgraded to design criteria based on improved knowledge of regional and local seismic and volcanic hazard. Slopes above the intake are benched and solidly bolted to mitigate potential rockfall. The rehabilitated tunnel is assumed to pass its maximum flow capacity of 15.6 $m^3 s^{-1}$ (550 cfs) under atmospheric, and not pressurized, conditions. The intake infrastructure is assumed to be modified to provide redundant capacity to close the tunnel if needed. Owing to this rehabilitation, extended closures of the tunnel are no longer anticipated. Because the fully rehabilitated tunnel is capable of passing its maximum flow capacity, lake elevation is stable and fluctuates little from its normal operating elevation of 1049 m (3,440 ft). Under this condition, the lake pool has the capacity to accommodate the inflow volume (69 million m^3; 56,000 ac-ft) of a probable maximum flood and a preceding unusual event without exceeding the maximum safe operating lake level (1055 m elevation; 3,460 ft). Therefore, risks associated only with volcanic eruption and during the period of rehabilitation construction when the tunnel is closed are evaluated.

Hypothetical failure mode scenario PFM 2-05—
An eruption of Mount St. Helens triggers a lahar that reaches Spirit Lake and generates a debris-laden water wave that damages the intake infrastructure. Consequently, the lake level rises to the elevation that induces internal seepage erosion and breaching of the blockage.

This hypothetical failure-mode scenario is identical to that hypothesized for the existing infrastructure. See discussion associated with potential failure mode scenario PFM 1-05.

Context—See discussion associated with potential failure mode scenario PFM 1-05.

Potential for intervention—See discussion associated with potential failure mode scenario PFM 1-05.

Likelihood of blockage breaching and release of the lake—The likelihood that this failure mode will lead to a breaching of the blockage and release of the lake is **REMOTE**, and the team has **MODERATE confidence** that this is the proper classification.

Hypothetical failure mode scenario PFM 2-11—
A major hydrologic event follows extended tunnel closure. Consequently, the lake level rises to the elevation that induces internal seepage erosion and breaching of the blockage.

Tunnel rehabilitation requires major repairs and upgrades, which will require several tunnel closures for extended periods of time. Rehabilitation repairs, as with major repairs to date, will likely be conducted during late fall and early winter owing to fisheries and environmental restrictions. With no outflow during repair activities, the lake level rises to a high and vulnerable level, at which time the tunnel is reopened. Following tunnel reopening, a series of substantial storms occurs and lake level rises and overtops the intake wall. Unless a phase of repair that provides redundant capability to close the tunnel intake has been completed, the rising lake level results in uncontrolled flow into the tunnel. Uncontrolled flow into a tunnel not fully rehabilitated damages support infrastructure, erodes weak rock, and induces tunnel blockage. Similar to the failure scenario associated with episodic repairs to the existing tunnel (PFM 1-11), the lake level rises to an elevation that initiates internal seepage erosion through the Spirit Lake blockage.

Context—The purpose of infrastructure rehabilitation is to mitigate the need for extended closures, to prevent uncontrolled flow into the tunnel, and to prevent support failure and erosion within the tunnel. But because the rehabilitation will require several extended closures to complete, the timing of various phases of rehabilitation will make the tunnel and intake more or less vulnerable to failure. Should the lake rise to or above the top of the intake structure, and the tunnel fails to provide adequate outflow, the lake could continue to rise until it reaches an elevation that induces internal seepage erosion through the Spirit Lake blockage. This failure mode can occur only during the period of rehabilitation construction. Once the tunnel is fully rehabilitated, the need for extended closures should be mitigated, and the threat of failure caused by this mode of artificially inflating the lake level will decrease sharply. All other context is similar to that presented for hypothetical failure mode scenario PFM 1-11.

Potential for intervention—See discussion associated with potential failure mode scenario PFM 1-11.

Likelihood of blockage breaching and release of the lake—The likelihood that this failure mode will lead to a breaching of the blockage and release of the lake is **REMOTE**, although the team has **LOW confidence** that this is the proper classification.

This potential failure mode is subject to substantial hydrological uncertainty, but it starts with the lake at its most vulnerable level. The likelihood of intervention is uncertain. Different phases of rehabilitation may make intervention more or less likely. The required rise of the lake level to a compromising level could happen swiftly under unusual hydrological conditions (see discussion for PFM 1-11).

Alternative 3—A Conduit Shallowly Buried Across the Debris Blockage Fed by a Permanent Pumping Facility

One alternative for a lake outlet is to replace the existing tunnel with a buried conduit to carry water across the blockage. Two alternatives for a buried conduit were evaluated: a shallowly buried conduit into which water is pumped over the blockage crest; and a more deeply buried conduit having a gravity-fed intake. Risks attached to a pump-fed conduit are evaluated first.

The team identified three potential failure modes (table 8-7), but two were judged not to be significant risk drivers (app. 1). At the time of the original analysis, a volcanic flow initiated by an eruption was deemed to be the only significant risk driver. An additional eruption-related failure mode not identified is provided in table 8-7 and noted below.

Table 8-7—Potential failure modes hypothesized for alternative 3: buried conduit and pumping facility

Potential failure mode ID	Potential failure mode description	Potential significant risk driver [a]	Failure likelihood (confidence) category
PFM 3-01	An eruption of Mount St. Helens generates a lahar (or other volcanic flow) that damages the barge or buries the conduit intake.	Y	Low (low to moderate)
PFM 3-02	An earthquake causes liquefaction and lateral spreading of sediment around the conduit intake. Sediment blocks the intake, and lateral spreading leads to intake damage.	N	
PFM 3-03	Avulsion of the channel draining the north slope of the volcano directs excess sediment to lake, which damages the pump system.	N	
	An eruption deposits substantial ash fall, which disables electrical systems on the pumping barge or induces mechanical failure of the pumps.	[b]	

[a] The rationale for not considering potential failure modes to be significant risk drivers is provided in appendix 1.

[b] This potential failure mode was not identified or evaluated. However, it is well known that volcanic ash falls can severely disrupt electrical systems, and the abrasive nature of the ash fall (ground-up bits of rock) could have adverse consequences on mechanical equipment. The eruption frequency of Mount St. Helens and its penchant for explosive eruptions (see chapters 2 and 7) indicate that ash falls greater than or equal to several centimeters thick at Spirit Lake have a relatively high probability of occurrence, especially over the lifespan (≥50 years) of the proposed outlet infrastructure.

Hypothetical failure mode scenario PFM 3-01—
An eruption of Mount St. Helens generates a lahar (or other volcanic flow) that damages the barge or buries the conduit intake. This event renders the outlet inoperable.

For this failure mode, an eruption of Mount St. Helens melts snow and ice in the crater and generates a lahar (or a pyroclastic flow or lava flow) of sufficient volume ($\geq 10^7$ m^3) and velocity to damage the pumping barge. This event also could partially bury the barge, bury the pumping intake, shear the discharge line, break fuel lines, or generate a debris-laden wave that overtops and damages the barge. Volcanic ash fall could disrupt electrical systems on the pump barge or have adverse effects on mechanical equipment and provide an additional means of rendering the outlet infrastructure inoperable. With the outlet inoperable, continued inflow under mean annual inflow rate raises lake level to an elevation that initiates internal seepage erosion through the Spirit Lake blockage.

Context—The distance from the center of the volcano crater to the lake is about 8 km (5 mi), and the barge is in the direct path of a lahar, pyroclastic flow, or lava flow. A lahar, pyroclastic flow, or lava flow would need to be of sufficient volume and velocity to rapidly displace water and cause waves, or to physically reach the barge and conduit intake. An inflow volume of about 10 million m^3 (8,100 ac-ft) would statically raise the lake about 1 m (3 ft); an inflow volume of 50 million m^3 (~40,000 ac-ft) would statically raise the lake 4.6 m (15 ft), and an inflow volume of 69 million m^3 (56,000 ac-ft) is required to statically raise the lake from its normal operating elevation at 1049 m (3,440 ft) to the maximum safe operating level of 1055 m (3,460 ft). A large and sudden change in lake level could damage the discharge line from the barge to the conduit intake. Lahars or pyroclastic flows from future eruptions could be of similar volume and velocity to that of the 1982 lahar. A pyroclastic flow would be hot, and interaction with water or wet sediment could trigger damaging phreatic explosions. Lava flows from future eruptions could be of volume similar to or larger than the 1982 lahar, but may flow more slowly and not reach the lake. Within the lake is substantial log debris that could wash up onto or slam into the pumping barge.

Part of the 1982 lahar entered the lake, but the change in elevation of lake level or any wave excitations resulting from this event are unknown. Pyroclastic flows from the 1980 eruptions reached the area of the proposed conduit alignment. Individual flow deposits range in thickness from <1 to 12 m (<3 to 40 ft) (Rowley et al. 1981). The volcano has erupted several lava flows, especially during the past 4,000 years. Many of these flows have traveled no more than 6 km (~4 mi) from the center of the volcano, but some have traveled much farther. The more viscous flows

(andesite and dacite) have traveled shorter distances than have more fluid basaltic lava flows.

Potential for intervention—Renewed volcanic activity could hinder intervention. The barge, conduit intake, or both may be compromised after this event. The static lake level may be higher after a lahar (or other volcanic flow) than before, making it more difficult to maintain the safe operating lake level.

Likelihood of blockage breaching and release of the lake—The likelihood that this failure mode will lead to a breaching of the blockage and release of the lake is **LOW**, and the team had **LOW to MODERATE confidence** that this is the proper classification.

Large lahars (>1 to 10 million m^3) are commonly clustered during periods of active eruption. But smaller lahars (<1 million m^3) that can travel at least a few kilometers are frequent. They are caused both by eruption and heavy rainfalls. The annual probability of a lahar reaching Spirit Lake is about 0.1 (see chapter 7). There has been at least one lahar of order 10^7 m^3 since the 1980 eruption that has reached the lake and likely would have affected the barge and conduit intake. Pyroclastic flows throughout the volcano's history of eruptions have reached the proposed conduit site. A lava flow capable of traveling 6 km (4 mi) or more is a relatively improbable event (annual probability about 0.001), but not beyond the realm of possibility. The predominant lava chemistry of eruptions over the past 4,000 years (dacite and andesite) favors shorter distance lava flows, but fluid basaltic lava flows occurred as recently as 1,900 years ago. The probability of eruption in the near future is high, and the probability of a lahar, or perhaps a pyroclastic flow, reaching the proposed barge or conduit intake site is also high.

Alternative 4—A Gravity-Fed Conduit More Deeply Buried Across the Debris Blockage

The team identified three potential failure modes for a gravity-fed buried conduit (table 8-8). But two of these failure modes were not considered to be significant risk drivers (app. 1). A volcanic flow initiated by an eruption is considered the only significant risk driver.

Hypothetical failure mode scenario PFM 4-01—
An eruption of Mount St. Helens generates a lahar (or perhaps a pyroclastic flow or lava flow) that buries the conduit intake. This event renders the outlet inoperable.

This failure mode is similar to that for the conduit associated with a pump barge. The lahar (or other volcanic flow) is assumed to bury and possibly damage the conduit intake.

Table 8-8—Potential failure modes hypothesized for alternative 4: buried conduit with free-flow intake

Potential failure mode ID	Potential failure mode description	Potential significant risk driver[a]	Failure likelihood (confidence) category
PFM 4-01	An eruption of Mount St. Helens generates a lahar (or perhaps a pyroclastic flow or lava flow) that buries the conduit intake.	**Y**	Low (low)
PFM 4-02	Earthquake causes liquefaction of debris blockage and lateral spreading, which damages conduit and intake structure.	N	
PFM 4-03	Extrafluvial landslide or debris flow from debris-avalanche sediment perched on Johnston Ridge blocks conduit intake or outlet.	N	
	Avulsion of channel draining north slope of volcano directs excess sediment to lake, which buries conduit intake.	[b]	

[a] The rationale for not considering potential failure modes to be significant risk drivers is provided in appendix 1.

[b] This potential failure mode was not considered for this alternative. Because it was deemed not to be a risk driver for alternative 3, it was not considered for alternative 4.

Context—Distance from the center of the volcano crater to the lake is about 8 km (5 mi), and the conduit intake is in the direct path of a lahar, pyroclastic flow, or lava flow. A lahar, pyroclastic flow, or lava flow would need to be of sufficient volume and velocity to physically reach the conduit intake or to rapidly displace water and cause debris-laden waves that could damage the intake. Lahars and pyroclastic flows from future eruptions could be of similar volume and velocity to that of the 1982 lahar. A pyroclastic flow would be hot, and interaction with water or wet sediment could trigger damaging phreatic explosions. Lava flows from future eruptions could be of similar or larger volume, but may flow more slowly and not reach the lake. Within the lake there is substantial log debris that could wash up onto or slam into the conduit intake.

Pyroclastic flows from the 1980 eruptions reached the area of the proposed conduit alignment. Individual flow deposits range in thickness from <1 to 12 m (<3 to 40 ft) (Rowley et al. 1981). The volcano has erupted several lava flows, especially during the past 4,000 years. Many of these flows have traveled no more than 6 km (4 mi) from the center of the volcano, but some have traveled much farther. The more viscous flows (andesite and dacite) have traveled shorter distances than have more fluid basaltic lava flows.

Potential for intervention—Renewed volcanic activity could hinder intervention. A buried conduit may have manholes providing access for inspection. Intervention may be achieved by pumping or siphoning rising lake water into access manholes.

This intervention effort is assumed to take considerably less time and effort than establishing a massive barge pumping effort to lower and stabilize the lake level. Such an intervention may be done with equipment air-lifted to the site, greatly increasing the probability of success.

Likelihood of blockage breaching and release of the lake—The likelihood that this failure mode will lead to a breaching of the blockage and release of the lake is **LOW**, although the team had **LOW confidence** that this is the proper classification.

Alternative 5—An Open Channel Across the Debris Blockage

In contrast to pipe-style outlets, which require controlled intakes or elaborate pumping systems, a channel excavated across the blockage provides a substantially different outlet alternative. Unlike pipe-style structures having outflow capacities limited by pipe diameter and intake control, outflow capacity through an open channel scales with the lake level. Safe outflow capacity is limited only by channel dimensions and erosion thresholds. Whereas pipe-style structures draining Spirit Lake are likely limited to outflow capacities of ≤20 $m^3 s^{-1}$ (a few hundred cubic feet per second), an outlet channel can pass discharges of several tens to several hundreds of cubic meters per second (thousands of cubic feet per second) depending on design. For purposes of evaluation, the team considered only a very conceptual open channel cut across the debris-avalanche deposit. The conceived channel is trapezoidal. It has an active channel and flood plain sufficiently wide (channel floor width = 15 m; 50 ft) and is sufficiently deep to pass the probable maximum flood discharge of ~1219 $m^3 s^{-1}$ (43,000 cfs), to allow channel meander, and to allow for storage of small landslides. Cut banks are assumed to have 2:1 side slopes. The channel is segmented into reaches having different gradients. An extended reach leading from the lake has a gradient of 0.001. But because the overall slope of the blockage west of the crest is about 2 to 3 percent, and both the Loowit channel (draining the volcano crater) and the North Fork Toutle River channel (see fig. 3-1) lie below the extension of this shallow gradient channel, the lower channel reach will need to have a gradient of about 0.025 to join those existing channels. Given these dimensions, the excavated channel could be as deep as 35 to 40 m (115 to 130 ft).

A Shields stress analysis for particle mobility reveals important channel constraints. Shields' equation relates shear stress (τ), median particle size of the channel bed (D_{50}), and a critical dimensionless shear stress for particle mobility (τ_*) as:

$$\tau_* = \frac{\tau}{(\rho_s - \rho) g D_{50}}$$

where ρ_s is particle density (2300 kg m^{-3} for volcanic rock) and ρ is water density. Manning's equation using a roughness coefficient of 0.04, channel dimensions and gradients noted above, and Shields equation with a critical dimensionless shear stress that ranges from 0.04 to 0.08 provide insights on discharges and sediment mobility along the conceptual channel reaches. Along the shallow gradient reach (S = 0.001), flow depths as great as 10 m (30 ft) result in a discharge as great as 900 m^3 s^{-1} (about 32,000 cfs). For a range of flow depths from 1 to 10 m (3 to 30 ft), particles ranging from 1 to 20 cm (0.4 to 8 in) diameter could mobilize (fig. 8-2; app. 2). By contrast, along the steeper gradient reach (S = 0.025), flow depths that exceed 5.25 m (17 ft) produce discharges that exceed 1200 m^3 s^{-1} (42,300 cfs), approximately the design PMF discharge. For depths that range from 1 to 5 m (3 to 15 ft), particles 0.25 to 2.5 m (10 in to 8 ft) diameter could mobilize. If flow depth along this steep reach achieved 10 m (30 ft), particles nearly 5 m (15 ft) diameter could mobilize (fig. 8-2; app. 2). This simple analysis shows that a channel across the blockage would require heavy reinforcement and thus would be equivalent to an engineered spillway that is many hundreds of meters (many thousands of feet) long.

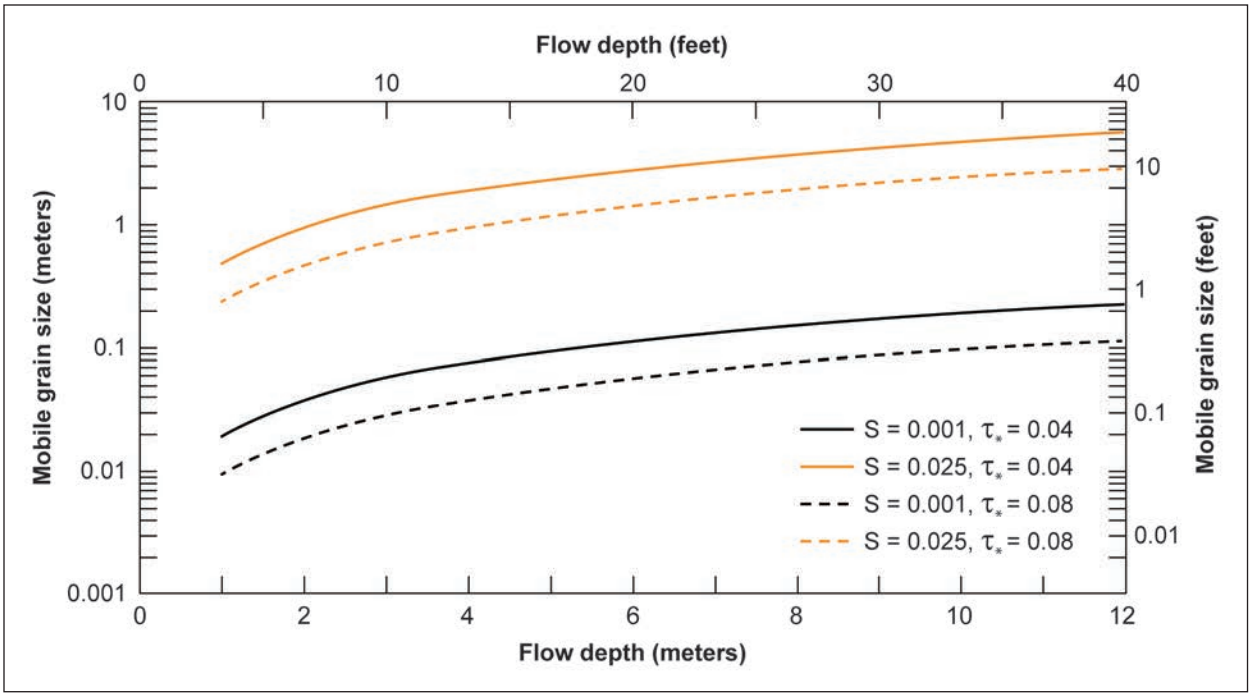

Figure 8-2—Mobile channel-bed grain size as a function of flow depth. Calculations assume a channel 15 m (50 ft) wide with 2:1 side slopes, and particle density of 2300 kg m^{-3} (see discussion in text and app. 2).

The team identified six potential failure modes for an open channel across the debris blockage (table 8-9). Three of the failure modes we judged not to be significant risk drivers (app. 1). The main risk drivers are associated with hydrologic, seismic, and volcanic processes. Because the hydrologic and seismic hazards considered are associated with an extrafluvial landslide, they are combined in the following evaluation.

Hypothetical failure mode scenario PFMs 5-02 and 5-06—A hydrologic or seismic event triggers a landslide into the channel, which blocks outflow, raises the lake level, and leads to a breach.

For this failure mode, a hydrologic or seismic event triggers a landslide from debris-avalanche sediment perched on the south-facing slope of Johnston Ridge, or from the side slopes of the channel across the debris blockage. The landslide enters the channel, blocks outflow, and impounds lake water. The lake rises swiftly and breaches the channel blockage; the resulting outflow incises through both the landslide blockage and through the channel bed, initiating a knickpoint. The knickpoint progresses headward and undermines the graded channel bed, which results in a larger, uncontrolled release of lake water.

Context—Using the design discharge capacity and the conceptual geometry above, any blockage that raises the lake level by 11.5 m (~40 ft) and then breaches suddenly could expose about 440 m^2 (4,700 ft^2) of channel cross-section to flow. If that flow exits the lake at a velocity of 3 m s^{-1} (10 ft s^{-1}), the proximal channel will just pass the probable maximum flood discharge (app. 2). But if the design capacity is exceeded, channel damage will occur and potentially undermine the infrastructure. If the channel intake is at the present-day normal operating lake level (1049 m; 3,440 ft) and the lake level rises 11.5 m (~40 ft), it will approach an elevation at which breaching of the Spirit Lake blockage becomes a concern. It would take about 135 million m^3 (110,000 ac-ft) of inflow volume to raise the lake that much. Under average inflow conditions (11.3 m^3 s^{-1}; 400 cfs), that lake rise would take about 4 to 5 months.

In January 2006, part of the debris-avalanche sediment perched on the south-facing slope of Johnston Ridge failed, resulting in a landslide that buried the channel floor, displaced the North Fork Toutle River, and temporarily blocked the channel. The landslide deposited about 600 000 m^3 (785,000 yd^3) of sediment on the channel floor, and the deposit is about 5 m (15 ft) thick (Major et al., in press). This landslide appears to have mobilized under static conditions. In general, walls of channels cut through the debris avalanche and overlying pyroclastic sediment can stand steeply for years. When they do fail, they commonly fail in small slumps.

Table 8-9—Potential failure modes hypothesized for alternative 5: open channel across debris blockage

Potential failure mode ID	Potential failure mode description	Potential significant risk driver[a]	Failure likelihood (confidence) category
PFM 5-01	Probable maximum flood event causes channel to downcut, inducing headward knickpoint erosion, which lowers channel intake and leads to uncontrolled release of lake.	N	
PFM 5-02	Hydrologic event triggers extrafluvial landslide from debris-avalanche sediment perched on Johnston Ridge above channel alignment. Landslide blocks channel until rising water breaches channel blockage.	**Y**	Moderate to high (low to moderate)
PFM 5-03	An earthquake induces liquefaction of the debris blockage near the upstream end of channel. Channel intake founders and causes uncontrolled release of lake water.	N	
PFM 5-04	Large woody debris from lake blocks channel intake. Lake level rises until logs are displaced or floated away. Lake water is released.	N	
PFM 5-05	A volcanic flow blocks the outlet channel, which raises lake level and leads to a breach.	**Y**	Remote (moderate)
PFM 5-06	Earthquake triggers extrafluvial landslide from debris-avalanche sediment perched on Johnston Ridge above channel alignment. Landslide blocks channel until rising water breaches channel blockage.	**Y**	Moderate to high (low to moderate)
	Rapid and deep (>3 m; >10 ft) incision of Loowit or North Fork Toutle River channel, into which open channel connects. This incision induces drop in base level and headward knickpoint erosion, which lowers channel intake and causes uncontrolled release of lake.	[b]	
	Extrafluvial landslide that blocks open channel is of sufficient depth and resistance that flow seeks new pathway across Spirit Lake debris blockage outside the design channel. Leads to rapid erosion and uncontrolled release of lake.	[b]	

[a] The rationale for not considering potential failure modes to be significant risk drivers is provided in appendix 1.

[b] These failure modes were not considered during the formal failure mode analysis. They are clouded by significant geomorphic and hydrologic uncertainty as to how the outlet system might respond to the hypothesized failure mode. But the Spirit Lake blockage at the foot of Mount St. Helens is a dynamic landscape. Five to more than 10 m (15 to more than 30 ft) of incision of the Loowit channel and North Fork Toutle River channel above and below the hypothesized connection point with the proposed open channel has occurred during single storm cycles (Mosbrucker et al. 2015). And the crest of the blockage is known to be composed of highly erodible material (see chapter 3). These geomorphic hazards are discussed in more detail at the end of this chapter.

Potential for intervention—An in-channel blockage would likely be detected by sensors monitoring lake level. Heavy equipment may be needed to remove debris. Pumping could be deployed if the channel blockage does not fail swiftly. Under average inflow conditions, there should be sufficient time to intervene and prevent the lake from rising to problematic levels.

Likelihood of blockage breaching and release of the lake—The likelihood that this failure mode will lead to a release of lake water is **MODERATE** to **HIGH**, but the team has **LOW** to **MODERATE confidence** that this release would not be catastrophic.

There are numerous factors (hydrologic, seismic, geomorphic) that could cause channel blockages of varying sizes and erosional resistance. To have substantial impacts on the outlet system, the channel blockage would have to be of sufficient depth and erosional resistance to allow the lake to rise at least 11.5 m (~40 ft), then rapidly release.

Channel blockage might be mitigated through relatively simple means. But there is a high likelihood that a channel blockage may not be detected quickly enough to prevent at least some release of the lake water. Access to the site is limited, and transporting heavy equipment to mitigate a blockage may not be feasible.

There are several unknowns associated with the physical properties of the materials through which the channel would be excavated. Uncertainty clouds how well channel side slopes will maintain design geometry, or the potential for side slopes to produce large slope failures. Observations of channels already carved through the area indicate slopes can stand quite steeply, but they are also susceptible to failure.

Consequences of breaching of the blockage and release of the lake—The magnitude of flow release owing to breaching of a landslide that blocks the channel is expected to be far smaller than that released by a catastrophic failure of the greater debris blockage that impounds Spirit Lake. Even if breaching of a channel blockage released a flood that transformed into a lahar, that lahar is not expected to have consequences exceeding those of the 1980s lahars in the population centers of Castle Rock, Lexington, Toledo, and Kelso-Longview. A U.S. Geological Survey model that examined the consequences of a breaching of Castle Lake (Denlinger 2012) showed that even a full release of that lake (~25 million m^3; 20,000 ac-ft) transformed to a lahar would spread across the flat plain behind the sediment retention structure and do little if any damage downstream. But there is no study routing a

1980s-magnitude lahar through the now evolved river-system topography. Although a lahar of this magnitude is not expected to affect population centers exceptionally, campers and residents in outlying areas could be severely affected.

Hypothetical failure mode scenario PFM 5-05—
A volcanic flow blocks the outlet channel, which raises the lake level and leads to a breach.

For this failure mode, an eruption of Mount St. Helens produces a lahar, pyroclastic flow, or lava flow that fills the outlet channel and blocks outflow. With the channel blocked, continued inflow under mean annual inflow raises the lake level to an elevation that initiates internal seepage erosion through the 1980 debris blockage, and the blockage fails.

Context—The volcanic context for this scenario is similar to that discussed for previous hypothetical failure modes. But in this scenario lahars and pyroclastic flows are likely to be fluidized, which may limit the depth of blockage in the channel (though 1980 pyroclastic flow units are as thick as 12 m [40 ft]; Rowley et al. 1981). Nonetheless, a pyroclastic flow would be hot, and interaction with water or wet sediment could trigger damaging phreatic explosions. A lava flow that blocked the channel could potentially provide bedrock control to regulate both lake level and outflow discharge. The context for a blocked channel is discussed in the preceding scenario.

Potential for intervention—An in-channel blockage would likely be detected by sensors monitoring the lake level. Heavy equipment may be needed to remove debris. Pumping could be deployed if the channel blockage does not fail swiftly. Under average inflow conditions, there should be sufficient time to intervene and prevent the lake from rising to problematic levels. Renewed volcanic activity could hinder intervention.

Likelihood of blockage breaching and release of the lake—The likelihood that this failure mode will lead to a breaching of the Spirit Lake blockage and to release of a large proportion of the lake is **REMOTE**, and the team had **MODERATE confidence** that this is the proper classification.

Large lahars (>1 to 10 million m^3) are commonly clustered during periods of active eruption, but smaller lahars (<1 million m^3) that can travel at least a few kilometers are frequent. They are caused both by eruption and heavy rainfalls. The annual probability of a lahar reaching Spirit Lake is about 0.1 (see chapter 7). There has been at least one lahar of order 10^7 m^3 since the 1980 eruption that has

reached the lake and likely would have affected the channel, and pyroclastic flows have repeatedly reached the lake throughout the volcano's eruptive history. In 1980, single pyroclastic flows deposited as much as 12 m (40 ft) of pumiceous sediment at this distance. Successful intervention may be likely before the lake rises to the level to breach the Spirit Lake debris blockage. A lava flow capable of traveling 6 km (4 mi) or more is a relatively improbable event (annual probability about 0.001), but not beyond the realm of possibility. The predominant lava chemistry of eruptions over the past 4,000 years (dacite and andesite) favors shorter distance lava flows, but fluid basaltic lava flows occurred as recently as 1,900 years ago. Though the probability of eruption in the near future is high, and the probability of a lahar, or perhaps a pyroclastic flow, reaching the proposed outlet channel is also high, it is likely that a channel blockage caused by a volcanic flow would be of relatively modest depth (≤10 m; ≤30 ft). Such a blockage would probably breach (or an intervention occur) before the lake rose to the level to induce seepage erosion and catastrophic release of the full lake volume. Thus, although the likelihood of breaching a channel blockage is high, the likelihood of a channel blockage leading to a catastrophic release of the full lake volume is remote provided the flowing water did not find a way around the channel and through the debris-avalanche blockage.

Consequences of breaching of the blockage and release of lake water—See discussion for PFM 5-02 for consequences of just a breaching of a channel blockage. See earlier discussion for consequences of a breaching of the Spirit Lake blockage.

Additional Geomorphic Issues Surrounding Potential Failure Modes of an Open Channel

There are two additional geomorphic issues that surround potential failure modes of an open channel (table 8-9). But because there is significant geomorphic and hydrologic uncertainty regarding how the channel system will respond, they were not formally considered during the PFMA process. One issue surrounds channel response to a rapid change of base level within the Loowit and/or North Fork Toutle River channels into which a channel across the blockage must connect (see fig. 3-1). The landscape of the upper North Fork Toutle River valley remains highly dynamic (e.g., Major et al., in press; Mosbrucker et al. 2015). During single storm cycles—most recently in November 2006—5 to >10 m (15 to >30 ft) of incision of the Loowit and North Fork Toutle River channels occurred both upstream and downstream of where the proposed open channel across the blockage likely would connect (Mosbrucker et al. 2015). If such rapid and dramatic incision occurred after channel construction, it is possible that the sudden drop in base level could

induce rapid knickpoint retreat through the unconsolidated blockage, undermine the constructed channel, and result in an uncontrolled release of lake water. There are several examples of rapid knickpoint retreat and mass failures along river channels following sudden drops in base level, especially following dam removals (e.g., Major et al. 2012, Tullos and Wang 2014, Wilcox et al. 2014). These examples demonstrate the speed and efficiency with which migrating knickpoints can destabilize channels. Furthermore, many small side channels presently entering the major drainage established across the avalanche deposit continue to erode headward. Over time, they could have the potential to undermine the design channel from outside its lateral boundaries.

A second issue surrounds an additional aspect to a response to an extrafluvial landslide or other fill that blocks the channel. Should a blockage of sufficient depth and erosional resistance fill the channel, it is possible that rather than incising through that blockage, lake water would seek an alternative pathway outside the design channel. If that should happen, uncontrolled flow across the Spirit Lake blockage could potentially lead to rapid incision and uncontrolled release of lake water.

Despite their significant geomorphic and hydrologic uncertainty, we highlight these mechanisms because they represent plausible potential failure modes. Any deliberations of a channel across the blockage should factor in consideration of these types of geomorphic issues as well as the potential failure modes formally considered in the risk assessment process. Compared to some other alternatives, there are vastly greater uncertainties surrounding a channel crossing a geomorphically dynamic landscape.

Summary

The options for releasing water from Spirit Lake are few. Barring a radical solution such as draining the lake and removing it from the landscape, the essential choice is between a pipe-style (i.e., tunnel or buried conduit) or open (i.e., open channel) outlet. Pipe-style options could be gravity-driven or pumped, but either approach would have similar characteristics. Each option has potential benefits and risks; here we summarize the positive and negative aspects.

The tunnel represents a known infrastructure with a proven track record of maintaining the lake level below the maximum operating level. A buried conduit was employed on a short-term basis while the tunnel was constructed and it also performed well. The amount of water that a pipe-style outlet can pass is inherently limited by pipe diameter and does not scale with inflow. A rehabilitated tunnel

or conduit is designed to pass flow only about 25 percent greater than the average annual inflow (11.3 $m^3 s^{-1}$; 400 cfs). Much greater inflows, including historical floods and the PMF thus inevitably raise the lake level. Such events create a hazardous situation only if they occur when the lake level is already high. If repair is required, the tunnel or conduit must be closed, heightening the possibility of raising the lake to a hazardous level. Failure of the tunnel does not lead immediately to failure of the blockage. Under most circumstances, many months are required for the lake to rise to the level where breaching can occur, offering the opportunity for intervention. The tunnel or other conduits are, by nature, somewhat insulated from incursions by volcanic processes and induced lake waves, although intake structures may be rendered inoperable. Moreover, conduits can be located away from zones of maximum hazard near the volcano. Tunnels are known to perform well during earthquakes. The existing tunnel is not capable, and other conduit systems may not be capable, of passing fish or other aquatic organisms both upstream and downstream.

An open channel, or engineered spillway, has the advantage that it can pass a much wider range of flows, and outflow scales with inflow. Channels lack mechanical infrastructure that can fail, and repairs do not necessarily require closure. Channels can also be engineered to pass fish and other aquatic organisms. On the other hand, an open channel would be exposed to the volcano, and subject to a wider range of volcanic, seismic, and hydrologic processes than would conduit systems. That wider exposure could lead to channel blockage. Similar to failed conduits, a blocked channel would require a period for the lake level to rise to a dangerous level, thus providing an opportunity for intervention. If the channel failed by incision, bypass, or an upstream-propagating knickpoint, such failure could occur much more rapidly (hours to days), precluding intervention. An open channel would require extensive reinforcement to protect the bed and banks against erosion and destabilization. Very large particles would have to armor the bed, or the spillway would have to be cast as concrete. In either case, these particles or hard channel boundaries would be resting on highly erodible material such that displacement of the armor or a breach of the channel could be catastrophic. The range of potential ways that a channel could fail exceed those of a closed conduit and are not as well understood. In addition, both construction of a new channel and the likelihood that some of that channel would be through a sediment-rich portion of the landscape would increase downstream sediment delivery at least temporarily until channels equilibrated.

Chapter 9: Uncertainties Affecting the Management of the Spirit Lake Outlet

Managing landscapes subject to a triad of volcanic, seismic, and hydrologic events (and their derivative geomorphic hazards) is inevitably fraught with uncertainties and a degree of risk. Events from these three hazards are fundamentally stochastic, and our present understanding is insufficient to support future forecasting and predictions in anything other than a broad statistical sense. Landscape managers and the greater public should understand that the future cannot be strictly foretold, but only anticipated within certain specified bounds.

In this report, we tried to characterize those bounds in as rigorous a fashion as current data and understanding permit. In so doing, we encountered a number of uncertainties and gaps in the data that, if addressed, would improve understanding of some of the issues facing decisionmakers developing a long-term strategy for managing the outlet of Spirit Lake. Here we discuss some of these uncertainties and consider what could reasonably be done to reduce or resolve them.

Better Resolution of the Critical Elevation for Blockage Failure

From previous analyses (Glicken et al. 1989, USACE 1983) and this report, it is clear that the elevation of the contact between the debris avalanche and overlying pyroclastic deposits at the crest of the blockage sets the safety limit for ensuring that a breakout flood does not occur. Although previous studies have provided a sound technical foundation for establishing safe operating elevations of the lake, a refined three-dimensional picture of how this contact is arrayed spatially would provide increased confidence for any management action.

Specifically, measurement and geophysical sensing technology that was not available in the 1980s but is currently available, including LiDAR and near-surface geophysical techniques such as ground-penetrating radar, seismic refraction, and electrical resistivity, could provide a more refined map of the varying elevations of the contact. Comparison of digital elevation models from 1984 and 2009 indicates the valley-filling deposits have consolidated little (USGS, unpublished data)[1], though investigation of possible consolidation could be pursued in greater detail. Thus, it is not anticipated that this elevation has changed dramatically since 1980, but its importance in establishing threshold elevations of the lake makes a reappraisal worthwhile. Firm establishment of the low point of this contact along the blockage crest and more refined estimates of the potential for deposit consolidation may allow refinement of the maximum safe operating level of the lake (see chapter 3).

[1] Unpublished data, U.S. Geological Survey. On file with: Jon Major, USGS Cascades Volcano Observatory, 1300 SE Cardinal Court, Bldg. 10, Suite 100, Vancouver, WA 98683.

Seismic Loading on the Blockage and Tunnel Due to Prolonged Shaking That Would Occur During a Cascadian Subduction Zone (CSZ) Earthquake

At the time of design and construction of the tunnel and its intake infrastructure, the potential for a M8–9 CSZ megathrust earthquake was not known for the Pacific Northwest. Although deep intraslab, shallow crustal, and volcanic earthquakes of lesser magnitudes were considered, no site-specific probabilistic seismic hazard analysis has been conducted. Prolonged (3 to 4 minute) shaking that could accompany a CSZ earthquake should be considered in any management decision.

An initial stability analysis of the blockage considered it safe from seismicity-induced failure. That analysis could be reconsidered in light of greater understanding of the potential for strong and prolonged shaking under a great CSZ earthquake. Moreover, provisional seismic velocity measurements (USACE 2016a) could be supplemented to better characterize the blockage material.

Detailed Geomorphic Investigations of the Channel and Landscape History and Potential for Erosion Within the Loowit Channel

One of the least well-understood dynamics of the Mount St. Helens landscape is the propensity for substantial geomorphic change along channels draining the north flank of the volcano. Recent surveys document as much as 15 m (50 ft) of vertical incision along some reaches of the Loowit channel during single storm events (Major et al., in press; Mosbrucker et al. 2015; Simon and Klimetz 2012). Yet, other reaches of the same channel are comparatively stable. Understanding controls on both vertical and lateral stability of channels in this area will provide information essential to determining the feasibility of establishing and maintaining an alternative outlet across the debris blockage without exacerbating the risk of an uncontrolled lake release owing to geomorphic instability.

Magnitude of the Probable Maximum Precipitation (PMP) and Probable Maximum Flood (PMF)

New data, measurement, and statistical techniques have improved our ability to define the largest meteorologic and hydrologic events that are likely to be experienced in the Mount St. Helens region. Because hydrologic analysis revealed that only an exceedingly rare combination of PMF-type floods could result in a rapid rise in lake level that could threaten the existing infrastructure and potentially lead to blockage failure, better understanding of the magnitude of this type of event

would be prudent. It is unlikely that further analysis will reveal a dramatic change in the level of the PMF, as the current value for this flood is consistent with a broad envelope curve for extreme floods (O'Connor et al. 2002). Nonetheless, a better understanding of the flood volumes associated with the PMF would improve assessment of risk associated with different alternatives.

Regular Piezometer Readings to Assess the Depth and Change in Ground-Water Level in the Debris Blockage

Piezometers in the blockage were installed and read regularly from 1982 to 1984 and intermittently afterward. Ground-water level appeared to have stabilized by the mid-1980s, and data show the ground-water gradient on the east side of the blockage crest flowed towards the lake, making east-to-west seepage erosion of the blockage highly unlikely at normal lake levels. Nonetheless, given the high risk associated with any seepage through the blockage, reestablishing regular readings of piezometers that remain, or installing new piezometers, would provide an additional check on the conclusion that seepage erosion in the absence of an elevated lake level is unlikely and also would provide a multidecade perspective on changes in ground-water flow within the blockage.

Modeling of Downstream Consequences of a Breakout of Spirit Lake

Throughout this report, we have used the lahar modeling work of Swift and Kresch (1983) in conjunction with analysis of Holocene lahars by Scott (1988b) as the basis for characterizing the downstream consequences of a breakout flood from Spirit Lake. But some things have changed since the 1980s that justify another look at the downstream effects of a breakout flood. The topography of the North Fork Toutle River valley has evolved considerably since the eruption. Construction of the Sediment Retention Structure and its operation and filling over the past few decades has potentially changed the way lahars might behave (e.g., Denlinger 2012). In potentially affected downstream communities, levees have been raised possibly affecting inundation levels, and development has proceeded in flood-prone areas. Furthermore, we now have better and more sophisticated 2- and 3-D flow-routing models and better knowledge of the dynamics of sediment entrainment and deposition for fluids of different compositions and rheologies. It is not clear how much these factors are likely to change the overall conclusions that a breakout flood would have dire consequences, but a more informed reanalysis seems warranted.

Better Understanding of the Character and Physical Properties of the Blockage at Depth

The debris blockage was drilled in the early 1980s as part of the characterization of the stratigraphy and material properties of the blockage (Glicken et al. 1989). Coupled with geophysical surveys noted above, additional drilling to provide a more complete 3-D picture of the character of the blockage at depth would help better understand what might happen if the blockage began to breach. Specifically, are there regions within the blockage where the size of subsurface material in the debris-avalanche deposit might be expected to resist vertical incision if a breakout were to occur? This information would be particularly useful to guide siting and design of an open channel.

Chapter 10: Other Considerations for Management of the Spirit Lake Outlet

In the course of writing this report, we encountered several issues that have bearing on any decisions regarding the Spirit Lake outlet but were beyond the scope of our charge or could not be dealt with under the constraints of time and resources. We briefly touch upon these issues here.

Outlet Redundancy

During the risk assessment process and at other junctures, the question was raised as to whether there should be redundant or backup mechanisms for getting water out of Spirit Lake. By this view, adoption of any new alternative for releasing water other than rehabilitating the existing tunnel would include maintaining the existing tunnel as a backup should the new design fail. This option was not rigorously analyzed. Although superficially an attractive option, a problem with this approach is that maintaining dual infrastructure could double the amount of repair and maintenance required to keep both outlets functioning. Because the overarching objective of the risk assessment is to identify alternatives that require less intervention for safely draining the lake, having to maintain two facilities instead of one appears impractical.

Massive Interventions

We did not consider what might be termed “extreme” options for dealing with potential hazards posed by Spirit Lake. The most extreme option involves outright draining of the lake by various means. Such an extreme and largely impractical option is very expensive and violates the mandate of the national monument, which was established so that “… geologic forces and ecological succession …continue substantially unimpeded.” Nevertheless, this extreme option would mitigate the threat of a future catastrophic breakout flood.

Ecological and Other Scientific Considerations

In focusing on the geophysical and engineering aspects of the Spirit Lake outlet, we did not evaluate the ecological consequences of any options. The broader context here is that the current operation and management of Spirit Lake and its outlet can be viewed as a kind of “grand experiment.” Although the presence of an engineered tunnel outlet means that this is not entirely a “natural” experiment, any change in management or construction of new infrastructure other than a rehabilitated tunnel will inevitably change the course of the experiment and trajectories of recovery that have been in place for more than three decades. An evaluation of the biophysical and scientific consequences of any change in strategy seems warranted.

Acknowledgments

This report was funded by the (USDA) Forest Service (USFS) Gifford Pinchot National Forest and Pacific Northwest Research Station as one part of an effort to evaluate options for management of the Spirit Lake outlet. The authors thank the U.S. Army Corps of Engineers (USACE) Portland District for facilitating a collaborative week-long effort to itemize potential failure modes and assess likelihoods of failure, and the U.S. Bureau of Reclamation and USFS Pacific Northwest Region for their participation in that process. Comments on early drafts were provided by the USFS and USACE. The National Academies of Sciences, Engineering, and Medicine's "Long-Term Management of the Spirit Lake/Toutle River System in Southwest, Washington" panel members posed questions that partly guided the scope of the document. The manuscript was improved by thoughtful and efficient reviews by Christopher Magirl, Patrick Pringle, and Bruce Marcot. We particularly thank Paul Anderson (Pacific Northwest Research Station) and Seth Moran (U.S. Geological Survey Cascade Volcano Observatory) for their institutional and personal support of our endeavor to highlight and summarize the interconnected issues surrounding hazards and risks within the complex landscape at Mount St. Helens.

English Equivalents

When you know:	Multiply:	To get:
Millimeters (mm)	0.0394	Inches (in)
Centimeters (cm)	0.394	Inches
Meters (m)	3.28	Feet (ft)
Kilometers (km)	0.621	Miles (mi)
Square kilometers (km^2)	0.386	Square miles (m^2)
Cubic meters (m^3)	1.308	Cubic yards (yd^3)
Cubic meters (m^3)	0.000811	Acre-feet (ac-ft)
Cubic kilometers (km^3)	0.2399	Cubic miles (mi^3)
Cubic meters per second ($m^3\ s^{-1}$)	35.3147	Cubic feet per second (cfs)
Liters per minute (lpm)	0.265	Gallons per minute (gpm)
Megapascals (MPa)	0.145	Kilopounds per square inch (ksi)
Newtons (kg m s^{-2})	0.225	Pound-force

References

Abe, K. 1992. Seismicity of the caldera-making eruption of Mount Katmai, Alaska in 1912. Bulletin of the Seismological Society of America. 82: 175–191.

Antos, J.A.; Zobel, D.B. 2005. Plant responses in forests of the tephra-fall zone. In: Dale, V.H.; Swanson, F.J.; Crisafulli, C.M., eds. Ecological responses to the 1980 eruption of Mount St. Helens. New York: Springer-Verlag: 47–58.

Atwater, B.F.; Hemphill-Haley, E. 1997. Recurrence intervals for great earthquakes of the past 3,500 years at northeastern Willipa Bay, Washington. Professional Paper 1576. Menlo Park, CA: U.S. Department of the Interior, Geological Survey. 108 p.

Atwater, B.F.; Musumi-Rokkaku, S.; Satake, K.; Tsuji, Y.; Ueda, K.; Yamaguchi, D.K. 2005. The orphan tsunami of 1700. Professional Paper 1707. Reston, VA: U.S. Department of the Interior, Geological Survey. 135 p.

Bacon, C.R. 1983. Eruptive history of Mount Mazama and Crater Lake caldera, Cascade Range, USA. Journal of Volcanology and Geothermal Research. 18: 57–115.

Bacon, C.R.; Mastin, L.G.; Scott, K.M.; Nathenson, M. 1997. Volcano and earthquake hazards in the Crater Lake region, Oregon. Open-File Report 97-487. Vancouver, WA: U.S. Department of the Interior, Geological Survey. 32 p.

Bergfeld, D.; Evans, W.C.; McGee, K.A.; Spicer, K.R. 2008. Pre- and post-eruptive investigations of gas and water samples from Mount St. Helens, Washington, 2002 to 2005. In: Sherrod, D.R.; Scott, W.E.; Stauffer, P.H., eds. A volcano rekindled: the renewed eruption of Mount St. Helens, 2004–2006. Professional Paper 1750. Reston, VA: U.S. Department of the Interior, Geological Survey: 523–542.

Bissell, V.C.; Hutcheon, R.J. 1983. Forecasting and data collection preparedness for streams affected by the Mt. St. Helens volcano. Portland, OR: National Oceanic and Atmospheric Administration, National Weather Service, Northwest River Forecast Center. 72 p.

Britton, J.P.; Askelson, S.K.; Budai, C.M.; Scofield, D.H. 2016. Repair of failing Spirit Lake outlet tunnel at Mount St. Helens. In: Crookston, B.; Tullis, B., eds. Hydraulic structures and water systems management. 6th IAHR International Symposium on Hydraulic Structures. doi:10.15142/T3170628160853.

Carey, S.; Gardner, J.; Sigurdsson, H. 1995. The intensity and magnitude of Holocene plinian eruptions from Mount St. Helens volcano. Journal of Volcanology and Geothermal Research. 66: 185202.

Chan, K.J. 2008. Late Quaternary volcanically influenced sedimentation in the Cowlitz River, WA—implications for hazard mitigation. Pullman, WA: Washington State University. 198 p. M.S. thesis.

Clynne, M.A.; Calvert, A.T.; Wolfe, E.W.; Evarts, R.C.; Fleck, R.J.; Lanphere, M.A. 2008. The Pleistocene eruptive history of Mount St. Helens, Washington, from 300,000 to 12,800 years before present. In: Sherrod, D.R.; Scott, W.E.; Stauffer, P.H., eds. A volcano rekindled: the renewed eruption of Mount St. Helens, 2004–2006. Professional Paper 1750. Reston, VA: U.S. Department of the Interior, Geological Survey: 593–627.

Clynne, M.A.; Ramsey, D.W.; Wolfe, E.W. 2005. Pre-1980 eruptive history of Mount St. Helens, Washington. Fact Sheet 2005-3045. Vancouver, WA: U.S. Department of the Interior, Geological Survey. 4 p.

Colle, B.A.; Mass, C.F. 2000. The 5–9 February 1996 flooding event over the Pacific Northwest: sensitivity studies and evaluation of the MM5 precipitation forecasts. Monthly Weather Review. 128(3): 593–617.

Crandell, D.R. 1987. Deposits of pre-1980 pyroclastic flows and lahars from Mount St. Helens volcano, Washington. Professional Paper 1444. Washington, DC: U.S. Government Printing Office. 91 p.

Crandell, D.R.; Hoblitt, R.P. 1986. Lateral blasts at Mount St. Helens and hazard zonation. Bulletin of Volcanology. 48: 27–37.

Denlinger, R.P. 2012. Effects of catastrophic floods and debris flows on the sediment retention structure, North Fork Toutle River, Washington. Open-File Report 2011-1317. Reston, VA: U.S. Department of the Interior, Geological Survey. 25 p.

Dewey, J.W.; Hopper, M.G.; Wald, D.J.; Quitoriano, V.; Adams, E.R. 2002. Intensity distribution and isoseismal maps for the Nisqually, Washington, earthquake of 28 February 2001. Open-File Report 02-346. Denver, CO: U.S. Department of the Interior, Geological Survey. 57 p.

Dobry, R.; Borcherdt, R.F.; Crouse, C.B.; Idriss, I.M.; Joyner, W.B.; Martin, G.R.; Power, M.S.; Rinne, E.E.; Seed, R.B. 2000. New site coefficients and site classification system used in recent building seismic code provisions. Earthquake Spectra. 16: 41–67.

Dowding, C.H.; Rozan, A. 1978. Damage to rock tunnels from earthquake shaking. ASCE Journal of the Soil Mechanics and Foundations Division. 104: 175–191.

Dunne, T.; Fairchild, L.H. 1984. Estimation of flood and sedimentation hazards around Mt. St. Helens. Shin Sabo. 36(4): 12–22; 37(1): 13–22.

Dzurisin, D.; Moran, S.C.; Lisowski, M.; Schilling, S.P.; Andersen, K.R.; Werner, C. 2015. The 2004–2008 dome-building eruption at Mount St. Helens, Washington: epilogue. Bulletin of Volcanology. 77(10): art 89. doi:10.1007/s00445-015-0973-4.

Endo, E.T.; Malone, S.D.; Noson, L.L.; Weaver, C.S. 1981. Locations, magnitudes, and statistics of the March 20–May 18 earthquake sequence. In: Lipman, P.W.; Mullineaux, D.R., eds. The 1980 eruptions of Mount St. Helens, Washington. U.S. Geological Survey Professional Paper 1250. Washington, DC: U.S. Government Printing Office: 93–107.

Evarts, R.C.; Ashley, R.P. 1993. Text that accompanies the geologic map of the Spirit Lake West Quadrangle, Skamania and Cowlitz Counties, Washington. Geologic Map GQ-1681. Reston, VA: U.S. Department of the Interior, Geological Survey. https://pubs.er.usgs.gov/publication/gq1681. (7 December 2016).

Evarts, R.C.; Ashley, R.P.; Smith, J.G. 1987. Geology of the Mount St. Helens area: record of discontinuous volcanic and plutonic activity in the Cascade Arc of southern Washington. Journal of Geophysical Research. 92(B10): 10155–10169.

Evarts, R.C.; Swanson, D.A. 1994. Geologic transect across the Tertiary Cascade Range, southern Washington. In: Swanson, D.A.; Haugerud, R.A., eds. Geologic field trips in the Pacific Northwest: 1994 Geological Society of America annual meeting. Seattle, WA: University of Washington, Department of Geological Science: Vol. 2, Chap. H: 1–31.

Fairchild, L.H. 1987. The importance of lahar initiation processes. In: Costa, J.E.; Wieczorek, G.F., eds. Debris flows/avalanches: process, recognition, and mitigation. Reviews in Engineering Geology. 7: 51–61.

Fairchild, L.H.; Wigmosta, M.S. 1983. Dynamic and volumetric characteristics of the 18 May 1980 lahars on the Toutle River, Washington. Proceedings of the symposium on erosion control in volcanic areas. Tech. Memorandum 1908. Tsukuba, Japan: Public Works Research Institute: 131–153.

Flück, P.; Hyndman, R.D.; Wang, K. 1997. Three-dimensional dislocation model for great earthquakes of the Cascadia subduction zone. Journal of Geophysical Research. 102(B9): 20539–20550.

Folk, R. 1980. Petrology of sedimentary rocks. Austin, TX: Hemphill Publishing Company. 102 p.

Foxworthy, B.L.; Hill, M. 1982. Volcanic eruptions of 1980 at Mount St. Helens: the first 100 days. U.S. Geological Survey Professional Paper 1249. Washington, DC: U.S. Government Printing Office. 125 p.

Glicken, H.X. 1996. Rockslide-debris avalanche of May 18, 1980, Mount St. Helens Volcano, Washington. Open-File Report 96-677. Vancouver, WA: U.S. Department of the Interior, Geological Survey. 90 p.

Glicken, H.; Meyer, W.; Sabol, M. 1989. Geology and ground-water hydrology of Spirit Lake blockage, Mount St. Helens, Washington, with implications for lake retention. U.S Geological Survey Bulletin 1789. Washington, DC: U.S. Government Printing Office. 33 p. + maps.

Goldfinger, C.; Nelson, C.H.; Morey, A.E.; Johnson, J.E.; Patton, J.R.; Karabanov, E.; Gutiérrez-Pastor, J.; Eriksson, A.T.; Gràcia, E.; Dunhill, G.; Enkin, R.; Dallimore, A.; Vallier, T. 2012. Turbidite event history—methods and implications for Holocene paleoseismicity of the Cascadia subduction zone. Professional Paper 1661-F. Reston, VA: U.S. Department of the Interior, Geological Survey. 170 p.

Gomberg, J.; Cascadia 2007 and Beyond Working Group. 2010. Slow-slip phenomena in Cascadia from 2007 and beyond—a review. Geological Society of America Bulletin. 122: 963–978.

Grant, W.C.; Weaver, C.S.; Zollweg, J.E. 1984. The 14 February Elk Lake, Washington, earthquake sequence. Bulletin of the Seismological Society of America. 74: 1289–1309.

Harr, R.D. 1981. Some characteristics and consequences of snowmelt during rainfall in western Oregon. Journal of Hydrology. 53(3): 277–304.

Hausback, B.P.; Swanson, D.A. 1990. Record of prehistoric debris avalanches on the north flank of Mount St. Helens, Washington. Geoscience Canada. 17: 142–145.

Hildreth, W. 2007. Quaternary magmatism in the Cascades—geologic perspectives. Professional Paper 1744. Reston, VA: U.S. Department of the Interior, Geological Survey. 125 p.

Hoblitt, R.P.; Crandell, D.R.; Mullineaux, D.R. 1980. Mount St. Helens eruptive behavior during the past 1,500 years. Geology. 8: 555–559.

Hoblitt, R.P.; Miller, C.D.; Vallance, J.W. 1981. Origin and stratigraphy of the deposit produced by the May 18 directed blast. In: Lipman, P.W.; Mullineaux, D.R., eds. The 1980 eruptions of Mount St. Helens, Washington. U.S. Geological Survey Professional Paper 1250. Washington, DC: U.S. Government Printing Office: 401–420.

Hoblitt, R.P.; Scott, W.E. 2011. Estimate of tephra accumulation probabilities for the U.S. Department of Energy Hanford site, Washington. Open-File Report. 2011-1064. Reston, VA: U.S. Department of the Interior, Geological Survey. 15 p.

Hoek, E.; Brown, E.T. 1980. Underground excavations in rock. London: Institution of Mining and Metallurgy. 527 p.

Hyndman, R.D.; Mazzotti, S.; Weichert, D.; Rogers, G.C. 2003. Frequency of large crustal earthquakes in Puget Sound–Southern Georgia Strait predicted from geodetic and geological deformation rates. Journal of Geophysical Research. 108(B1): 2033. doi:10.1029/2001JB001710.

International Seismological Centre. 2017. ISC-GEM instrumental earthquake catalogue (1900–2012). http://www.isc.ac.uk/iscgem/index.php. (January 12, 2017).

Janda, R.J.; Meyer, D.F.; Childers, D. 1984. Sedimentation and geomorphic changes during and following the 1980–1983 eruptions of Mount St. Helens, Washington. Shin Sabo. 37(2): 10–21; 37(3): 5–19.

Janda, R.J.; Scott, K.M.; Nolan, K.M.; Martinson, H.A. 1981. Lahar movement, effects, and deposits. In: Lipman, P.W.; Mullineaux, D.R., eds. The 1980 eruptions of Mount St. Helens, Washington. U.S. Geological Survey Professional Paper 1250. Washington, DC: U.S. Government Printing Office: 461–478.

Jing-Ming, W.; Litehiser, J.J. 1985. The distribution of earthquake damage to underground facilities during the 1976 Tang-Shan earthquake. Earthquake Spectra. 1: 741–757.

Johnson, M.G.; Beschta, R.L. 1980. Logging, infiltration capacity, and surface erodibility in western Oregon. Journal of Forestry. 78: 334–337.

Jones, J.A. 2000. Hydrologic processes and peak discharge response to forest removal, regrowth, and roads in 10 small experimental basins, western Cascades, Oregon. Water Resources Research. 36: 2621–2642.

Kanamori, H.; Given, J.W.; Lay, T. 1984. Analysis of seismic body waves excited by the Mount St. Helens eruption of May 18, 1980. Journal of Geophysical Research. 89(B3): 1856–1866.

Kelsey, H.M.; Nelson, A.R.; Hemphill-Haley, E.; Witter, R.C. 2005. Tsunami history of an Oregon coastal lake reveals a 4600 yr record of great earthquakes on the Cascadia subduction zone: Geological Society of America Bulletin. 117: 1009–1032.

Kelsey, H.M.; Witter, R.C; Hemphill-Haley, E. 2002. Plate-boundary earthquakes and tsunamis of the past 5500 yr, Sixes River estuary, southern Oregon. Geological Society of America Bulletin. 114: 298–314.

Kiser, E.; Palomeras, I.; Levander, A.; Zelt, C.; Harder, S.; Schmandt, B.; Hansen, S.; Creager, K.; Ulberg, C. 2016. Magma reservoirs from the upper crust to the Moho inferred from high-resolution Vp and Vs models beneath Mount St. Helens, Washington State, USA. Geology. 44: 411–414.

Leavesley, G.H.; Lusby, G.C.; Lichty, R.W. 1989. Infiltration and erosion characteristics of selected tephra deposits from the 1980 eruption of Mount St. Helens, Washington, USA: Hydrological Sciences Journal. 34: 339–353.

Lehre, A.K.; Collins, B.D.; Dunne, T. 1983. Post-eruption sediment budget for the North Fork Toutle River drainage, June 1980–June 1981: Zeitschrift für Geomorphologie. 46(suppl.): 143–165.

Lin, T.; Baker, J. 2011. Probabilistic seismic hazard deaggregation of ground motion prediction models. In: Proceedings, 5th international conference on earthquake geotechnical engineering. London: International Society of Soil Mechanics and Geotechnical Engineering. 12 p.

Lipman, P.W.; Moore, J.G.; Swanson, D.A. 1981. Bulging of the north flank before the May 18 eruption—geodetic data. In: Lipman, P.W.; Mullineaux, D.R., eds. The 1980 eruptions of Mount St. Helens, Washington. U.S. Geological Survey Professional Paper 1250. Washington, DC: U.S. Government Printing Office: 143–155.

Lipman, P.W.; Mullineaux, D.R., eds. 1981. The 1980 eruptions of Mount St. Helens, Washington. U.S. Geological Survey Professional Paper 1250. Washington, DC: U.S. Government Printing Office. 844 p.

Lombard, R.E.; Miles, M.B.; Nelson, L.M.; Kresch, D.L.; Carpenter, P.J. 1981. The impact of mudflows of May 18 on the lower Toutle and Cowlitz Rivers. In: Lipman, P.W.; Mullineaux, D.R., eds. The 1980 eruptions of Mount St. Helens, Washington. U.S. Geological Survey Professional Paper 1250. Washington, DC: U.S. Government Printing Office: 693–699.

Major, J.J.; Kingsbury, C.G.; Poland, M.P.; LaHusen, R.G. 2008. Extrusion rate of the Mount St. Helens lava dome estimated from terrestrial imagery—November 2004–December 2005. In: Sherrod, D.R.; Scott, W.E.; Stauffer, P.H., eds. A volcano rekindled: the renewed eruption of Mount St. Helens, 2004–2006. Professional Paper 1750. Reston, VA: U.S. Department of the Interior, Geological Survey: 237–255.

Major, J.J.; Mark, L.E. 2006. Peak flow responses to landscape disturbances caused by the cataclysmic 1980 eruption of Mount St. Helens, Washington. Geological Society of America Bulletin. 118: 938–958. doi:10.1130/B25914.1.

Major, J.J.; Mosbrucker, A.R.; Spicer, K.R. [In press]. Sediment erosion and delivery from Toutle River basin after the 1980 eruption of Mount St. Helens—a 30-year perspective. In: Dale, V.H.; Crisafulli, C.M., eds. Ecological responses revisited 35 years after the 1980 eruptions of Mount St. Helens. New York: Springer-Verlag.

Major, J.J.; Pierson, T.C.; Dinehart, R.L.; Costa, J.E. 2000. Sediment yield following severe volcanic disturbance—a two-decade perspective from Mount St. Helens. Geology. 28: 819–822.

Major, J.J.; Pierson, T.C.; Scott, K.M. 2005. Debris flows at Mount St. Helens, Washington, USA. In: Jakob, M.; Hungr, O., eds. Debris-flow hazards and related phenomena. Berlin: Springer-Praxis: 685–731.

Major, J.J.; Scott, K.M. 1988. Volcaniclastic sedimentation in the Lewis River valley, Mount St. Helens, Washington—processes, extent, and hazards. U.S. Geological Survey Bulletin 1383-D. Washington, DC: U.S. Government Printing Office. 38 p.

Major, J.J.; Voight, B. 1986. Sedimentology and clast orientations of the 18 May 1980 southwest flank lahars, Mount St. Helens, Washington. Journal of Sedimentary Petrology. 56: 691–705.

Major, J.J.; Yamakoshi, T. 2005. Decadal-scale change of infiltration characteristics of a tephra-mantled hillslope at Mount St. Helens, Washington. Hydrological Processes. 19: 3621–3630.

McCaffrey, R.; Qamar, A.I.; King, R.W.; Wells, R.; Khazaradze, G.; Williams, C.A.; Stevens, C.W.; Vollick, J.J.; Zwick, P.C. 2007. Fault locking, block rotation, and crustal deformation in the Pacific Northwest. Geophysical Journal International. 169: 1315–1340.

McCrory, P.A.; Blair, J.L.; Waldhauser, F.; Oppenheimer, D.H. 2012. Juan de Fuca slab geometry and its relation to Wadati-Benioff zone seismicity. Journal of Geophysical Research. 117(B9), B09306. doi:10.1029/2012JB009407.

McNutt, S.R. 1996. Seismic monitoring and eruption forecasting of volcanoes—a review of the state-of-the-art and case histories. In: Scarpa, R.; Tilling, R.I., eds. Monitoring and mitigation of volcano hazards. Berlin: Springer-Verlag: 99–146.

Meyer, D.F. 1995. Stream-channel changes in response to volcanic detritus under natural and augmented discharge, South Coldwater Creek, Washington. Open-File Report 94-519. Vancouver, WA: U.S. Department of the Interior, Geological Survey. 137 p.

Meyer, D.F.; Janda, R.J. 1986. Sedimentation downstream from the 18 May 1980 North Fork Toutle River debris avalanche deposit, Mount St. Helens, Washington. In: Keller, S.A.C., ed. Mount St. Helens: five years later. Cheney, WA: Eastern Washington University Press: 68–86.

Meyer, D.F.; Martinson, H.A. 1989. Rates and processes of channel development and recovery following the 1980 eruption of Mount St. Helens, Washington: Hydrological Sciences Journal. 34: 115–127.

Meyer, W.; Carpenter, P.J. 1983. Filling of Spirit Lake, Washington, May 18, 1980, to July 3, 1982. Open-File Report 82-771. Tacoma, WA: U.S. Department of the Interior, Geological Survey. 19 p.

Meyer, W.; Schuster, R.L.; Sabol, M.A. 1994. Potential for seepage erosion of landslide dam: Journal of Geotechnical Engineering. 120: 1211–1229.

Mosbrucker, A.R.; Spicer, K.R.; Major, J.J.; Saunders, D.R.; Christianson, T.S.; Kingsbury, C.G. 2015. Digital database of channel cross-section surveys, Mount St. Helens, Washington. Data Series 951. Reston, VA: U.S. Department of the Interior, Geological Survey. 9 p.

Mullineaux, D.R. 1996. Pre-1980 tephra-fall deposits erupted from Mount St. Helens, Washington. U.S. Geological Survey Professional Paper 1563. Washington, DC: U.S. Government Printing Office. 95 p.

Mullineaux, D.R.; Crandell, D.R. 1981. The eruptive history of Mount St. Helens. In: Lipman, P.W.; Mullineaux, D.R., eds. The 1980 eruptions of Mount St. Helens, Washington. U.S. Geological Survey Professional Paper 1250. Washington, DC: U.S. Government Printing Office: 3–15.

Myers, B.; Driedger, C. 2008. Eruptions in the Cascade Range during the past 4,000 years. General Information Product 63. Vancouver, WA: U.S. Department of the Interior, Geological Survey. 1 p.

Nelson, A.R.; Kelsey, H.M.; Witter, R.C. 2006. Great earthquakes of variable magnitude at the Cascadia subduction zone. Quaternary Research. 65: 354–365.

O'Connor, J.E.; Grant, G.E.; Costa, J.E. 2002. The geology and geography of floods. In: House, P.K.; Webb, R.H.; Baker, V.R.; Levish, D.R. Ancient floods, modern hazards: principles and application of paleoflood hydrology. Washington, DC: American Geophysical Union. Water Science and Application. 5: 359–385.

Oppenheimer, D.; Eaton, J.; Jayko, A.; Lisowski, M.; Marshall, G.; Murray, M.; Simpson, R.; Stein, R.; Beroza, G.; Magee, M.; Carver, G.; Dengler, L.; McPherson, R.; Gee, L.; Romanowicz, B.; Gonzalez, F.; Li, W.H.; Satake, K.; Somerville, P.; Valentine, D. 1993. The Cape Mendocino, California, earthquakes of April 1992: subduction at the triple junction. Science. 261(5120): 433–438.

Pallister, J.S.; Hoblitt, R.P.; Crandell, D.R.; Mullineaux, D.R. 1992. Mount St. Helens a decade after the 1980 eruptions: magmatic models, chemical cycles, and a revised hazards assessment. Bulletin of Volcanology. 54: 126–146.

Parsons, T.; Trehu, A.M.; Luetgert, J.H.; Miller, K.; Kilbride, F.; Wells, R.E.; Fisher, M.A.; Flueh, E.; ten Brink, U.S.; Christensen, N.I. 1998. A new view into the Cascadia subduction zone and volcanic arc: implications for earthquake hazards along the Washington margin. Geology. 26: 199–202.

Petersen, M.D.; Cramer, C.H.; Frankel, A.D. 2002. Simulations of seismic hazard for the Pacific Northwest of the United States from earthquakes associated with Cascadia subduction zone: Pure and Applied Geophysics. 159: 2147–2168.

Petersen, M.D.; Frankel, A.D.; Harmsen, S.C.; Mueller, C.S.; Haller, K.M.; Wheeler, R.L.; Wesson, R.L.; Zeng, Y.; Boyd, O.S.; Perkins, D.M.; Luco, N.; Field, E.H.; Wills, C.J.; Rukstales, K.S. 2008. Documentation for the 2008 update of the United States National Seismic Hazard Maps. Open-File Report 2008–1128. Reston, VA: U.S. Department of the Interior, Geological Survey. 61 p.

Petersen, M.D.; Moschetti, M.P.; Powers, P.M.; Mueller, C.S.; Haller, K.M.; Frankel, A.D.; Zeng, Y.; Rezaeian, S.; Harmsen, S.C.; Boyd, O.S.; Field, E.H.; Chen, R.; Luco, N.; Wheeler, R.L.; Williams, R.A.; Olsen, A.H.; Rukstales, K.S. 2015. Seismic hazard maps for the conterminous United States, 2014. Scientific Investigations Map 3325. Reston, VA: U.S. Department of the Interior, Geological Survey. 6 sheets.

Petersen, M.D.; Moschetti, M.P.; Powers, P.M.; Mueller, C.S.; Haller, K.M.; Frankel, A.D.; Zeng, Y.; Rezaeian, S.; Harmsen, S.C.; Boyd, O.S.; Field, N.; Chen, R.; Rukstales, K.S.; Luco, N.; Wheeler, R.L.; Williams, R.A.; Olsen, A.H. 2014. Documentation for the 2014 update of the United States National Seismic Hazards Maps. Open-File Report 2014-1091. Reston, VA: U.S. Department of the Interior, Geological Survey. 243 p.

Pierson, T.C. 1985. Initiation and flow behavior of the 1980 Pine Creek and Muddy River lahars, Mount St. Helens, Washington: Geological Society of America Bulletin. 96: 1056–1069.

Pierson, T.C. 1999. Transformation of water flood to debris flow following the eruption-triggered transient-lake breakout from the crater on March 19, 1982. In: Pierson, T.C., ed. Hydrologic consequences of hot-rock/snowpack interactions at Mount St. Helens volcano, Washington, 1982–1984. Professional Paper 1586. Reston, VA: U.S. Department of the Interior, Geological Survey: 19–36.

Pierson, T.C.; Major, J.J. 2014. Hydrogeomorphic effects of explosive volcanic eruptions on drainage basins: Annual Review of Earth and Planetary Sciences. 42: 469–507.

Pierson, T.C.; Pringle, P.T.; Cameron, K.A. 2011. Magnitude and timing of downstream channel aggradation and degradation in response to a dome-building eruption at Mount Hood, Oregon. Geological Society of America Bulletin. 123: 3–20.

Power, J.A.; Murray, T.L.; Marson, J.N.; Laguerta, E.P. 1996. Preliminary observations of seismicity at Mount Pinatubo by use of the seismic spectral amplitude measurement (SSAM) system, May 13–June 18, 1991. In: Newhall, C.G.; Punongbayan, R.S., eds. Fire and mud—eruptions and lahars of Mount Pinatubo, Philippines. Seattle, WA: University of Washington Press: 269–283.

Pringle, P.T. 2002. Roadside geology of Mount St. Helens National Volcanic Monument and vicinity. Information Circular 88, rev. edition. Olympia, WA: Washington Department of Natural Resources, Division of Geology and Earth Resources. 122 p.

Pringle, P.T. 2008. Roadside geology of Mount Rainier National Park and vicinity. Information Circular 107. Olympia, WA: Washington Department of Natural Resources, Division of Geology and Earth Resources. 190 p.

Pringle, P.T.; Cameron, K.A. 1999. Eruption-triggered lahar on May 14, 1984. In: Pierson, T.C., ed. Hydrologic consequences of hot-rock/snowpack interactions at Mount St. Helens volcano, Washington, 1982–1984. Professional Paper 1586. Reston, VA: U.S. Department of the Interior, Geological Survey: 81–103.

Pringle, P.T.; Schuster, R.L.; Logan, R.L. 1998. New radiocarbon ages of major landslides in the Cascade Range, Washington. Washington Geology. 26: 31–39. [Errata: Washington Geology. 26: 59.]

PRISM Climate Data. 2016. Corvallis, OR: Oregon State University, PRISM Climate Group. http://prism.oregonstate.edu. (12 December 2016).

Rowley, P.D.; Kuntz, M.A.; Macleod, N.S. 1981. Pyroclastic-flow deposits. In: Lipman, P.W.; Mullineaux, D.R., eds. The 1980 eruptions of Mount St. Helens, Washington. U.S. Geological Survey Professional Paper 1250. Washington, DC: U.S. Government Printing Office: 489–512.

Sager, J.W.; Chambers, D.R. 1986. Design and construction of the Spirit Lake outlet tunnel, Mount St. Helens, Washington. In: Schuster, R.L., ed. Landslide dams—processes, risk, and mitigation. Geotechnical Special Publication 3. New York: American Society of Civil Engineers: 42–58.

Sarna-Wojcicki, A.M.; Shipley, S.; Waitt, R.B.; Dzurisin, D.; Wood, S.H. 1981. Areal distribution, thickness, mass, volume, and grain size of air-fall ash from the six major eruptions of 1980. In: Lipman, P.W.; Mullineaux, D.R., eds. The 1980 eruptions of Mount St. Helens, Washington. U.S. Geological Survey Professional Paper 1250. Washington, DC: U.S. Government Printing Office: 577–600.

Satake, K.; Shimazaki, K.; Tsuji, Y.; Ueda, K. 1996. Time and size of a giant earthquake in Cascadia inferred from Japanese tsunami records of January 1700. Nature. 379: 246–249.

Satake, K.; Wang, K.; Atwater, B.F. 2003. Fault slip and seismic moment of the 1700 Cascadia earthquake inferred from Japanese tsunami descriptions: Journal of Geophysical Research. 108(B11). doi:10.1029/2003JB002521.

Schilling, S.P.; Carrara, P.E.; Thompson, R.A.; Iwatsubo, E.Y. 2004. Post-eruption glacier development within the crater of Mount St. Helens, Washington, USA. Quaternary Research. 61: 325–329.

Schilling, S.P.; Thompson, R.A.; Messerich, J.A.; Iwatsubo, E.Y. 2008. Use of digital aerophotogrammetry to determine rates of lava dome growth, Mount St. Helens, Washington, 2004–2005. In: Sherrod, D.R.; Scott, W.E.; Stauffer, P.H., eds. A volcano rekindled: the renewed eruption of Mount St. Helens, 2004–2006. Professional Paper 1750. Reston, VA: U.S. Department of the Interior, Geological Survey: 145–167.

Schuster, R.L. 1983. Engineering aspects of the 1980 Mount St. Helens eruptions. Bulletin of the Association of Engineering Geologists. 20: 125–143.

Schuster, R.L.; Logan, R.L.; Pringle, P.T. 1992. Prehistoric rock avalanches in the Olympic Mountains, Washington. Science. 258(5088): 1620–1621.

Scott, K.M. 1988a. Origins, behavior, and sedimentology of lahars and lahar-runout flows in the Toutle-Cowlitz River system. U.S. Geological Survey Professional Paper 1447-A. Washington, DC: U.S. Government Printing Office. 74 p.

Scott, K.M. 1988b. Origins, behavior, and sedimentology of prehistoric catastrophic lahars at Mount St. Helens, Washington. Geological Society of America. Special Paper 229: 23–36.

Scott, K.M. 1989. Magnitude and frequency of lahars and lahar-runout flows in the Toutle-Cowlitz River System. U.S. Geological Survey Professional Paper 1447-B. Washington, DC: U.S. Government Printing Office. 33 p.

Scott, W.E.; Sherrod, D.R.; Gardner, C.A. 2008. Overview of 2004 to 2006, and continuing, eruption of Mount St. Helens, Washington. In: Sherrod, D.R.; Scott, W.E.; Stauffer, P.H., eds. A volcano rekindled: the renewed eruption of Mount St. Helens, 2004–2006. Professional Paper 1750. Reston, VA: U.S. Department of the Interior, Geological Survey: 3–22.

Simon, A. 1999. Channel and drainage-basin response of the Toutle River system in the aftermath of the 1980 eruption of Mount St. Helens, Washington. Open-File Report 96-633. Vancouver, WA: U.S. Department of the Interior, Geological Survey. 130 p.

Simon, A.; Klimetz, D. 2012. Analysis of long-term sediment loadings from the upper North Fork Toutle River system, Mount St. Helens, Washington. Technical Report 77. Washington, DC: U.S. Department of Agriculture, Agricultural Research Service, National Sedimentation Laboratory. 91 p.

Stanley, W.D.; Johnson, S.Y.; Qamar, A.I.; Weaver, C.S.; Williams, J.M. 1996. Tectonics and seismicity of the southern Washington Cascade Range. Bulletin of the Seismological Society of America. 86: 1–18.

Suter, C.; Pringle, P.T.; Schuster, R.L. 2013. New environmental and radiocarbon evidence for ages of two Holocene landslide-dammed lakes in the southern Washington Cascade Range, USA. In: [Abstract] Northwest Scientific Association 84th annual meeting. 78–79.

Swanson, F.J.; Collins, B.D.; Dunne, T.; Wicherski, B.P. 1983. Erosion of tephra from hillslopes near Mount St. Helens and other volcanoes. In: Proceedings of the symposium on erosion control in volcanic areas. Tech. Memorandum 1908. Tsukuba, Japan: Ministry of Construction, Public Works Research Institute: 183–221.

Swift, C.H.; Kresch, D.L. 1983. Mudflow hazards along the Toutle and Cowlitz Rivers from a hypothetical failure of Spirit Lake blockage. Water Resources Investigations Report 82-4125. Reston, VA: U.S. Department of the Interior, Geological Survey. 10 p. + map plates.

Tullos, D.; Wang, H.-W. 2014. Morphological responses and sediment processes following a typhoon-induced dam failure, Dahan River, Taiwan. Earth Surface Processes and Landforms. 39: 245–258. doi:10.1002/esp.3446.

U.S. Department of the Army, Corps of Engineers [USACE]. 1983. A comprehensive plan for responding to the long-term threat created by the eruption of Mount St. Helens, Washington. Portland, OR: Portland District. 187 p.

U.S. Department of the Army, Corps of Engineers [USACE]. 2014a. Engineering and design—safety of dams: policy and procedures. Regulation 1110-2-1156. Washington, DC. 528 p. http://www.publications.usace.army.mil/Portals/76/Publications/EngineerRegulations/ER_1110-2-1156.pdf. (15 December 2016).

U.S. Department of the Army, Corps of Engineers [USACE]. 2014b. Mount St. Helens long-term sediment management plan update. Limited reevaluation report. Portland, OR: Portland District. 26 p. http://www.nwp.usace.army.mil/Portals/24/docs/projects/MSH_EIS/Final_Draft_MSH-LRR.pdf. (15 December 2016).

U.S. Department of the Army, Corps of Engineers [USACE]. 2016b. Spirit Lake Project loading conditions, unpublished engineering notes: Portland District Corps of Engineers, Portland, Oregon.

U.S. Department of the Army, Corps of Engineers [USACE]. 2016a. Earthquake design and evaluation for civil works projects. Regulation ER-1110-2-1806. Washington, DC. 28 p. http://www.publications.usace.army.mil/Portals/76/Publications/EngineerRegulations/ER_1110-2-1806.pdf. (15 December 2016).

U.S. Department of the Interior, Geological Survey [USGS]. 2017. Earthquake hazards program. http://www.earthquake.usgs.gov/earthquakes/. (January 12, 2017).

Vallance, J.W.; Schneider, D.J.; Schilling, S.P. 2008. Growth of the 2004–2006 lava-dome complex at Mount St. Helens, Washington. In: Sherrod, D.R.; Scott, W.E.; Stauffer, P.H., eds. A volcano rekindled: the renewed eruption of Mount St. Helens, 2004–2006. Professional Paper 1750. Reston, VA: U.S. Department of the Interior, Geological Survey: 169–208.

Voight, B. 1981. Time scale for the first moments of the May 18 eruption. In: Lipman, P.W.; Mullineaux, D.R., eds. U.S. Geological Survey Professional Paper 1250. Washington, DC: U.S. Government Printing Office: 69–86.

Waite, G.P.; Moran, S.C. 2009. Vp structure of Mount St. Helens, Washington, USA, imaged with local earthquake tomography. Journal of Volcanology and Geothermal Research. 182: 113–122.

Waitt, R.B. 1981. Devastating pyroclastic density flow and attendant air fall of May 18—stratigraphy and sedimentology of deposits. In: Lipman, P.W.; Mullineaux, D.R., eds., The 1980 eruptions of Mount St. Helens, Washington. U.S. Geological Survey Professional Paper 1250. Washington, DC: U.S. Government Printing Office: 439–460.

Waitt, R.B. 1989. Swift snowmelt and floods (lahars) caused by great pyroclastic surge at Mount St. Helens volcano, Washington, 18 May 1980. Bulletin of Volcanology. 52: 138–157.

Waitt, R.B.; Dzurisin, D. 1981. Proximal airfall deposits from the May 18 eruption—stratigraphy and field sedimentology. In: Lipman, P.W.; Mullineaux, D.R., eds. U.S. Geological Survey Professional Paper 1250. Washington, DC: U.S. Government Printing Office: 601–616.

Waitt, R.B.; Pierson, T.C.; MacLeod, N.S.; Janda, R.J.; Voight, B.; Holcomb, R.T. 1983. Eruption-triggered avalanche, flood, and lahar at Mount St. Helens—effects of winter snowpack. Science. 221(4618): 1394–1397.

Walder, J.S.; Watts, P. 2003. Evaluating tsunami hazards from debris flows. In: Locat, J.; Mienert, J., eds. Submarine mass movements and their consequences. Dordrecht, The Netherlands: Springer: 155–162

Walder, J.S.; Watts, P.; Waythomas, C.F. 2006. Case study: mapping tsunami hazards associated with debris flow into a reservoir. Journal of Hydraulic Engineering. 132: 1–11.

Wang, K.; Wells, R.; Mazzotti, S.; Hyndman, R.D.; Sagiya, T. 2003. A revised dislocation model of interseismic deformation of the Cascadia subduction zone. Journal of Geophysical Research. 108(B1). doi:10.1029/2001JB001227.

Wang, Z.; Ormsbee, L. 2005. Comparison between probabilistic seismic hazard analysis and flood frequency analysis. Eos. 86(5): 45–56.

Weaver, C.S.; Grant, W.C.; Shemeta, J.E. 1987. Local crustal extension at Mount St. Helens, Washington. Journal of Geophysical Research. 92(B10): 10170–10178.

Weaver, C.S.; Smith, S.W. 1983. Regional tectonic and earthquake hazard implications of a crustal fault zone in southwestern Washington. Journal of Geophysical Research. 88(B12): 10371–10383.

Wells, R.E.; Blakely, R.J.; Weaver, C.S. 2002. Cascadia microplate models and within-slab earthquakes. In: Kirby, S.H.; Wang, K.; Dunlop, S., eds. The Cascadia subduction zone and related subduction systems—seismic structure, intraslab earthquakes and processes, and earthquake hazards. Open-File Report 02-328. Menlo Park, CA: U.S. Department of the Interior, Geological Survey: 17–23.

Wells, R.E.; McCaffrey, R. 2013. Steady rotation of the Cascade arc. Geology. 41: 1027–1030.

Wells, R.E.; Weaver, C.S.; Blakely, R.J. 1998. Fore-arc migration in Cascadia and its neotectonic significance. Geology. 26: 759–762.

White, J.D.L.; Houghton, B.F. 2006. Primary volcaniclastic rocks. Geology. 34: 677–680.

Wigmosta, M.S.; Burges, S.J. 1997. An adaptive modeling and monitoring approach to describe the hydrologic behavior of small catchments. Journal of Hydrology. 202: 48–77.

Wilcox, A.C.; O'Connor, J.E.; Major, J.J. 2014. Rapid reservoir erosion, hyperconcentrated flow, and downstream deposition triggered by breaching of 38 m tall Condit Dam, White Salmon River, Washington. Journal of Geophysical Research Earth Surface. 119: 1376–1394. doi:10.1002/2013JF003073.

Williams, H.F.; Hutchinson, I.; Nelson, A.R. 2005. Multiple sources for late-Holocene tsunamis at Discovery Bay, Washington State, USA. The Holocene. 15: 60–73.

Willingham, W.F. 2005. The Army Corps of Engineers' short-term response to the eruption of Mount St. Helens. Oregon Historical Quarterly. 106: 174–203.

Wynn, J.; Mosbrucker, A.; Pierce, H.; Spicer, K. 2016. Where is the hot rock and where is the ground water—using CSAMT to map beneath and around Mount St. Helens. Journal of Environmental and Engineering Geophysics. 21(2): 79–87.

Yamaguchi, D.K.; Hoblitt, R.P. 1995. Tree-ring dating of pre-1980 volcanic flowage deposits at Mount St. Helens, Washington. Geological Society of America Bulletin. 107: 1077–1093.

Yamaguchi, D.K.; Pringle, P.T.; Lawrence, D.B. 1995. Field sketches of late-1840s eruptions of Mount St. Helens, Washington. Washington Geology. 23: 3–8.

Youd, T.L. 1978. Major cause of earthquake damage is ground failure. Civil Engineering. 48(4): 47–51.

Youd, T.L.; Wilson, R.C.; Schuster, R.L. 1981. Stability of blockage in North Fork Toutle River. In: Lipman, P.W.; Mullineaux, D.R., eds. The 1980 eruptions of Mount St. Helens, Washington. U.S. Geological Survey Professional Paper 1250. Washington, DC: U.S. Government Printing Office: 821–828.

Zehfuss, P.H.; Atwater, B.F.; Vallance, J.W.; Brenniman, H.; Brown, T.A. 2003. Holocene lahars and their by-products along the historical path of the White River between Mount Rainier and Seattle. In: Swanson, T.W., ed. Western cordillera and adjacent areas: Geological Society of America Field Guide. 4: 209–223.

Zheng, S.; Wu, B.; Thorne, C.; Simon, A. 2014. Morphological evolution of the North Fork Toutle River following the eruption of Mount St. Helens, Washington. Geomorphology. 208: 102–116.

Appendix 1: Potential Failure Modes

The Potential Failure Mode Analysis (PFMA) evaluated five alternative outlets:

- Alternative 1—Existing tunnel and intake.
- Alternative 2—Major rehabilitation of the existing tunnel and intake.
- Alternative 3—A conduit shallowly buried across the debris blockage, fed by a permanent pumping facility.
- Alternative 4—A gravity-fed conduit more deeply buried across the debris blockage.
- Alternative 5—An open channel across the debris blockage.

All failure modes considered are listed here with the rationale for exclusion of those modes not considered to be significant risk drivers. Asterisks identify the potential failure modes considered to be key risk drivers of the Spirit Lake outflow project.

Alternative 1—Existing Tunnel and Intake

PFM 1-01: Probable maximum flood event overtops intake structure and induces tunnel failure. The lake rises to an elevation that overtops the debris blockage.

Because the pyroclastic deposits are variably thick along the crest of the blockage and are highly erodible, they are unlikely to hold back impounded lake water. Therefore, the blockage is expected to fail through internal seepage erosion of those deposits before the lake rises to the level that overtops the blockage.

***PFM 1-02:** A probable maximum flood event induces tunnel failure. Consequently, the lake level rises to an elevation that induces internal seepage erosion and breaching of the blockage.

PFM 1-03: An earthquake causes significant displacement along faults crossing the tunnel, which leads to tunnel blockage or failure. The lake rises to an elevation that overtops the debris blockage.

Because the pyroclastic deposits are variably thick along the crest of the blockage and are highly erodible, they are unlikely to hold back impounded lake water. Therefore, the blockage is expected to fail through internal seepage erosion of those deposits before the lake rises to the level that overtops the blockage.

***PFM 1-04:** An earthquake causes significant displacement along faults crossing the tunnel, which leads to tunnel blockage or failure. The lake rises to an elevation that leads to internal seepage erosion.

***PFM 1-05:** An eruption triggers a lahar that flows into Spirit Lake and generates a debris-laden wave that damages the intake structure and blocks flow into the tunnel. The lake rises to an elevation that leads to internal seepage erosion.

PFM 1-06: A landslide or rockfall from the hillslope above the tunnel intake damages its infrastructure and blocks flow into the tunnel.

The intake structure is cut into bedrock on the western margin of Spirit Lake. Bedding and flow planes dip out of the slope at 30 to 40 degrees. But the friction angle for this bedrock is 45 to 50 degrees. Therefore, although these dip slopes are in a favorable orientation for instability, they are below the critical angle for slope failure. The upper bench above the intake is highly fractured but is pinned with 24-ft rock bolts. The lower bench above the intake is stabilized with shotcrete and bolts. Thirty-foot drains and drain boards were installed in wet areas. To block the tunnel, a slope failure would need to fill the plunge pool that leads to the tunnel entrance. The slope design and engineering protections should provide adequate defense against such slope failures.

PFM 1-07: An earthquake induces liquefaction of the debris blockage.

This failure mechanism was examined by Youd et al. (1981) and found to not be a significant risk. But megathrust earthquakes on the Cascadia subduction zone and local earthquakes on the St. Helens seismic zone were not known, or only poorly known, at the time of that analysis. Liquefaction would have to deform the debris blockage by at least 18 m (60 ft) vertically for the normal lake stage to induce internal seepage erosion. But if the lake were highly elevated, the amount of vertical drop owing to liquefaction would be less. Based on deposit geometry, it would take at least 400 m (1,300 ft) of lateral movement to produce 18 m (60 ft) of vertical drop by spreading failure owing to liquefaction. The average slope on the blockage is 3 percent, which is below the 5 percent slope typical for mass failure owing to liquefaction to occur (Youd et al. 1981). The likelihood of such a large slope deformation owing to liquefaction is remote, but potential liquefaction and deformation caused by strong, long-duration shaking from a Cascadia megathrust earthquake, or a strong local St. Helens seismic zone earthquake should be evaluated.

PFM 1-08: An earthquake damages the intake structure, which allows uncontrolled flow into the tunnel. The tunnel subsequently fails.

The tunnel intake was designed to a seismic coefficient of 0.2 g. The intake is keyed into bedrock. An earthquake would need to generate a peak ground acceleration well above 0.2 g to significantly damage the intake infrastructure. The intake appears well designed and constructed to defend against seismic events.

PFM 1-09: Localized failure of the tunnel lining leads to partial collapse and reduction of tunnel capacity.

These sorts of failures have happened episodically during the 30-year operation of the tunnel. Each time the tunnel has undergone sufficient distress to potentially compromise design flow depth in the tunnel and the ability of the lake freeboard to temporarily accommodate unusual hydrological events, the tunnel has been repaired. These episodes of distress have not led to tunnel failure or to debris-blockage failure. Although the tunnel is likely to undergo future distress unless it is rehabilitated, future distress of the type that has happened historically is not expected to lead to tunnel failure.

PFM 1-10: Slope failure by any mechanism blocks the tunnel outlet portal. Tail water accumulation in the tunnel creates hydraulic shock that induces tunnel failure.

Slope material above the outlet is relatively thin and unconsolidated and unlikely to provide sufficient volume to plug the outlet even if a shallow landslide occurred. The bedrock bedding planes dip into the slope, thus bedrock failure is unlikely. Furthermore, the tunnel outlet is visible from the road leading to Johnson Ridge Observatory, thus a slope failure is unlikely to go undetected long enough to back up a sufficient volume of water to initiate a tail-water event. Monitoring gauges at the tunnel inlet would provide notice if water began backing up in the tunnel.

***PFM 1-11:** Extended closure during a major tunnel repair operation leads to a precarious lake level and is followed by a hydrological event that results in uncontrolled flow into the tunnel. The tunnel subsequently fails.

PFM 1-12: Extended closure during a major repair leads to a precarious lake level followed by an earthquake.

The probability of an earthquake of sufficient magnitude to cause sufficient damage to close the tunnel occurring at the conclusion of an extended maintenance closure that elevates the lake to a high level is an unlikely coincidence. Therefore, this mechanism is not considered to be a significant risk driver.

Alternative 2—Major Rehabilitation of the Existing Tunnel and Intake

Owing to similarities in the factors driving risk for alternatives 1 and 2, only the four original risk factors for alternative 1 were considered. And because the tunnel is assumed to have been fully rehabilitated in alternative 2, the hydrologic and seismic risk factors are deemed to no longer be significant. Therefore, only the

volcanic loading and operations and maintenance risks were formally evaluated. Because the rationales for excluding potential risk factors for alternative 2 are the same as for alternative 1, we do not repeat them here and refer the reader to the prior discussions.

Alternative 3—A Conduit Shallowly Buried Across the Debris Blockage Fed By a Permanent Pumping Facility

***PFM 3-01:** An eruption of Mount St. Helens generates a lahar (or other volcanic flow) that damages the barge or buries the conduit intake. This event renders the outlet inoperable.

PFM 3-02: An earthquake causes liquefaction and lateral spreading of sediment around the conduit intake. Sediment blocks the intake, and lateral spreading leads to intake damage.

The intensity of seismic loading required to initiate this event is a low-probability event. Furthermore, the blockage was deemed to be stable against liquefaction (Youd et al. 1981). Seismic loading is unlikely to render the barge inoperable, and damage to the connections between the barge and conduit may be limited in extent. Therefore, this mechanism leading to ultimate breaching of the blockage is considered unlikely.

PFM 3-03: Avulsion of the channel draining the north slope of the volcano directs excess sediment to the lake, which then damages the pump system.

This type of loading has a high probability of happening, but the consequent damages can be relatively easily repaired or prevented. There is sufficient time after initiation of avulsion to allow for intervention. Excess sediment loading by fluvial transport is not likely to render the barge/conduit system inoperable. It may cause some damage to the pumps or conduit, but such damage could likely be managed by onsite maintenance personnel.

Alternative 4—A Gravity-Fed Conduit More Deeply Buried Across the Debris Blockage

***PFM 4-01:** An eruption of Mount St. Helens generates a lahar (or perhaps a pyroclastic flow or lava flow) that buries the conduit intake. This event renders the outlet inoperable.

PFM 4-02: An earthquake causes liquefaction of debris blockage and lateral spreading, which damages the conduit and intake structure.

The intensity of seismic loading required to initiate this event is a low-probability event. Furthermore, the blockage was deemed to be stable against liquefaction (Youd et al. 1981). Seismic loading is unlikely to render the conduit inoperable,

although conduit performance under a strong, long-duration Cascadia megathrust event is unknown.

PFM 4-03: An extrafluvial landslide or debris flow from debris-avalanche sediment perched on Johnston Ridge blocks the conduit intake or outlet.

Depending upon the siting of the intake, there may or may not be sufficiently unstable material nearby to result in a landslide or debris flow that could block the intake. If the conduit outlet became blocked, the team anticipated that sufficient hydraulic head would build and breach the blockage before the lake rose to dangerous levels. Release of water by breaching of a blockage at the conduit outlet is limited by conduit capacity. There are two opportunities for intervention: uncovering the outlet structure, or pumping water from the lake into the conduit through access manholes, thus limiting potential damage.

Alternative 5—An Open Channel Across the Debris Blockage

PFM 5-01: A probable maximum flood event causes the channel to downcut, inducing headward knickpoint erosion that lowers the channel intake and leads to uncontrolled release of the lake.

This was not considered to be a significant risk driver because it was assumed that stream power and sediment transport would be managed in the channel design. Furthermore, the probable maximum flood (PMF) is a very low-probability event. The channel design would accommodate a conservative design flow. If the channel is designed to meet the flow requirements of the estimated PMF discharge, then this potential failure mode is not a significant risk driver for the project.

***PFM 5-02:** A hydrologic event triggers an extrafluvial landslide from debris-avalanche sediment perched on Johnston Ridge above the channel alignment. The landslide blocks the channel until rising water breaches the channel blockage.

PMF 5-03: An earthquake induces liquefaction of the debris blockage near the upstream end of the channel. The channel intake founders and causes an uncontrolled release of lake water.

The intensity of seismic loading required to initiate this event is a low-probability event. Furthermore, the blockage was deemed to be stable against liquefaction (Youd et al. 1981). Seismic loading is unlikely to render the channel intake inoperable. Therefore, this mechanism leading to ultimate breaching of the blockage is considered unlikely. But the potential for liquefaction should be reevaluated in light of the potential for strong, long-duration shaking during a Cascadia megathrust event.

PFM 5-04: Large woody debris from the lake blocks the channel intake. The lake level rises until logs are displaced or floated away. Lake water is released.

Woody debris is unlikely to block the channel intake to the point that no water can pass through. This is considered a very unlikely mechanism to generate failure of the channel or failure of the debris blockage.

***PFM 5-05:** A volcanic flow blocks the outlet channel, which raises the lake level and leads to a breach.

***PFM 5-06:** An earthquake triggers an extrafluvial landslide from debris-avalanche sediment perched on Johnston Ridge above the channel alignment. The landslide blocks the channel until rising water breaches the channel blockage.

Appendix 2: Derivation of Discharge and Threshold Particle Mobility for Trapezoidal Channel

Discharge and sediment transport thresholds for a conceptual trapezoidal channel can be estimated from Manning's equation, channel geometry, and the Shields equation for critical shear stress. The trapezoidal channel as conceived for risk assessment purposes has the following geometry:

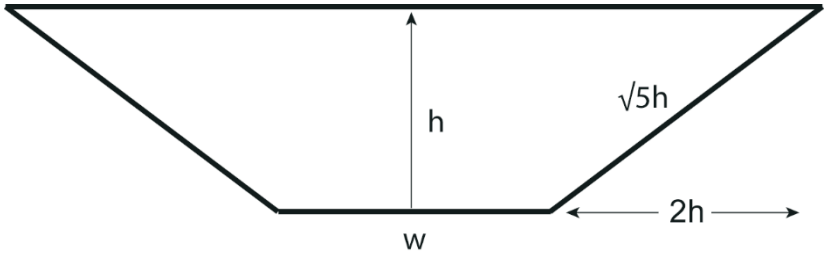

where *w* is bottom width, *h* is channel depth, *S* is slope of the channel centerline, and the channel has 2:1 side slopes. From this geometry, cross sectional area, *A*, is computed as:

$$A = h\frac{w+(w+4h)}{2} = h(w+2h) = 2h^2 + wh$$

wetted perimeter, *P*, is computed as:

$P = w + 2\sqrt{5}h$

and hydraulic radius, *R*, is computed as (*A/P*):

$$R = \frac{2h^2+wh}{2\sqrt{5}h+w}$$

From Manning's equation, we compute flow velocity as

$$v = \frac{R^{2/3}S^{1/2}}{n}$$

where *n* is Manning's roughness coefficient. For the given geometry, Manning's equation can be written as

$$v = \left[\frac{2h^2+wh}{2\sqrt{5}h+w}\right]^{2/3}\frac{s^{1/2}}{n}$$

Flow discharge, *Q*, is given by $A \times v$, which can be written as

$$Q = [2h^2 + wh]\left[\left[\frac{2h^2+wh}{2\sqrt{5}h+w}\right]^{2/3}\frac{s^{1/2}}{n}\right]$$

The Shields equation for particle mobility is given by

$$\tau_* = \frac{\tau}{(\rho_s - \rho) g D_{50}}$$

where τ is shear stress ($\rho g h S$), ρ_s is particle density, ρ is water density, g is gravitational acceleration, D_{50} is median particle size on the channel bed, and τ_* is a critical dimensionless shear shear stress for particle mobility. Rearrangement of the Shields stress equation yields

$$D_{50} = \frac{\tau}{(\rho_s - \rho) g \tau_*}$$

We compute discharge and particle mobility as functions of flow depth and slope for the following parameter values:

W = 15 m

S = 0.001 and 0.025

n = 0.04

ρ_s = 2300 kg m^{-3}, a common density for volcanic rocks

ρ = 1000 kg m^{-3}

τ_* = 0.04 and 0.08, which represent bounding values common for gravel-bed rivers.

Table A2-1—Discharge and mobile particle size as functions of depth, slope, roughness and critical shear stress

Depth	A	P	R	v at S = 0.001	Q at S = 0.001	v at S = 0.025	Q at S = 0.025	τ at S = 0.001	τ at S = 0.025	Mobile D_{50} at S = 0.001, $\tau_* = 0.04$	Mobile D_{50} at S = 0.025, $\tau_* = 0.04$	Mobile D_{50} at S = 0.001, $\tau_* = 0.08$	Mobile D_{50} at S = 0.025, $\tau_* = 0.08$
Meters	m^2	*Meters*		$m\ s^{-1}$	$m^3\ s^{-1}$	$m\ s^{-1}$	$m^3\ s^{-1}$	$N\ m^{-2}$	$N\ m^{-2}$	*Meters*			
1	17	19	0.9	0.7	12	3.6	60	10	245	0.02	0.48	0.01	0.24
1.5	27	22	1.2	0.9	25	4.6	125	15	368	0.03	0.72	0.01	0.36
2	38	24	1.6	1.1	40	5.4	205	20	490	0.04	0.96	0.02	0.48
2.5	50	26	1.9	1.2	60	6.1	305	25	613	0.05	1.20	0.02	0.60
3	63	28	2.2	1.3	85	6.7	425	29	735	0.06	1.44	0.03	0.72
3.5	77	31	2.5	1.5	110	7.3	560	34	858	0.07	1.68	0.03	0.84
4	92	33	2.8	1.6	145	7.8	720	39	980	0.08	1.92	0.04	0.96
4.5	108	35	3.1	1.7	180	8.4	905	44	1103	0.09	2.16	0.04	1.08
5	125	37	3.3	1.8	220	8.8	1105	49	1225	0.10	2.40	0.05	1.20
5.25	134	38	3.5	1.8	245	9.1	1215	51	1286	0.10	2.52	0.05	1.26
5.5	143	40	3.6	1.9	265	9.3	1330	54	1348	0.11	2.64	0.05	1.32
6	162	42	3.9	1.9	315	9.7	1580	59	1470	0.12	2.88	0.06	1.44
6.5	182	44	4.1	2.0	370	10.2	1850	64	1593	0.13	3.13	0.06	1.56
7	203	46	4.4	2.1	430	10.6	2150	69	1715	0.13	3.37	0.07	1.68
8	248	51	4.9	2.3	565	11.4	2820	78	1960	0.15	3.85	0.08	1.92
9	297	55	5.4	2.4	720	12.1	3605	88	2205	0.17	4.33	0.09	2.16
10	350	60	5.9	2.6	900	12.8	4500	98	2450	0.19	4.81	0.10	2.40
11	407	64	6.3	2.7	1100	13.5	5510	108	2695	0.21	5.29	0.11	2.64
11.5	437	66	6.6	2.8	1215	13.9	6065	113	2818	0.22	5.53	0.11	2.76
12	468	69	6.8	2.8	1330	14.2	6650	118	2940	0.23	5.77	0.12	2.88

Q = water discharge; v = water velocity; τ = shear stress; N = Newton (unit of force); S = channel slope; τ* = critical dimensionless shear stress.

Pacific Northwest Research Station

Website	http://www.fs.fed.us/pnw
Telephone	(503) 808-2592
Publication requests	(503) 808-2138
FAX	(503) 808-2130
E-mail	pnw_pnwpubs@fs.fed.us
Mailing address	Publications Distribution Pacific Northwest Research Station P.O. Box 3890 Portland, OR 97208-3890

Federal Recycling Program
Printed on Recycled Paper

U.S. Department of Agriculture
Pacific Northwest Research Station
1220 SW 3rd Ave., Suite 1400
P.O. Box 3890
Portland, OR 97208-3890